

AD-A179 741

A METHOD TO OBTAIN TIME DEPENDENT ELECTRON EIGENSTATE
POPULATIONS WITH EL (U) MISSION RESEARCH CORP SANTA

1/2

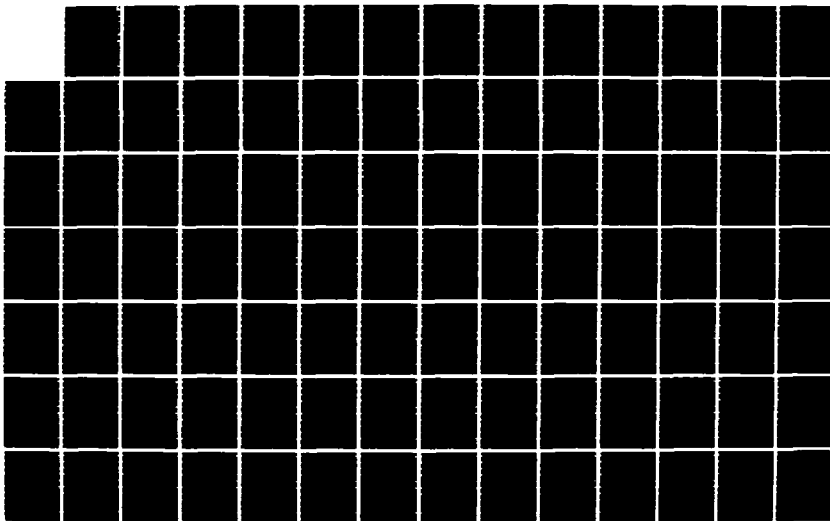
BARBARA CA D H SOMLE 01 JUL 86 MRC-R-1006

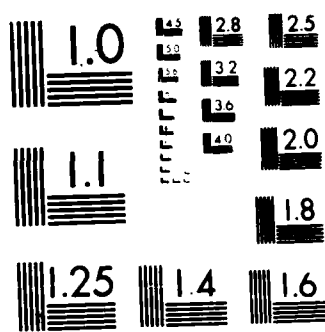
UNCLASSIFIED

DNA-TR-86-283 DNA001-85-C-0035

F/G 28/8

NL





MICROCOPY RESOLUTION TEST CHART
NATIONAL BUREAU OF STANDARDS 1964 A

AD-A179 741

10-FILE 100

(12)

DNA-TR-86-283

A METHOD TO OBTAIN TIME DEPENDENT ELECTRON EIGENSTATE POPULATIONS WITH ELECTRON COLLISIONS AND AN ARBITRARY RADIATION FIELD

D. H. Sowle
Mission Research Corporation
P. O. Drawer 719
Santa Barbara, CA 93102-0719

1 July 1986

Technical Report

CONTRACT No. DNA 001-85-C-0035

Approved for public release;
distribution is unlimited.

THIS WORK WAS SPONSORED BY THE DEFENSE NUCLEAR AGENCY
UNDER RDT&E RMSS CODE B322085760 Z99QMXZA00002 H2590D.

Prepared for
Director
DEFENSE NUCLEAR AGENCY
Washington, DC 20305-1000

DTIC
SELECTED
APR 3 0 1987
S E D

Destroy this report when it is no longer needed. Do not return to sender.

PLEASE NOTIFY THE DEFENSE NUCLEAR AGENCY
ATTN: TITL, WASHINGTON, DC 20305 1000, IF YOUR
ADDRESS IS INCORRECT, IF YOU WISH IT DELETED
FROM THE DISTRIBUTION LIST, OR IF THE ADDRESSEE
IS NO LONGER EMPLOYED BY YOUR ORGANIZATION.



UNCLASSIFIED

SECURITY CLASSIFICATION OF THIS PAGE

MD-101-1974

REPORT DOCUMENTATION PAGE

2a. REPORT SECURITY CLASSIFICATION UNCLASSIFIED		2b. RESTRICTIVE MARKINGS	
2a. SECURITY CLASSIFICATION AUTHORITY N/A since Unclassified		3. DISTRIBUTION/AVAILABILITY OF REPORT Approved for public release; distribution is unlimited.	
2b. DECLASSIFICATION/DOWNGRADING SCHEDULE N/A since Unclassified		5. MONITORING ORGANIZATION REPORT NUMBER(S) DNA-TR-86-283	
4. PERFORMING ORGANIZATION REPORT NUMBER(S) MRC-R-1006		7a. NAME OF MONITORING ORGANIZATION Director Defense Nuclear Agency	
5a. NAME OF PERFORMING ORGANIZATION Mission Research Corporation	6b. OFFICE SYMBOL (If applicable) MRC	7b. ADDRESS (City, State, and ZIP Code) Washington, DC 20305-1000	
5c. ADDRESS (City, State, and ZIP Code) P.O. Drawer 719 Santa Barbara, CA 93102-0719	8a. NAME OF FUNDING/SPONSORING ORGANIZATION 8b. OFFICE SYMBOL (If applicable) RAAE/Schwartz		
9. PROCUREMENT INSTRUMENT IDENTIFICATION NUMBER DNA 001-85-C-0035		10. SOURCE OF FUNDING NUMBERS	
		PROGRAM ELEMENT NO 62715H	PROJECT NO Z99QMXZ
		TASK NO A	WORK UNIT ACCESSION NO DH 200761
11. TITLE (Include Security Classification) A METHOD TO OBTAIN TIME DEPENDENT ELECTRON EIGENSTATE POPULATIONS WITH ELECTRON COLLISIONS AND AN ARBITRARY RADIATION FIELD			
12. PERSONAL AUTHOR(S) Sowle, Dave H.			
13a. TYPE OF REPORT Technical	13b. TIME COVERED FROM 850101 TO 860701	13c. DATE OF REPORT (Year, Month, Day) 860701	13d. PAGE COUNT 118
14. SUPPLEMENTARY NOTATION This work was sponsored by the Defense Nuclear Agency under RDT&E RMSS Code B322035760 Z99QMXZA00002 H2590D.			
15. COSAT CODES		16. SUBJECT TERMS (Continue on reverse if necessary and identify by block number) Radiative Collisional Transitions, Opacity Eigenstate Population, Non-LTE Opacity	
FIELD 9	GROUP 1	SUB-GROUP 2	
20		3	
17. ABSTRACT (Continue on reverse if necessary and identify by block number) A computer module has been written which solves the time dependent electron eigenstate population problem under the influence of electron collisions as well as spontaneous and induced radiative transitions to bound or free states. Degree of ionization is automatically included. Electron velocity distribution must be represented by a Maxwellian. Radiation is represented as photon groups, called "features," with flat central regions and Lorentz-like tails. Photon features can be superimposed, so that a rather general line and continuum combination can be represented. Check out examples discussed in the final section indicate that photoionization may be a more important phenomenon at high altitude than is generally appreciated.			
20. DISTRIBUTION/AVAILABILITY OF ABSTRACT <input type="checkbox"/> UNCLASSIFIED/UNLIMITED <input checked="" type="checkbox"/> SAME AS RPT <input type="checkbox"/> DTIC USERS		21. ABSTRACT SECURITY CLASSIFICATION UNCLASSIFIED	
22a. NAME OF RESPONSIBLE INDIVIDUAL BETTY L. FOX		22b. TELEPHONE (Include Area Code) (202) 325-7042	22c. OFFICE SYMBOL DNA/STII

DD FORM 1473, 84 MAR

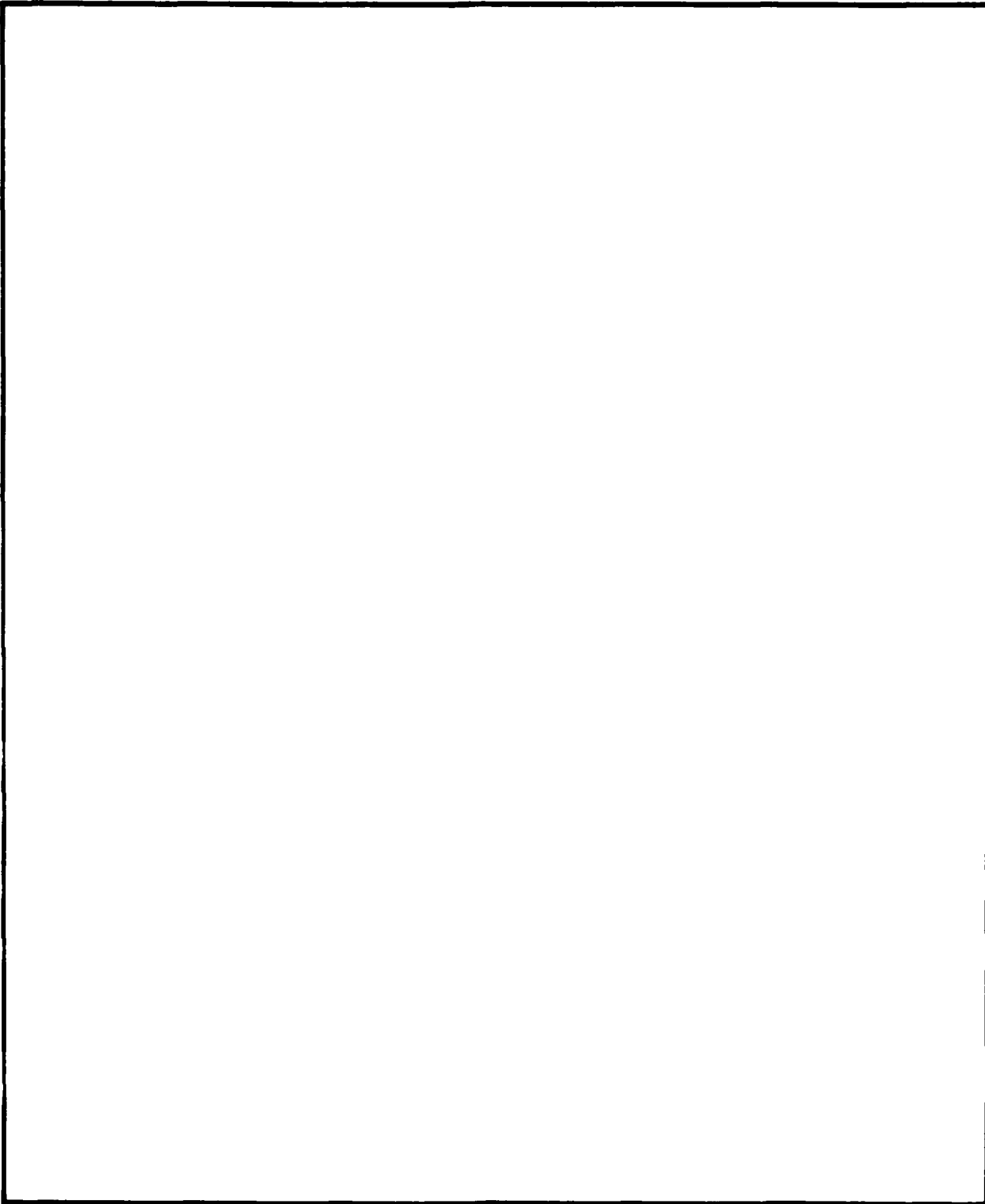
33 APR edition may be used until exhausted.

All other editions are obsolete.

SECURITY CLASSIFICATION OF THIS PAGE

UNCLASSIFIED

UNCLASSIFIED
SECURITY CLASSIFICATION OF THIS PAGE



SECURITY CLASSIFICATION OF THIS PAGE
UNCLASSIFIED

CONVERSION TABLE

angstrom	1.000 000 X E -10	meters (m)
atmosphere (normal)	1.013 25 X E +2	kilo pascal (kPa)
bar	1.000 000 X E + 2	kilo pascal (kPa)
barn	1.000 000 X E -28	meter ² (m ²)
British thermal unit (thermochemical)	1.054 350 X E + 3	joule (J)
calorie (thermochemical)	4.184 000	joule (J)
cal (thermochemical)/cm ²	4.184 000 X E -2	mega joule/m ² (MJ/m ²)
curie	3.700 000 X E +1	*giga becquerel (GBq)
degree (angle)	1.745 329 X E -2	radian (rad)
degree Fahrenheit	t _k = (t°F + 459.67)/1.8	degree kelvin (K)
electron volt	1.602 19 X E -19	joule (J)
erg	1.000 000 X E -7	joule (J)
erg/second	1.000 000 X E -7	watt (W)
foot	3.048 000 X E -1	meter (m)
foot-pound-force	1.355 818	joule (J)
gallon (U.S. liquid)	3.785 412 X E -3	meter ³ (m ³)
inch	2.540 000 X E -2	meter (m)
jerk	1.000 000 X E +9	joule (J)
joule/kilogram (J/kg)(radiation dose absorbed)	1.000 000	Gray (Gy)
kilotons	4.183	terajoules
kip (1000 lbf)	4.448 222 X E +3	newton (N)
kip/inch ² (ksi)	6.894 757 X E +3	kilo pascal (kPa)
ktap		newton-second/m ² (N-s/m ²)
micron	1.000 000 X E +2	meter (m)
mil	1.000 000 X E -6	meter (m)
mile (international)	2.540 000 X E -5	meter (m)
ounce	1.609 344 X E +3	kilogram (kg)
pound-force (lbs avoirdupois)	2.834 952 X E -2	newton (N)
pound-force inch	4.448 222	newton-meter (N·m)
pound-force/inch	1.129 848 X E -1	newton/meter (N/m)
pound-force/foot ²	1.751 268 X E +2	kilo pascal (kPa)
pound-force/inch ² (psi)	4.788 026 X E -2	kilo pascal (kPa)
pound-mass (lbm avoirdupois)	6.894 757	kilogram (kg)
pound-mass-foot ² (moment of inertia)	4.535 924 X E -1	kilogram-meter ² (kg·m ²)
pound-mass/foot ³	4.214 011 X E -2	kilogram/meter ³ (kg/m ³)
rad (radiation dose absorbed)	1.601 846 X E +1	**Gray (Gy)
roentgen	1.000 000 X E -2	coulomb/kilogram (C/kg)
shake	2.579 760 X E -4	second (s)
slug	1.000 000 X E -8	kilogram (kg)
torr (mm Hg, 0° C)	1.459 390 X E +1	kilo pascal (kPa)
	1.333 220 X E -1	

*The becquerel (Bq) is the SI unit of radioactivity; 1 Bq = 1 event/s.

**The Gray (Gy) is the SI unit of absorbed radiation.

TABLE OF CONTENTS

Section		Page
	CONVERSION TABLE	iii
	LIST OF ILLUSTRATIONS	vi
	LIST OF TABLE	vii
1	SCOPE.....	1
2	REQUIREMENTS.....	4
2.1	Systems.....	4
2.2	Physics.....	4
2.3	Mathematics.....	6
2.4	Computer.....	7
3	METHOD ADOPTED FOR EIGENSTATE SOLUTION.....	10
3.1	Summary of Method.....	10
3.2	Summary of Method Rationale.....	11
3.3	Major Elements of the Method.....	14
3.3.1	Adding Ionization States.....	14
3.3.2	Deleting Ionization States.....	15
3.3.3	Adding an Artificial Eigenstate.....	16
3.3.4	Deleting Eigenstates.....	19
3.3.4.1	Before Calculations Commence.....	19
3.3.4.2	During Calculation.....	19
3.3.5	Stiff Equation Problem.....	21
3.3.6	Normalization Problems.....	22
3.3.6.1	Inherent Numerics Problem.....	22
3.3.6.2	Set Separation Problem.....	23
3.3.6.3	Gauss Elimination Problem.....	25
3.3.7	Sorting Algorithm.....	26
3.3.8	Freezing Problem.....	28
3.3.9	Gauss Elimination.....	31
3.3.9.1	Quasi-Steady Equations.....	31
3.3.9.2	Differential Equations.....	35
4	RADIATION SPECTRUM AND LINE SHAPE.....	36
4.1	Nomenclature.....	36
4.2	Spectral Features.....	36
4.3	Lines.....	37
4.4	Line Widths.....	38

TABLE OF CONTENTS (Concluded)

Section	Page
5 RATES.....	40
5.1 Stark Width.....	40
5.2 Spontaneous Emission.....	41
5.3 Electron Bound-Bound Collisions.....	41
5.4 Electron Bound-Free Collisions and Three Body Recombination.....	42
5.4.1 Contribution from Eigenstates Above the Continuum	44
5.5 Radiative Ionization and Recombination.....	45
5.5.1 Radiative Recombination.....	45
5.5.2 Photoionization.....	49
5.6 Bound-Bound Radiative Rates.....	51
5.7 Oscillator Strength.....	56
5.7.1 Oscillator Strength for Real States.....	56
5.7.2 Oscillator Strength to the Artificial State.	57
5.7.2.1 Radiation Oscillator Strength.....	61
5.7.2.2 Electron Collision Oscillator Strength.....	63
6 BASIC DATA.....	66
7 SAMPLE RESULTS.....	68
7.1 Collisional-Radiative Recombination and Ionization..	68
7.1.1 Recombination Coefficient for Hydrogen.....	69
7.1.2 Ionization Coefficient for Hydrogen.....	75
7.2 Approach to Steady State Without Radiation.....	80
7.2.1 Time Development of Hydrogen.....	82
7.2.2 Hydrogen Steady State vs Electron Density...	82
7.2.3 Time Development of Nitrogen.....	82
7.2.4 Nitrogen Steady State vs Electron Density...	86
7.2.5 Value of Electron Density for Equilibrium in Optically Thin Plasma.....	88
7.3 Approach to Steady State with Planck Radiation.....	92
7.4 Steady State with Line Radiation.....	97
8 LIST OF REFERENCES.....	105

LIST OF ILLUSTRATIONS

Figure		Page
1	Hydrogen Collisional Radiative Recombination Coefficient at 250°K.	70
2	Hydrogen Collisional Radiative Recombination Coefficient at 1000°K.	71
3	Hydrogen Collisional Radiative Recombination Coefficient at 4000°K.	72
4	Hydrogen Collisional Radiative Recombination Coefficient at 16,000°K.	73
5	Hydrogen Collisional Radiative Recombination Coefficient at 64,000°K.	74
6	Hydrogen Collisional Radiative Ionization Coefficient at 4000°K.	76
7	Hydrogen Collisional Radiative Ionization Coefficient at 16,000°K.	77
8	Hydrogen Collisional Radiative Ionization Coefficient at 64,000°K.	78
9	Hydrogen Ionization.	83
10	Steady State Hydrogen.	84
11	Nitrogen in 10^{14} electrons at 3 eV.	85
12	Nitrogen at 1-eV.	87
13	Nitrogen at 10-eV, optically thin.	89
14	Optically thin nitrogen at 10-eV, more detail.	90
15	Nitrogen in a 1-eV Planck spectrum without collisions..	94
16	Nitrogen in 1.0 eV Planck radiation and 10-eV electrons.	96

LIST OF ILLUSTRATIONS (Concluded)

Figure		Page
17	Nitrogen with 1 line.	98
18	Nitrogen with 2 lines.	100
19	Nitrogen with 3 lines.	101
20	Nitrogen with 4 lines.	103
21	Nitrogen with and without 4 lines.	104

Table		
1	0 ¹⁺ Data.	67

Accredited For	
YES	<input checked="" type="checkbox"/>
NO	<input type="checkbox"/>
Distribution	
Approved	<input type="checkbox"/>
Justification	<input type="checkbox"/>
By	
Distribution/	
Availability Codes	
Email and/or	<input type="checkbox"/>
Post	<input type="checkbox"/>
Special	
A-1	



SECTION 1

SCOPE

Many military systems, particularly SDI systems, have trans-nuclear missions which require successful propagation of electromagnetic signals through the atmosphere. Signals of interest may be radio, radar, infra-red emissions, optical, UV, X-ray, or even atomic atoms or ions. Many of the above wavelength ranges are sensitive to the presence and especially to the structure of plasma or atomic and molecular emitters and absorbers produced or modified by atmospheric nuclear explosions. The range of yield and altitude of interest spans kilotons to tens of megatons and ground surface to hundreds of kilometers.

The atmospheric test data base is sparse except near the surface, and lacks measurements of quantities critical to modern systems even there. Many observables of interest cannot be obtained in underground tests. Consequently it is necessary to rely heavily on theoretical predictions.

For these purposes theory is required to provide two distinct services. It is required to serve as a mechanism for interpolating between field test events and extrapolating from them for observables which have been measured, and it is required to predict observables which have not been measured.

To maximize confidence in theoretical results for cases remote from the data base or for observables not available in the data base it is not sufficient to carry out the most careful and complete treatment feasible on each individual test event, or even on several classes of test

event. It is necessary to do the above with a single unified theoretical model, to provide the best assurance against an overlooked effect or a misunderstood transition in dominant physics.

For this reason an attempt to construct a calculation of nuclear fireball development applicable over the entire range of yield and altitude is underway. In addition to its direct utility in predictions of fireball conditions for events far from test data, the major utility of such a model is to provide predictions of the environment in which early time structure of plasma and emitters forms. This structure is believed to develop at later times into the most critical feature for many modern systems.

Nuclear fireballs develop by processes of transport of radiant and material energy. Basic to the transport is the distribution of ion species and the electron eigenstate populations within each important atomic ion, for these control both the chemical energy stored and the material opacity. The opacity in turn controls radiation transport of energy, under most conditions a most important mechanism. Therefore a requirement on a unified theoretical model is the ability to calculate atomic ion species distribution and electron eigenstate distribution within each atomic ion important either to observables affecting system performance or to radiative transport of energy.

Depending on burst conditions and the system requirements, the calculation must be reliable for times from microseconds to minutes, for temperatures from kilovolts to a few hundred degrees Kelvin, and for electron densities from, say, $10^6/\text{cm}^3$ or less to $10^{22}/\text{cm}^3$ or more. Further, it must handle radiation fields from sparse line spectra to Planckian. In particular, it must handle conditions which span the range from extreme non-thermodynamic equilibrium to local thermodynamic equilibrium.

This report describes a method developed to satisfy this need. It calculates monatomic ion species populations and electron eigenstate populations within each ion species over the above range of conditions.

SECTION 2 REQUIREMENTS

2.1 SYSTEMS.

At a level this deep in theoretical modelling the only system requirement laid on the method is that it be capable of handling chemical elements important to systems (emitters, absorbers, etc.) but not important to energy or material transport. This is simply accomplished, by allowing for mixtures of a large number of arbitrary elements to be present at any point in space. The price paid for this capability is some storage on nonvirtual memory computers and, presumably, almost nil on virtual memory machines.

2.2 PHYSICS.

Consider a chemical element immersed in a field consisting of hot ions, electrons, and photons. It is necessary to find the rate at which energy is being absorbed or emitted by this element. To do so one must know the distribution of ionization, or charge, states of the element, the distribution of electrons in the eigenstates of each charge state, and the rate of collisional and radiative processes from each eigenstate to all others. Perhaps the simplest way to think of the problem is to consider a single array of eigenstates for an element; that is, consider the ground state of the lowest charge state (neutral or negative ion) as the base state and all other states, including higher ionization states, as excited states. In fact, this has turned out to be the best way to accomplish the numerical solution. In the case of hydrogen one has

the ground state of the neutral atom, call it $H^0(1)$, and its excited states plus a single eigenstate corresponding to a bare proton, $H^1(1)$. In the case of oxygen one has, at present, the ground state of an oxygen atom with attached electron, $O^{1-}(1)$, followed by the ground state neutral, $O^0(1)$ at about an eV excitation energy, then all the excited states of O^0 , followed by all the states of O^1 , through $O^8(1)$, the bare oxygen nucleus.

The basic problem then is to find the electron distribution among eigenstates of an element. Once that is done, charge distribution, energetics, and opacity all follow easily.

The processes which act to redistribute electrons among the eigenstates include electron collisions, radiatively induced transitions, spontaneous radiation and heavy ion collisions. Heavy ion collisions are less important than the others and have been neglected, although the numerical solution is so organized that heavy ion processes can be introduced in a very straightforward manner if they ever appear to be necessary. Another restriction, which presently appears to be more important, is that di-electronic recombination and its inverse, Auger type processes, are neglected. Di-electronic recombination sometimes is the most important recombination mechanism under conditions of high electron temperature and low electron density. But under those conditions very little recombination occurs; this is the justification for reducing the complexity of the initial code version by neglecting such processes.

The processes treated are: bound-bound electron collisions (upward and downward in excitation energy), bound-free electron collisions along with the inverse three body recombination, bound-bound radiation induced transitions up and down, bound-free radiation induced transitions (ionization and recombination), and bound-bound spontaneous emission (down only).

For most rates a factor of two to three is the limit of current knowledge; for some important ones the situation is better but for many it is even worse. A factor of three error in a single rate coefficient can result in as much as a factor of three error in population, while an unfortunate coincidence involving such errors in several rate coefficients can result in even greater error in population.

Uncertainty in the correct value of rate coefficients is a fundamental limitation on accuracy of theory. In a situation as complex as this, the only satisfactory method of approach is sensitivity analysis, where the effects of modification in key rate coefficients are assessed by inserting modified values into the code and comparing results.

2.3 MATHEMATICS.

The major mathematical requirement on the method is generality, due to the extremely broad range of conditions over which the method is to be applied. This means that one is not allowed to use most normal methods designed for special limiting cases; LTE, coronal, etc., but must adopt a general method which is capable of handling both those limiting cases and intermediate cases. In short, the equations must be solved directly.

Given that important physical parameters, especially rate coefficients but also energy levels in some cases, have substantial uncertainties, the only firm mathematical accuracy requirement on the method is that it yield answers accurate to better than, say, a factor of three or so. Unfortunately it is difficult if not impossible to analyze the final effect of a mathematical approximation buried deep in such a complex set of equations as those which must be solved, so it is most unwise to allow any unnecessary inaccuracies in the math. Certainly it is almost always easier to do the math correctly than to analyze the implication of an approximation. Nevertheless it has been necessary to give up mathematical

rigor at a few points in the method to meet finite computer time requirements. The impact of such approximations on the final results have been assessed by comparison of these calculations with results obtained from more precise methods. Enough precise results are available to provide reasonable assurance of the mathematical soundness of our method.

2.4 COMPUTER.

Computer requirements are that the coded implementation of the method be transportable among mainframes, fit within memory available on a Cray-class computer and that this portion of the code require at most a few hours of CP time on such equipment to complete calculation of a fireball history.

The transportability requirement creates some tedious but straightforward limitations on code and data structure, mainly due to the fact that Crays do not have virtual memory operating systems.

The memory requirement does not appear to be limiting.

However, the CP time requirement has been the major driving force in almost every aspect of design and implementation of the method. The time allowed for any method implemented to solve the eigenstate population equations can be estimated as follows. As an average, take M eigenstates per ionization state, Z ionization states simultaneously present per element, E elements present per spacial zone, C space zones, and T time increments per problem. Then the number of eigenstate solutions necessary to complete a problem is

$$N = MZECT \quad . \quad (1)$$

A reasonable minimum number of eigenstates necessary to get a decent value of opacity is, say,

M = 10 .

It is difficult to imagine a scheme so wise that it can solve a problem without computing for 3 or 4 ionization states simultaneously present under severe conditions, but perhaps only half the space cells will have severe conditions, take

Z = 2 .

The number of elements per cell is at least 2 (N and 0) and more likely to average 3,

E = 3.

Space zones depend on the dimensionality of the problem, let D be the number of space dimensions, then C is at least 100 per dimension,

C = 10^{2D} .

Finally, one expects a problem to be completed in about a thousand time steps, so take

T = 1000.

Then

$$N = 6 \times 10^{4+2D}$$

and if the total time spent on the method is to be H hours, the time allowed per eigenstate solution is

$$t = 1.7 \times 10^{-5} \frac{3600 H}{10^{20}} = \frac{6 \times 10^{-2} H}{10^{20}} .$$

Given that H is to be of order 1, we find that for a three dimensional code

$$t = 6 \times 10^{-8} \text{ sec} .$$

This is hopeless for foreseeable equipment. To have a reasonable chance, we must limit ourselves to one space dimension so that

$$t = 6 \times 10^{-4} \text{ sec} = 0.6 \text{ msec} .$$

This translates into 12 msec to solve all eigenstates and charge states for a given element in one spacial zone per time cycle. Not much time. To date we are within a factor of two to ten of the goal, depending on the complexity of the radiation field, for the MRC ELXSI computer (a 4 to 5 MIP machine). All things being as advertised, this should place us at or better than the goal on a CRAY.

SECTION 3
METHOD ADOPTED FOR EIGENSTATE SOLUTION

3.1 SUMMARY OF METHOD.

- (a) Transition rates for all processes are calculated connecting states of Z to all eigenstates of $Z-1$, Z , and $Z+1$.
- (b) Eigenstates for all ion charge states of a given element are arranged in a linear array ordered on increasing state energy referenced to the lowest energy state of the element (ground state neutral or ground state negative ion). Call the total number of equations in this array L .
- (c) The total state array is sorted into two linear arrays, one set to be solved with a quasi-steady approximation and the other to be solved as differential equations.
- (d) These two sets of equations are each further broken down into sets of closely coupled equations, for a total of M sets, $1 \leq M \leq L$.
- (e) Each of the M sets is solved by Gauss elimination using initial conditions derived from the original linear array of length L .

- (f) Sets initially containing a major fraction of the total elemental electron population are renormalized to their initial total populations. Sets initially containing a minor fraction of the total elemental electron population are allowed major population changes, but minor changes are strongly damped.
- (g) Effective set-to-set transition rates are calculated based on individual eigenstate rates and populations.
- (h) The pair of sets with the fastest interset rate is solved as a pair of coupled differential equations for total set population, with relative eigenstate population unchanged.
- (i) The resultant sets from step (h) are amalgamated into a single set, reducing the number of sets by 1.
- (j) Steps (h) through (i) are repeated until only one set, encompassing all eigenstates of all ionization states, remains.
- (k) Because absolute normalization was lost in step (f), the final set is renormalized to conserve atomic ions.

3.2 SUMMARY OF METHOD RATIONALE.

The overriding objective in developing the method was to minimize CP time without too much loss in accuracy. The principal tactic has been to maximize allowable time step. The process consisted of recognition of a problem, curing it, recognition of problems created by the cure, curing them etc. until no new problems appeared. The result is cumbersome logically, but it is quite rugged, adequately accurate, and relatively fast in execution.

The first step is to decide how many ionization states and eigenstates per ion must be calculated. This is done before any rates are calculated. Rate calculation is expensive; the order of 10^2 rates and inverses must be calculated for each eigenstate.

All rates connecting each eigenstate of ion Z to all other eigenstates present of ions Z-1, Z, and Z+1 are then calculated.

To make it automatic that eigenstate equations in adjacent ionization states be grouped together for solution where appropriate, eigenstate data for all values of Z present are stacked in a single linear array indexed on increasing eigenenergy. This arrangement turns out to save some storage and simplify some logic, as added bonuses.

The method is required to work for situations where some or all states approach LTE. This guarantees a severe stiff differential equation problem. Stiff equations can be solved assuming them to be quasi-steady. A criterion to distinguish between stiff and "limp" behavior is straightforward; but some efficiency must be sacrificed here. We must allow equations to go from stiff to "limp" as well as from limp to stiff and unfortunately criteria which identify every stiff equation, once met, force equations to remain stiff forever. Accordingly a less efficient criterion is applied and the linear array of eigenstate equations is sorted into two arrays or sets, the QS set to be solved under a quasi-steady assumption and the DE set to be solved as ordinary differential equations.

Under circumstances of interest, normalization problems exist if the two sets are solved in a straightforward manner. Some or all of these problems were created by breaking the equations into two sets. To address these problems, each of the two sets, QS and DE, is further broken down into sets of closely coupled equations.

Each QS set is then solved by Gauss elimination separately, using initial conditions from all other sets as input, and each DE set is similarly solved separately by a different version of Gauss elimination.

The resultant set electron populations are incompatible in general, since changes in other set populations were neglected when finding eigenstate population in a given set. The basic way adopted to handle this is to renormalize each set back to its initial population, so that only the electron distribution within each set has been changed, calculate effective rates between the sets, then solve differential equations for set populations.

The situation at this point is similar to that at the beginning of the process, a number of linear differential equations for set (rather than eigenstate) populations must be solved. If we were guaranteed that the number of sets were less than the number of initial equations we could simply repeat the process (sort into QS and DE, sort into closely coupled equations, solve) iteratively until only one set, including all eigenstates, remained. Unfortunately, it is not true that under all circumstances each such iteration would reduce the number of sets.

The technique actually used is to analytically solve only for populations of the two most closely coupled sets, neglecting effects of the others. These two sets are amalgamated into a single set, rates among the reduced number of sets are adjusted and the process repeated until only one set remains.

This time splitting technique for set populations has its own version of the stiff equation problem. It is always far less severe than that of the original eigenstate set and appears only to affect sets with minor fractions of total electron population, but it is bad enough to require fixing. The fix adopted is empirical rather than rigorous and is

targeted against the specific problem encountered. Because the time splitting scheme locks set populations together by pairs, a low population set strongly influenced by two high population sets and requiring a major population adjustment can become locked into a position where the adjustment is impossible. To avoid this eventuality, at the end of the Gauss elimination procedure, the Gauss answer for set population is accepted for minor population sets with major population changes, but all sets with major population are renormalized as are minor population sets with minor population changes.

With this modification the process of sorting equations into sets, solving for relative populations within the sets by Gauss elimination, then solving for set population by time splitting works adequately. It is only necessary to add a final, overall, normalization since we have allowed the absolute normalization to be broken occasionally after the Gauss elimination step.

3.3 MAJOR ELEMENTS OF THE METHOD.

3.3.1 Adding Ionization States.

A time cycle begins for some chemical element with one or more contiguous ionization states, Z , present, and with a distribution of electrons in their eigenstates. Circumstances may require addition of another state of ionization one unit charge above the highest present or one unit below the lowest present. In preparation for this, an ion state above the highest and one below the lowest present are added without populations, if such ion states exist for the element. At this point the maximum number of charge states which may possibly be considered has been determined.

3.3.2 Deleting Ionization States.

It is important to avoid calculating and processing unnecessary rates, to save time. Before any rates are calculated, "temperatures" are defined for all processes which might control creation or destruction of charge states. At present there are three such temperatures, one is electron temperature, one is the temperature of that Planck spectrum which contains the same total radiant flux as the actual (line or continuum) spectrum, and one is that of a grey body spectrum with the same mean photon energy as the actual spectrum.

The highest density ion species, $D(Z_m)$, is then determined.

To eliminate the lowest state of ionization, Z , the equilibrium ratio, R_e , of Z to $Z+1$ is estimated using the coldest of the three temperatures, then it must be true that both

$$D(Z) < r D(Z_m)$$

and either

$$D(Z+1) < f D(Z_m) \quad (2)$$

or

$$R_e < R_q$$

where the current value of r is 10^{-3} and f is currently 0.1 if $D(Z)=0$ or 0.05 if $D(Z)$ is nonzero (to make it more difficult to eliminate an existing ion state than one just added). The value of R_q used is 10^{-5} .

If an ion state is eliminated, its density is added to $Z+1$ (without modifying eigenstate distribution in $Z+1$) and the process repeated until the test (2) fails.

To eliminate the highest state of ionization, Z , the equilibrium ratio, R_e , of Z to $Z-1$ is estimated using the hottest of the three temperatures and the sequence of tests (2) applied to it. Again this test is repeated until it fails.

At this point only those ion states with significant populations, plus those which may gain significant populations in this cycle are present.

3.3.3 Adding an Artificial Eigenstate.

There are two reasons for limiting the number of eigenstates per ionization state to about 10, which implies principal quantum number limited to 3 or 4. The first reason is that reliable data is generally very incomplete at higher quantum numbers for elements of interest so that a more complete representation would be interspersed liberally with either gaps or guesswork. The second reason is that CP restrictions do not allow a large number of eigenstates to be represented. The number of state-to-state rate coefficients which must be calculated is proportional to the square of the number of states represented, and time spent in the Gauss elimination routine is proportional to the cube of the number of states.

Nevertheless, there may be tens to thousands of eigenstates between the uppermost state represented and the ionization continuum. The higher states must be taken into account if correct ionization and recombination rates to the interesting lower states are to be obtained. This is accomplished by creating an artificial eigenstate to represent the upper states not modeled.

To create such a state one first finds the number of states lying between the uppermost state modeled and the ionization continuum. This is determined by the amount by which the ionization potential is depressed due to polarization effects of the plasma. From reference 1, pp. 137-140, the energy of this depression is roughly

$$E_D = (Z+1) e^2 / \rho_D \quad (3)$$

where Z is the degree of ionization, e (esu) is electron charge, and ρ_D is Debye length,

$$\rho_D = [kT/(4\pi e^2 N_e (1 + \langle Z^2 \rangle / \langle Z \rangle))]^{1/2} \quad (4)$$

with k Boltzmann's constant, T the electron temperature, and N_e electron density.

Assuming the upper levels to be hydrogenic, the principal quantum number of the level which lies at the ionization continuum is given by

$$E_H (Z+1)^2 / S_M^2 = E_D \quad (5)$$

or

$$S_M = (Z+1) \sqrt{E_H / E_D} \quad .$$

where E_H is the ionization potential of hydrogen in vacuo. States above S_M are ignored. If the principal quantum number of the highest energy state represented is S_N , then the artificial state must represent all states from S_N to S_M .

Parameters to represent the artificial state must be calculated. The basic parameters are calculated as simple integrals weighted

by the degeneracy of the upper states. For hydrogenic states the degeneracy of a state with principal quantum number n is

$$g_n = 2n^2 . \quad (6)$$

Then the degeneracy of the artificial state, g_A , is the sum of degeneracies of its constituents multiplied by the degeneracy of the ground state of the next higher state of ionization,

$$g_A = g_{Z+1} \int 2n^2 dn = \frac{2}{3} (S_M^3 - S_N^3) (2S_+ + 1) (2L_+ + 1) \quad (7)$$

where S_+ is the spin quantum number of the ground state of $Z+1$ and L_+ is the orbital quantum number of $Z+1$.

The mean energy of the artificial state, E_A , is

$$\begin{aligned} E_A &= V \int (1 - Q^2/n^2) 2n^2 dn / \int 2n^2 dn \\ &= V (1 - 3Q^2 (S_M^3 - S_N^3) / (S_M^3 - S_N^3)) \end{aligned} \quad (8)$$

where V is the vacuum ionization potential of the ground state ion Z and Q is the ground state of Z principal quantum number. The factor Q^2 scales the ionization potential, V , to its equivalent hydrogenic value.

Similarly, the mean principal quantum number of the artificial state, Q_A , is given by

$$Q_A = \int n^2 n^2 dn / \int 2n^2 dn = \frac{3}{4} (S_M^4 - S_N^4) / (S_M^3 - S_N^3) . \quad (9)$$

Parameters for Stark broadening and for rate coefficient calculations must also be generated. The Stark broadening term for the state

is estimated from the lead term in equation (46) and the crucial oscillation strength calculations are discussed in section 5.7.2.

3.3.4 Deleting Eigenstates.

3.3.4.1 Before Calculations Commence. In a situation where the hottest effective temperature (see 3.3.2) is small compared to the excitation energy of some eigenstate it may be appropriate to save some calculation time by neglecting that eigenstate. Accordingly, after unnecessary ions have been removed as described in section 3.3.2 the three following tests are made, from highest excitation state for which data exists to the ground state of the highest ionization state present.

Is the equilibrium ratio of ion $Z+1$ to ion Z greater than about 10^{-5} ?

Is the fractional population of eigenstate s greater than 10^{-3} ?

Is the energy of state s less than ten times the hottest temperature?

If any of the three tests is met, then eigenstate s and all lower eigenstates are accepted. If all tests fail, s is deleted and the tests are applied to $s-1$.

The principal virtue of this procedure is to eliminate upper states from consideration under benign conditions. For example, undisturbed cells at the beginning of a problem, or material late in a problem which has recombined and fallen to the ground state.

3.3.4.2 During Calculations. If the value of E_0 from (3) is so large that the energy from some states s , E_s , satisfies

$$E_s > V - E_D \quad (10)$$

then these states are removed.

There are two physics problems associated with this procedure. The minor one is that all eigenstates lying above the effective ionization potential

$$A \equiv V - E_D \quad (11)$$

still exist, even though they lie above the ground state of $Z+1$. In principle, account should be taken of these states. One straightforward procedure might be to add the combined oscillator strength to these states from state s to that from state s to the ground state of $Z+1$, on the assumption that electrons raised to states above the ground state of $Z+1$ will be lost (of course, they might even lie above some excited state of $Z+1$, to complicate matters). A procedure such as this has not been implemented because the numerical effect doesn't seem important under conditions where our treatment is credible and more serious problems exist where the treatment becomes questionable due to the second physics problem, as follows.

If electrons become so closely packed that their Debye spheres begin to overlap (at 1-eV this would be $N_e \geq 10^{20}$) the potential energy wells of neighboring ions begin to overlap; the plasma begins to show liquid or solid properties! The concept of an isolated ionic system of eigenstates begins to fail, electrons no longer have all space available for orbits, they must find channels between ions. We have not addressed this problem and hope never to be required to do so.

What has been done is entirely ad hoc. The last 4 eigenstates are retained independent of the outcome of the three tests discussed in the foregoing.

3.3.5 Stiff Equation Problem.

To find the populations of all M eigenstates of (all ionization states of) some element, the solution is required to the set of equations:

$$\frac{dN_s}{dt} = T_s + \sum_{k=1}^M \alpha_{ks} N_k - N_s \left[\sum_{k=1}^M \alpha_{sk} + B_s \right] \quad (12)$$

for s from 1 to M .

In (12), all terms are inherently non negative, α_{ij} is the rate of transfer from state i to state j due to all causes, per unit population of state i and per unit time, N_j is population of state i and the terms T_s and B_s refer to sources and sinks of population outside the set of M equations.

Equation sets like (12) are infamous for having so called "stiff" equation difficulties when any straightforward method of solution is applied. This occurs whenever for some value of s , the input terms tend to cancel the output terms, driving the time step toward zero while N_s is, in fact, nearly constant in time. In our case such a problem is guaranteed since we wish to handle cases where equilibrium is approached, where the inputs and outputs effectively cancel for all s . Given that a one dimensional radiation transport problem will typically consist of thousands of radiation and hydro time steps, hundreds of cells, and several elements per cell (N, O , etc.) with perhaps 40 eigenstates per element (say 10 states each for 4 ionization states), a stiff equation problem would be catastrophic.

To avoid stiff equation difficulties the M equations are sorted into a set of "Quasi-steady" equations (hereafter referred to as "QS") and a set of "Differential" equations (hereafter referred to as "DE") which are treated separately. This separation is currently based on the condition:

$$\Delta t \sum_{k=1}^M \alpha_{sk} > G \quad (13)$$

where Δt is the time step, arbitrary for purposes of this test, and G is some sizable number; $G = e^3 = 20.1$ is the value currently in use, but the precise value of G does not appear to be critical.

This test is made independently each time the set is to be advanced, so a given equation is able to be advanced as QS or DE as appropriate to current conditions; no equation becomes frozen into one mode or the other.

3.3.6 Normalization Problems.

Three classes of normalization problems arise when solving these equations by the chosen method.

3.3.6.1 Inherent Numerics Problem. The first class of normalization problems is inherent in eq (12). To demonstrate it, sum (12) over all s to obtain

$$d(\sum N_s)/dt = \sum T_s - \sum N_s B_s \quad (14)$$

where the terms containing α 's have cancelled. If the set were isolated as it would have been had we not separated the equations into two classes, then T_s and B_s would be zero for all s and, ideally, $\sum N_s$ would be constant. Almost any method of numerical solution will lose this precision but that is easy to correct; simply sum N_s before and after solution then multiply the new values by the ratio to force conservation of total number.

3.3.6.2 Set Separation Problem. The second class of normalization problem is caused by separation of the equations into sets to be treated differently. Now T_s and B_s are no longer zero in general. It becomes possible to lose or gain population excessively from one set to another. The problem is even deeper than it appears, for it is not only possible but fairly common for a subset of DE equations to be coupled more tightly to some subset of QS equations than it is to the remaining DEs, and the reverse also occurs. So it is not necessarily true that a common normalization factor, however derived, will be appropriate to all DEs or all QSs.

After the separation into DE and QS a further separation into subsets is made to locate equations which are significantly more closely coupled to each other than to others. The precise method for accomplishing this is discussed in section 3.3.7.

Depending on circumstances, and the separation algorithm, after this process there are a number of distinct equation sets which may vary from 1 (all are DE or all are QS and all are reasonably coupled together) to M (none tightly coupled to another in the same class). The next step in the solution is to collect the terms in equation (12) for each subset. T_s and B_s thus are constructed from $N_{k'} x_{k'}$ and $t_{sk'}$.

$$T_s = \sum_{k'} N_{k'} x_{k'}, \quad B_s = \sum_{k'} t_{sk'} \quad (15)$$

where k' does not belong to the set to which s belongs. After solution, most sets are renormalized to a value such that total population within the set is close to its original value (see section 3.3.8). Thus the step mainly redistributes electrons among the eigenstates of the subset, without allowing the total population of the subset to change.

Next, effective α 's are constructed connecting each set m to all other sets n

$$\alpha_{nm} = \sum_s N_s \sum_k \alpha_{sk} / \sum_s N_s \quad (16)$$

where s belongs to set n and k belongs to set m .

Then values of n' and m' are found for which $\alpha_{n'm'} + \alpha_{m'n'}$ is a maximum. These two sets are then solved as a differential equation independent of all other sets.

$$\dot{N}_n = \alpha_{mn} N_m - \alpha_{nm} N_n$$

$$\dot{N}_m = \alpha_{nm} N_n - \alpha_{mn} N_m$$

$$N_n(t+\Delta t) = N_n(t)E + T\alpha_{mn}/(\alpha_{nm} + \alpha_{mn})(1-E) \quad (17)$$

where

$$E \equiv \exp [-(\alpha_{nm} + \alpha_{mn}) \Delta t]$$

$$T \equiv N_n(t) + N_m(t)$$

This solution preserves normalization and finds a new value for the relative populations of eigenstates in the sets n' and m' .

Sets n' and m' are then amalgamated into a single set, set-to-set α 's readjusted, and the process repeated until only one set, comprising all eigenstates, remains. The solution is then complete.

This rather peculiar form of time splitting has the advantage of giving priority to the fastest reactions and of approaching the correct steady state solution. However, if Δt is too large, it will approach the steady state solution too slowly; its behavior is similar to an implicit difference scheme in this respect.

3.3.6.3 Gauss Elimination Problem. The third and final class of normalization problems arises from the particular method chosen to solve each subset of equations, that of Gaussian elimination (see section 3.3.9 for rationale and form of implementation). For present purposes, the important feature of Gaussian elimination is that the equations are formulated in such a way as to eliminate the derivative in eq (12). Then eq (14) takes the form

$$\Sigma T_s = \Sigma N_s B_s \quad (18)$$

and (18) is the only normalization condition. If T_s is large and B_s is small compared to some weighting of the α 's in (12), then the total population of the set may increase by orders of magnitude. If B_s is large and T_s small, the total population may decrease by orders of magnitude. If, as is always the case when populations approach steady state, both T_s and B_s are small, then the equation set approaches indeterminacy and N_s approaches zero for all s .

To avoid this problem, T_s is compared to the bound-bound input terms for that state of the set with the largest population, s' ,

$$T_{s'} < \epsilon \sum_k \alpha_{ks'} N_k \quad ? \quad (19)$$

and B_s is compared to bound-bound output terms,

$$\sum_k \alpha_{s'k} < \epsilon B_s \quad ? \quad (20)$$

If either test fails then the state s' is removed from the set, held constant, and becomes a source and sink of electrons for the remaining members of the set, so that they will have appropriate values of T_s , B_s .

The current value of ϵ is 10^{-6} but the precise value is not crucial.

3.3.7 Sorting Algorithm.

The sorting algorithm currently in use is applied separately to DE and QS, potentially breaking each of these major groupings into smaller sets of equations.

The first requirement is that all members of a set be contiguous in index, which is equivalent to being contiguous in energy since the indexing system for eigenstates runs from low energy states to high. This condition produces some unnecessary sets occasionally but prevents the possibility of, say, including the ground states of two ions in a single set relegating the excited states connecting them to another set. Should such a situation occur, the intermediate states may not be able to come to the correct configuration since they will be unable to alter the ratio between the two ground states.

The second condition for membership of state i in a set is applied only to QS equations. It requires that for some member j of the set,

$$(\alpha_{ij} + \alpha_{ji}) \Delta t > G \quad . \quad (21)$$

This test is similar to that of (13) and the same value of G is currently used. The difference is that it insists that state i meet the QS test for some individual state j in the set, rather than that i meet the

test globally through the sum of α_{ij} over all j . It prevents the possibility of i being QS with respect to some member outside the set but not to members of the set. An example is the upper state of charge state Z being QS because it is coupled tightly to the ground state of $Z+1$, which may be handled as a differential equation, and upper state of Z not coupled as tightly to any other state.

The final criterian applies to both DE and QS. It is that for state i to be included in the set, it must be true that for some state j in the set either

$$\alpha_{ij} \geq \alpha_{ik} \text{ for all } k \text{ (where } k \text{ can be DE or QS)}$$

or

$$\alpha_{ji} \geq \alpha_{jk} \text{ for all } k.$$

That is, the transition rate from i to some member of the set must be the largest transition rate out of i , or the transition rate from some member of the set to i must be its largest transition rate.

These criteria sound quite restrictive and may, in fact, be overdone. However, because of the tendency of eigenstates to transfer most rapidly to an adjacent state, the results of application are not as restrictive in practice as might seem to be the case. Breakpoints in sets typically occur where one wants them, at states with dipole forbidden transitions to neighbors and between states for which data exists and the artificial uppermost state of an ion.

When electron density is very low a situation occurs where the largest rate for many excited states is spontaneous emission to the ground state. Then most sets consist of a single state which is advanced by the time splitting method described in 3.3.6.2. No problem ensues, not even a noticeable penalty in CP time, for in this situation the equations have benign behavior and the time splitting technique is faster than Gauss elimination, the method used to redistribute population within a set.

3.3.8 Freezing Problem.

The elements of the method for solution can be summarized as follows. In order to avoid stiff differential equation problems the equations for eigenstate population were broken into two sets, one set of stiff equations (QS) for which solution methods exist and another set of limp equations (DE) for which other methods of solution exist. However, the best methods we have found are imperfect. To counter these imperfections the equations may be further sorted into smaller sets.

Now what we would like to do in the interest of simplicity and cleanliness of logic is redistribute eigenstate populations within each of the final sets as influenced by initial conditions of all other sets; then renormalize the population of each set to its initial value to prevent an instability due to overcorrection; and finally to adjust the relative set populations with the time splitting technique. This approach works well for almost all situations but fails in situations similar to the following.

Suppose ion $Z+1$ is recombining to ion Z . Also suppose equation set A consists of the lowest states of $Z+1$ and perhaps the highest states of Z and is highly populated. Set A is rapidly feeding electrons into set B, the intermediate states of Z . Set B has a small population despite the electrons received from A because it rapidly feeds them downward to set C, the lower lying states of Z . Set C is also highly populated. Further, suppose set B is currently some how underpopulated. Situations similar to this are common for either recombination or ionization. They present a choice between: (i) a stiff equation problem where the time step is controlled by insisting that the population of the low population set B not change too much in a cycle or (ii) a stability problem where the population of set B fluctuates wildly while sloshing electrons erratically between sets A and C.

Application of our desired method can, under exceptionally unlucky circumstances, proceed as follows if the time step is chosen to be appropriate to the A to C transfer, as one would wish, rather than the much smaller time step appropriate for B from A or B to C.

First, the sets are solved independently using initial conditions. This results in an appropriately modest depletion of set A, an enormous relative net increase in population of B (since it was assumed underpopulated - it gains more from A than it loses to C and both the gain and loss are very large compared to the population of B because of the large time step), and a negligible increase in the population of C (essentially equal to the too low initial population of B).

The next step of the method renormalizes all three sets back to their original population, nipping this incipient instability in the bud. The result is redistributed eigenstate populations within each set but initial total set populations.

Now the method looks at the effective set-to-set transition rates and picks out the maximum, say it is B to C. New B and C populations are then found from (17); if the time step is as large as assumed it is likely that B and C will come to the steady state ratio they would have if state A weren't present, which keeps set B population below its correct value, and, since B started with too low a value, not enough electrons have been transferred to C. Sets B and C are then combined into a set (B,C) with relative B to C population frozen. New rates are calculated between A and the combined sets (B,C) and finally the two sets A and (B,C) solved with (17).

To the degree that electrons are properly distributed in all three sets the result is that A is correctly depleted, C is correctly enhanced except for the incorrect sharing of electrons between B and C

(minor because B has low population), and B is left with a population frozen at too low a value with no way to build it up to the proper value. In fact, because the population of B is kept too small, the electrons in B will be incorrectly distributed and, to some extent this is also true for A and C so neither the set populations, the electron distributions nor the rates will be quite right.

There are two mathematically sound ways to cure this sort of problem, (i) reduce the time step to a value which produces a small relative change in set B population from both A to B and B to C transitions and (ii) elaborate (17) to handle three sets simultaneously. The former is unacceptable because of CP time restrictions and the latter has not been tried because there is no guarantee that a more elaborate 4 or 5 set problem would not occur.

What has been done instead is an empirical reduction in the degree of renormalization of small population sets after the initial solution. The problem only occurs for sets with small population and would not exist if such sets were not renormalized after the initial solution for electron distribution within the set. Therefore the renormalization procedure is modified to the following:

- (1) The renormalization factor, R, is calculated for the set
- (2) If the set population is larger than some fraction, f , of the total element (all Zs) population, renormalize. The present value of f is 1/3.
- (3) If the set population is less than f then replace R by the function

$$R' = Ra + 1 - a \quad (22)$$

and renormalize using R' .

The function a is given by

$$a = \exp(|2-R-1/R|) \quad (23)$$

From (23) one sees that for $R \gg 1$ or $R \ll 1$ the function a approaches zero and R' therefore approaches 1. In this case almost no renormalization takes place, the modified value of set population is accepted, allowing low population sets to approach their proper population. On the other hand, when R' is near unity, a approaches unity faster than R and renormalization is accepted, preventing oscillation about the correct value.

The approach is inelegant but yields good answers without significant penalty in wasted CP time.

3.3.9 Gauss Elimination.

3.3.9.1 Quasi-Steady Equations. In the quasi-steady approximation the derivative in (12) is small compared to other terms and is neglected. The set of equations reduces to a set of linear algebraic equations for $1 \leq s \leq m$,

$$N_s(S_{s,m} + B_s) = T_s + I_{s,m} \quad (24)$$

where for convenience we have defined the bound-bound output term

$$S_{s,m} \equiv \sum_{k=1}^m \alpha_{sk} \quad , \quad \alpha_{s,s} = 0 \quad (25)$$

and the bound-bound input term

$$I_{s,m} = \sum_{k=1}^m N_k a_{ks} , \quad a_{s,s} = 0 \quad (26)$$

There are at least three standard approaches to solution of the set (24): determinants, iteration, and Gauss elimination. Both determinants and Gauss elimination are quite sensitive to round off errors so our initial choice was iteration despite the fact that it is reputed to be the slowest of the three methods. The allegation was amply verified by our experience and eventually we were driven to Gauss elimination.

The advantage of Gauss elimination is that it is faster than iteration. Its advantage relative to the method of determinants is that it was easier to analyze its sensitivity to round off problems. In fact, we were able to devise a modification of the technique which completely eliminates this problem for equation systems like (24).

To see how to do this consider the mechanics of Gauss elimination. Initially one has the m equations (24) in m unknowns, N_s . The set is reduced to $m-1$ equations in $m-1$ unknowns by substituting the m^{th} equation into all the others, then to $m-2$ equations in $m-2$ unknowns by substituting the $m-1$ equation into the remainder, etc., until only one equation in one unknown (N_1) remains. This can be solved. Then N_1 is substituted to find N_2 etc., until all N_s are found.

Given that all terms of (24) are nonnegative as is our case, the only way to produce a serious round off error is by some step which requires a subtraction. This occurs when substituting the m^{th} equation into any equation s as follows.

Write the equations for N_s and N_m in the form

$$N_s(S_{s,m} + B_s) = T_s + I_{s,m-1} + \alpha_{m,s} N_m \quad (27)$$

$$N_m(S_{m,m} + B_m) = T_m + I_{m,s-1} + \alpha_{s,m} N_s + I_{s+1,m-1} \quad (28)$$

The subscript $m-1$ is allowed on the last term because $\alpha_{m,m} = 0$. Now substitute (28) into (27) and collect terms to yield an equation of the same form as (24)

$$N_s(S'_{s,m-1} + B'_s) = T'_s + I'_{s,m-1} \quad (29)$$

where

$$T'_s = T_s + \alpha_{m,s} T_m / (S_{m,m} + B_m) \quad (30)$$

$$I'_{s,m-1} = \sum_{k=1}^{m-1} N_k \alpha'_{ks} \quad (31)$$

$$\alpha'_{ks} = \alpha_{ks} + \alpha_{m,s} \alpha_{km} / (S_{m,m} + B_m) \quad k \neq s \quad (32)$$

and the multiplier of N_s is

$$S'_{s,m-1} + B'_s = S_{s,m-1} + \alpha_{sm} + B_s - \alpha_{ms} \alpha_{sm} / (S_{m,m} + B_m) \quad (33)$$

Equation (29) has the same form as the original (24) but with m index reduced by unity, as was described. The problem is that the single subtraction, in (33), will sometimes nearly cancel the multiplier of N_s for some values of s . Very bad answers result when this occurs.

However, further study of (33) shows that the subtraction can be eliminated. Look more closely at the second and fourth terms on the RHS of (33)

$$\begin{aligned}
 \alpha_{sm} &= \alpha_{ms} \alpha_{sm} / (S_{m,m} + B_m) \\
 &= \alpha_{sm} (S_{m,m} + B_m - \alpha_{ms}) / (S_{m,m} + B_m) \\
 &= \alpha_{sm} (S_{m,s-1} + \alpha_{ms} + S_{m,s+1} + B_m - \alpha_{ms}) / (S_{m,m} + B_m) . \quad (34)
 \end{aligned}$$

The only subtraction cancels!

In fact, we can use the same modification of α as in (32) to find

$$S'_{s,m-1} = \sum_{k=1}^{m-1} \alpha'_{s,k} \quad (35)$$

and define

$$B'_s = B_s + \alpha_{sm} B_m / (S_{m,m} + B_m) \quad (36)$$

and Eq. (29) has the proper form with no subtractions. Accordingly no round off problem exists until the number of equations approaches the biggest integer which can be represented by the computer word length (10^7 for the smallest modern machines), or perhaps the square of the biggest integer (10^{14}).

Indeed, back substitution of answers into the original equations, when m is around 40, show discrepancies of at most the last three bits for a 32 bit word.

3.3.9.2 Differential Equations. Eq. (12) can be converted to a simple first order difference scheme by substituting

$$dN_s/dt = (N_s(t+\Delta t) - N_s(t))/\Delta t \quad (37)$$

Then (12) can be written

$$N_s(t+\Delta t) (S'_{s,m} + B'_s) = T'_s + I'_{s,m} \quad (38)$$

which is identical in form to (24), if we define

$$\alpha'_{k,s} \equiv \Delta t \alpha_{ks}$$

$$S'_{s,m} \equiv \sum_{k=1}^m \alpha'_{s,k}$$

$$B'_s \equiv \Delta t B_s$$

$$T'_s \equiv N_s(t) + \Delta t T_s$$

$$I'_{s,m} = \sum N_k \alpha'_{ks} \quad (39)$$

Having done this, the same Gauss elimination routine as was used for quasi-steady equations can be used to obtain a first order implicit solution for differential equations.

SECTION 4

RADIATION SPECTRUM AND LINE SHAPE

4.1 NOMENCLATURE.

One speaks of "lines" meaning spectral emission or absorption features as well as energy quanta absorbed from the spectrum or emitted to the spectrum by an ion. When translated into Fortran such usage can be very confusing. Therefore in the following, the radiation spectrum represented by a set of numbers denoting frequencies, energy flux, etc. has no lines. It has "features." A "line" will be associated with an atom or ion, it refers to energy quanta absorbed from the radiation field or emitted to that field associated with transitions among electronic eigenstates.

4.2 SPECTRAL FEATURES.

The convention adopted is to represent the radiation field as being composed of a number of spectral "features," hopefully less than 100 of them in a real problem, although 1000 are allowed. Each feature is defined by four parameters; its central energy, v_f (eV), its central, or core intensity, U_C (erg/cm²/sec/eV) or (erg/cm²/sec/eV/sr), its core half width, W_f (eV), and a parameter denoting the strength of its tail, U_T (erg-eV/cm²/sec) or (erg-eV/cm²/sec/sr). The feature intensity is calculated from parameters as

$$U = \begin{cases} U_C & \text{if } |v - v_f| \leq W_f \\ U_T / (v - v_f)^2 & \text{if } |v - v_f| > W_f \end{cases} \quad (40)$$

In addition to these four parameters there are three rules of logic: (1) each feature is associated with a "level", level 1 feature parameters are stored first, followed by level 2, etc. Levels are distinguished on the basis of core width; roughly speaking, core width should become narrower by at least about a factor of four when the level increases. That is, higher levels represent narrow features superimposed on broader ones, (2) within a given level, features are stored sequentially on the basis of central energy, v_f , (3) level 1 represents the continuum; its features have $U_T = 0$. There are 9 levels allowed. There is no limit on the number of features allowed in each level, only on the total number of features. The logic at present requires at least one feature to be in level 1, although its intensity may be zero.

The system is believed capable of representing a radiation field to any desired degree of accuracy needed for energy transport and the associated problem of eigenstate population as well as output spectrum for systems analysis and data comparison.

4.3 LINES.

Atomic (ionic) lines are also modeled with four parameters, representing a Doppler broadened line core with Lorentzian wings. The parameters are central energy, v_L (eV), Lorentzian central cross section σ_L (cm²), Lorentzian half width, W_L (eV), and the Doppler width to Lorentzian width ratio, x .

$$W = W_L \sqrt{\pi + x^2}$$

$$\sigma_C = \sigma_L / \sqrt{1 + x^2 / \pi}$$

$$x_C = \begin{cases} 2.490606 + 0.539095 \times 1.65668 & , \quad x \leq 4 \\ 1.74623 \times 1.08419 & , \quad x > 4 \end{cases} \quad (41)$$

then

$$\sigma(v) = \begin{cases} \sigma_C \exp [-(v - v_L)^2 / W^2] , & \frac{|v - v_L|}{W_L} \leq x_C \\ \frac{\sigma_L}{1 + (v - v_L)^2 / W_L^2} , & \frac{|v - v_L|}{W_L} > x_C \end{cases} \quad (42)$$

This representation gives the correct central cross section and the correct cross section in the far wing always. For x less than about 3 it has a maximum error, as compared to the more correct Voight profile, of under 30 percent, occurring at the transition point, x_C . When $x > 3$, the error, an underestimate of cross section, becomes worse, but when $x > 3$, the wing portion is less than 10^{-4} of the center so this error cannot seriously affect any overlap integral, thus cannot seriously affect any rate.

4.4 LINE WIDTHS.

The Doppler width of a line is given by

$$w_D = v_L / c \sqrt{2 \theta_i / M} \quad (43)$$

where c is light speed in vacuo, θ_i is heavy ion temperature, and M is heavy ion mass.

The Lorentzian width is the sum of widths of the two eigenstates involved in the transition. For each of these states, width is

$$W_L = 4\pi/\Gamma \quad (44)$$

where Γ is the effective lifetime of the state of ion Z against all forms of decay, plus thermal electron induced Stark broadening, Γ_S .

$$\Gamma = \Gamma_S + \Gamma_{SP} + \Gamma_{EB} + \Gamma_{EF} + \Gamma_{ER} + \Gamma_{PF} + \Gamma_{PR} + \Gamma_{PB} \quad (45)$$

where Γ_{SP} is spontaneous emission rate to all lower states of Z , Γ_{EB} is electron collisional bound-bound rate to all states of Z , Γ_{EF} is electron collisional ionization rate to all states of $Z+1$, Γ_{ER} is electron three-body recombination rate to all states of $Z-1$, Γ_{PF} is photo ionization rate to all states of $Z+1$, Γ_{PR} is radiative recombination rate to all states of $Z-1$, and Γ_{PB} is bound-bound photo induced transition rate to all states of Z .

These rates are calculated in the order shown in (45), from left to right, because the rates become increasingly sensitive to state width from left to right. In principle one should iterate (45) to obtain a self consistent state width. In practice, the bound-bound photo transition rate is the most sensitive to width; if Γ_{PB} changes Γ by as much as 25%, that one contribution is iterated.

The method for calculating each of these rates is described in the following section 5.

SECTION 5 RATES

In the following discussion the convention is adopted that the parenthetical expression (a,b) means "from a to b."

5.1 STARK WIDTH.

The net effect of Stark shifts due to bombarding thermal electrons is to broaden eigenstate energy. This process does not cause transitions between states but, because its effect on line width is similar, it is discussed here. To a first approximation Stark broadening is not dependent on state width, so it is appropriate to calculate it before other contributions to state width have been evaluated.

A formula for thermal electron Stark broadening, Γ_s , is given in eq (526) of Ref. 2. This formula can be fit within a few percent over the interesting range of electron temperature, θ , by

$$\Gamma_s = W_s N_e / \sqrt{\theta} [1 + r/(A_s + r) + C_s \theta^{p_s}] \quad (46)$$

where r is the ratio of θ to the Rydberg (13.6 eV) and W_s , A_s , C_s , and p_s are parameters adjusted to give a best fit to Griem's formula for each eigenstate. These parameters are derived at the time eigenstate data is collected and treated as eigenstate data (see section 6).

5.2 SPONTANEOUS EMISSION.

Spontaneous emission is also insensitive to state width and is the second contribution to state width, the first actual transition rate, calculated. From Ref. 3., p. 58, the spontaneous radiative transition rate from upper state k to lower state ℓ is

$$r_{sp}(k, \ell) = (8\pi^2 e^2 v^2) / (mc^3) (g_\ell / g_k) f_{\ell k} \quad (47)$$

in c.g.s. units. In (47), r_{sp} is in units of sec^{-1} , e (e.s.u.) is electron charge, $m(g)$ is electron mass, c (cm/sec) is lightspeed, the g 's are state degeneracies and $f_{\ell k}$ is the oscillator strength from state ℓ to state k . In more convenient units (47) becomes

$$r_{sp}(k, \ell) = A_r (E_k - E_\ell)^2 (g_\ell / g_k) f_{\ell k} \quad (48)$$

where the E 's (eV) are state energies and

$$A_r = 4.33927 \times 10^7 \text{ eV}^{-2} \text{ sec}^{-1} \quad (49)$$

5.3 ELECTRON BOUND-BOUND COLLISIONS.

Burgess (Ref. 4) gives a formula for electron collision cross section from lower state ℓ to upper state k as

$$\sigma_{\ell k} (\text{cm}^2) = A R_y^2 \bar{g} f_{\ell k} / [E(E_k - E_\ell)] \quad , \quad E > E_k - E_\ell \quad (50)$$

where $A = 1.28 \times 10^{-15} \text{ cm}^2$, R_y is the Rydberg, \bar{g} is the Gaunt factor, $f_{\ell k}$ is the oscillator strength, E is electron energy and E_k , E_ℓ are the state energies

To convert (50) into a rate for electrons at temperature θ one multiplies by electron velocity then averages over a Boltzmann distribution to obtain

$$r_{EB}(\ell, k) = C_{EC} f_{\ell k} / [(\theta^{1/2}(E_k - E_\ell))] \exp(-(E_k - E_\ell)/\theta) \quad (51)$$

$$C_{EC} = 6 \times 10^{-6} \text{ eV}^{3/2} \text{ sec}^{-1}$$

where \overline{g} was taken to be 0.4 and θ and E are in units of eV.

By detailed balance, the downward rate from k to ℓ is

$$r_{EB}(k, \ell) = C_{EC} f_{\ell k} g_\ell / [g_k \theta^{1/2} (E_k - E_\ell)] \quad (52)$$

5.4 ELECTRON BOUND-FREE COLLISIONS AND THREE BODY RECOMBINATION.

In Ref. 6., Lotz gives a general formula along with necessary parameters which gives a good fit to measured electron collisional ionization cross sections and rate coefficients for any atom or ion in the lower portion of the periodic table. His fit is based on the ratio

$$x = \Delta E / \theta \quad (53)$$

where ΔE is change in energy, ground state Z to ground state $Z+1$. He suggests that ionization rates from excited states be approximated by simply substituting the appropriate value of ΔE . We have adopted this suggestion and generalized it to include excited states of $Z+1$ as well.

For our application, his formula can be well fit to the simpler formula

$$r_{EF}(k, p) = (A_L / \theta^{3/2}) N_e E_1(x) / x^{P_L} \quad , \quad (54)$$

where

$$x = (E_p + V_a - E_k) / \theta \quad , \quad (55)$$

θ is electron temperature, N_e electron density, E_1 the first order exponential integral, E_p and E_k are state energies in $Z+1$ and Z respectively. V_a is the effective ionization energy of Z , and A_L and P_L are parameters fit to Lotz's formula for ion Z . These parameters are derived by comparing the sum of (54) over p to the Lotz formula for state k of Z .

It is easy to criticize this procedure but criticism can be readily countered by comparison of the formula to data except for the generalization to excited states of $Z+1$ (for which there is no data). That criticism must be countered by a challenge to find a better formula, coupled with the observation that ionization rates to excited states of $Z+1$ are almost always too low to control state populations.

The reverse reaction, three-body recombination, can be derived from r_{EF} by use of the principle of detailed balance, which yields

$$r_{EB}(p, k) = [N_e g_k \exp(x)] / [Q_e \theta^{3/2} g_p] r_{EF}(k, p) \quad (56)$$

$$Q_e = 6.037 \times 10^{21} \text{ eV}^{-3/2} \text{ cm}^3$$

where g_k and g_p are statistical weights and Q_e is the partition function of a free electron at 1-eV temperature.

5.4.1 Contribution from Eigenstates Above the Continuum.

The quantity V_a in (55) is the ionization potential depressed by polarization effects of the plasma. In all our formulae, states which lie above V_a are neglected. But these eigenstates still exist and the oscillator strength to them still exists so they may possibly have some influence. To evaluate the magnitude of influence of such states we constructed and implemented a simple model. It goes as follows. The infinite number of eigenstates which lie between V_a and the vacuum ionization potential, V , all lie above the ground state energy of ion state $Z+1$, in most cases extremely close to this ground state. So assume any bound-bound electron collision to one of these states to be instantly followed by another collision which frees the electron, resulting in a ground state $Z+1$ ion.

To evaluate this model we need to sum (51) over all states above S_m and add the resulting rate to $r_{EF}(k,1)$ (from Eq. 54), that is, to the electron collisional ionization rate to the ground state of $Z+1$.

If all states are assumed hydrogenic, Kramers rule (65) is adopted, and in the exponential, upper state energy is taken to be V_a to produce a simple overestimate of the effect, one finds

$$r_{Z,1} = 2 C_{EC} N_e / (V \theta^{1/2}) \exp[-(V_a - E_Z) / \theta] \ell^3 I \quad (57)$$

where

$$I \equiv \sum_{S_m+1}^{\infty} k^5 / (k^2 - \ell^2)^4$$

A reasonably good approximation to I may be found by defining

$$a = S_m^2 - \ell^2 \quad , \quad b = (S_m + 1)^2 - \ell^2 \quad , \quad c = (S_m + 1.7)^2 - \ell^2 \quad (58)$$

then

$$I = S_m^5/a^4 + (S_m + 1)^5/b^4 + 1/2 \left[(\ell^4/3)/c^3 + \ell^2/c^2 + 1/c \right]$$

The term (57) is added to the electron bound-free rate when $p = 1$. Its most important effect should occur at high electron density when S_m becomes low.

To date no case where the additional rate (57) is important has been found. This has discouraged us from seeking corresponding effects for other processes. Further, unless we are able to find some case of potential interest for which the effect matters, we will delete it from the code to save time, storage, and eliminate unnecessary complication.

5.5 RADIATIVE IONIZATION AND RECOMBINATION.

5.5.1 Radiative Recombination.

The radiative recombination coefficient from state k of ion Z to state ℓ of ion $Z-1$ can be obtained from the inverse photoionization cross section through the principle of detailed balance, but not as simply as for collision processes.

Let $\sigma(\ell, Z-1; k, Z; \nu) \equiv \sigma$ be the photoionization cross section at frequency ν from ℓ to k . $\alpha(k, Z; \ell, Z-1) \equiv \alpha$ be the radiative recombination coefficient from k to ℓ .

Then in general, for these processes only,

$$\dot{N}_\ell = \alpha N_e N(Z, k) - N_\ell \int_{v_0}^{\infty} dU(v) dv \quad (59)$$

where N_e is electron density, $N(Z, k)$ is the density of Z ions in state k , N_ℓ is density of $Z-1$ ions in state ℓ , v_0 is the minimum frequency which can ionize from ℓ to k and $U(v)$ is the photon omnidirectional spectral flux (photons/cm²/sec/Hz).

To apply detailed balance, assume (59) to be written for equilibrium conditions. Then \dot{N}_ℓ must be zero and $U(v)$ must be Planckian,

$$U(v) = P(\epsilon) = C_p \epsilon^2 / (\exp(t) - 1) \quad (60)$$

where

$$t \equiv \epsilon / \theta \quad ,$$

$$C_p = (8 \pi \epsilon_0^3) / (h^3 c^2) \quad ,$$

ϵ (eV) is photon energy, θ (eV) is temperature, ϵ_0 converts from eV to ergs, h is Planck's constant and c is the speed of light. Substitute (60) for $U(v)$ in (59) and set $\dot{N}_\ell = 0$ to obtain

$$\frac{N_\ell}{N_e N(Z, k)} = \frac{1}{\epsilon_0} \int_{\epsilon_0}^{\infty} P(\epsilon) d\epsilon \quad (61)$$

The population ratio in front of the integral can be found for equilibrium conditions thermodynamically, by taking the ratio of partition functions

$$\frac{N_\ell}{N_e N(Z, k)} = \frac{Q_\ell}{Q(e) Q_k} = h^3 g_\ell \exp(x) / [g_k 2(2\pi mkT)^{3/2}] \quad (62)$$

In our units this is

$$\frac{N_\ell}{N_e N(Z, k)} = g_\ell \exp(x) / (g_k Q_e \theta^{3/2}) \quad (63)$$

where $Q_e = 6.03704 \times 10^{21} \text{ cm}^{-3} \text{ eV}^{-3/2}$ and

$$x \equiv (E_k + I_{z-1} - E_\ell) / \theta \quad (64)$$

is the ratio of energy required to ionize state ℓ and then bring the ion to state k , to the temperature.

Now we have the multiplier of the integral in (61) in terms of known quantities and must evaluate the integral. To do that requires an expression for the photoionization cross section.

Begin with Kramer's formula for ionization of hydrogen from principle quantum number n

$$\sigma_k(v) = (64\pi^4 m Z^4 e^{10}) / (3\sqrt{3} \alpha^6 \bar{g}) / (n^5 v^3) \quad (65)$$

where m is electron mass, e is electron charge and \bar{g} is the Gaunt factor.

Somehow (65) must be generalized to apply to ions other than hydrogen and to be specific with respect to the final state of the ion Z .

We chose to generalize (65) beyond hydrogen by eliminating as much specific Z and n dependence as possible, replacing it with energy dependence, through the hydrogenic formula for ionization potential

$$I_Z = (2\pi^2 m Z^2 e^4) / (h^2 n^2) \quad (66)$$

Substitution of (66) into (65) to eliminate Z dependence and conversion to our units results in

$$\sigma(\epsilon) = C_H I_Z^2 / (n \epsilon^3) \quad (67)$$

where

$$C_H = (16e^2 \hbar \bar{g}) / (3\sqrt{3} m c \epsilon_0) = 3.2275 \cdot 10^{-17} \text{ cm}^2 \text{ eV}$$

if the Gaunt factor, \bar{g} , is taken equal to 0.3.

To use (67) for specific states, the simplest method is to just replace I by

$$I_Z = E_k + I - E_\ell \quad (68)$$

where I is ionization potential of the ground state of $Z-1$.

Substitution of (68) into (67) followed by substitution of (60), (63), and (67) into (61) leads to

$$\alpha = (p(\ell, k) C_H C_p \theta^{1/2} g_\ell) / (Q_e n g_k) F(x)$$

where

$$F(x) \equiv x^2 e^x \int_{x_0}^{\infty} dt / [t(e^t - 1)] , \quad x_0 = I_Z / \theta \quad (69)$$

and the constant $p(\ell, k)$ will be unity unless data on a specific transition indicates otherwise.

An approximation for $F(x)$ good to better than 1% everywhere is

$$F(x) = \begin{cases} x^2 e^x [1/x + (\ln x)/2 - x(1+x/2)/12 - .62772] , & x < 0.25 \\ x^2 e^x E_1(x) [x^2 + a_1 x + a_2] / [x^2 + b_1 x + b_2] , & 0.25 \leq x < 4.3 \\ x^2 e^x E_1(x) , & 4.3 \leq x < 60 \\ x , & 60 \leq x \end{cases} \quad (70)$$

with $a_1 = 2.9823$, $a_2 = 2.4416$, $b_1 = 3.5329$, $b_2 = 0.38094$ and $E_1(x)$ is the first order exponential integral.

5.5.2 Photoionization.

The rate of photoionization from state ℓ of ion Z to state k of ion $Z+1$ is given by

$$r_{\ell, k} = \int_{v_0}^{\infty} \sigma U(v) dv \quad (71)$$

where σ is given by (67) and $U(v)$ is the omnidirectional spectral flux described in Section 4.2, eq. (40).

To bring (40) into proper units, (71) becomes

$$r_{\ell,k} = C_H \epsilon_0^{-1} \sum_f v_f^{-1} I_z^2/n \int_f U(\epsilon)/\epsilon^3 d\epsilon \quad (72)$$

where the subscript f denotes a spectral feature.

The representation of U given in (40) requires three types of integrals to be carried out in (72) corresponding to a rising tail of U if $\epsilon < v_f - W_f$, a constant U if $v_f - W_f < \epsilon < v_f + W_f$ and a falling tail if $\epsilon > v_f + W_f$. If the threshold energy for ionization, ϵ_T , lies below the feature core, all three types of integral are present etc.

The simplest type is that of constant U , applicable to the core. Then

$$\int U d\epsilon / \epsilon^3 = U_C / 2(1/B^2 - 1/T^2) \quad (73)$$

where $B \equiv \max(v_f - W_f, \epsilon_T)$, $T \equiv v_f + W_f$

The two types of feature tail integrals can be handled with a single equation.

If below the core, (rising tail),

$$x \equiv v_f / \epsilon_T$$

$$y \equiv v_f / (v_f - W_f)$$

If above the core, (falling tail),

$$x = \max[v_f / \epsilon_T, v_f / (v_f + W_f)]$$

$$y = 0$$

Then

$$\int U d\varepsilon / \varepsilon^3 = (U_T / v_f^4) \left\{ 3 \ln \left[\frac{(1-x)}{(1-y)} \right] + 2(x-y) + (x^2 - y^2)/2 + (y-x)/[(1-y)(1-x)] \right\} \quad (74)$$

5.6 BOUND-BOUND RADIATIVE RATES.

To calculate the transition rate from lower eigenstate, ℓ , to upper eigenstate, k , of ion Z due to photon induced transitions, the integral

$$r_{\ell k} = \int dU dE \quad (75)$$

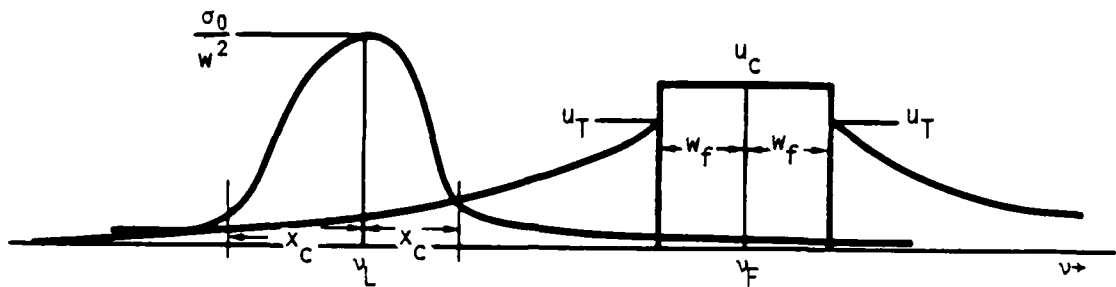
must be evaluated using the line model (41) for σ and the feature model (40) for U .

Given $r_{\ell k}$, the inverse rate may be obtained from detailed balance and is

$$r_{k\ell} = (g_\ell / g_k) r_{\ell k} \quad (76)$$

The integral (75) may be sensitive to the line width, (45) and the terms, T_{PB} , due to photo induced transitions in one or both of the states ℓ and k may dominate line width. Thus the rate $r_{\ell k}$ (and $r_{k\ell}$) implicitly depends upon itself as well as all other rates to and from ℓ and k . To partially account for this without incurring too much CPU penalty, if the rates $r_{\ell k}$ and $r_{k\ell}$ increase the line width by as much as 25%, the rates $r_{\ell k}$ and $r_{k\ell}$ are recalculated at the new line width. This will not cover all cases, but should cover all rapid transitions, which are the ones of most importance.

Evaluation of the overlap integral (75) is, of course, the heart of the rate calculation. The line and feature models were designed to be realistic, yet allow analytic evaluation of the overlap as far as possible. The sketch below illustrates the problem.



The central line frequency, v_L may be located anywhere with respect to the central feature frequency, v_F and x_C may be larger, smaller, or identical to W_f .

Eight logically distinct cases are recognized. Two are handled by simple analytic formulae and the other six by various sequences of calls to four subroutines. Three of the four subroutines evaluate analytic formulae; alas, the fourth is a numerical integration. Perhaps someday we will find an adequate analytic approximation for this one also.

Case 1 Line versus Continuum

If the feature is in level 1 of the spectral description it has no tail, $U_T = 0$, and can be assumed very broad with respect to the line. Thus in (75) one can take U to be constant at the value U_C and use infinite limits for the integral. In that case an exact integral exists for a Voight profile (which is a better representation than (45))

$$\int \sigma U dE = \pi U_C \sigma_L W_L / (\nu_L \epsilon_0) \quad (77)$$

where ϵ_0 converts ergs to eV and the symbols are defined in (41) and (42).

Case 2 Line and Spectral Feature Well Separated

This is another especially simple case, and should be appropriate for most spectral features for any given line. If $(W_f + W_L X_C) / |\nu_f - \nu_L| \leq 0.25$ then

$$\int \sigma U dE = \pi W_L \sigma_L U_T / (\nu_f - \nu_L)^2 + 2 \sigma_L (U_T / W_f + U_C W_f) / A^2 \quad (78)$$

where

$$A \equiv 1 + (\nu_f - \nu_L) / W_L$$

The other cases are: (3) cores don't overlap, line below feature, (4) cores don't overlap, line above feature, (5) cores partially overlap, line below feature, (6) cores partially overlap, line above feature, (7) feature core contained in line core, and (8) line core contained in feature core. Each of these cases is handled by a special sequence of calls to subroutines which evaluate the following four types of integrals.

Type 1

$$T_1 \equiv \int_a^b [1 + (v - v_L)^2/W_L^2]^{-1} (v - v_f)^{-2} dv = P(a) - P(b) \quad (79)$$

The primitive of (79) is

$$W_L P(v) = (1 + (1+\alpha)^2)^{-2} \{ \alpha \ln [1 + (y+\alpha)^2] + (\alpha^2-1) \tan^{-1} (y+\alpha) - 2\alpha \ln y - (1+\alpha^2)/y \} \quad (80)$$

where

$$y \equiv (v - v_f)/W_L, \quad \alpha \equiv (v_f - v_L)/W_L$$

Round off errors are a good possibility in evaluating, or differencing, (80). The scheme used is to define a function, τ , with expansions of some terms in (80) such that, if $\alpha/y > 10^{-2}$:

$$\begin{aligned} \tau(y) &= \alpha \ln \{1 + [2\alpha + (1+\alpha^2)/y]\} \\ &+ (\alpha^2-1) \tan^{-1} (y+\alpha) - (1-\alpha^2)/y - (\alpha^2-1)\pi/2 \end{aligned} \quad (81)$$

If $\alpha/y \leq 10^{-2}$:

$$\tau(y) = [-(\alpha^2+1)^2/3 + (\alpha/y)(9\alpha^4+2\alpha^2+1)/2]/y^3 \quad (82)$$

Then

$$T_1 = \sigma_L U_T [\tau(b) - \tau(a)] / [W_L(1+\alpha^2)] \quad (83)$$

Type 2

$$\begin{aligned} T_2 &\equiv \int_a^b U_C \sigma_L / [1 + (v - v_L)^2 / W_L^2] dv \\ &= U_C \sigma_L W_L \{ \tan^{-1} [(v_f - v_L + w_f) / W_L] - \tan^{-1} [(v_f - v_L - w_f) / W_L] \} \quad (84) \end{aligned}$$

Similarly to type 1, to avoid round off or truncation problems:

If $|y| > 5$

$$\tau(y) = -y^{-1} + y^{-3}/3$$

If $|y| < 10^{-3}$

$$\tau(y) = y - y^3/3 \quad (85)$$

Else

$$\tau(y) = \tan^{-1} y$$

Then

$$T_2 = U_0 \sigma_L W_L [\tau(b) - \tau(a)]$$

where $b \equiv (v_f - v_L + w_f) / W_L$ and $a \equiv (v_f - v_L - w_f) / W_L$

Type 3

$$T_3 = \int_a^b e^{-(v - v_L)^2 / W_L^2} dv \quad (86)$$

Standard formulae exist for approximating this integral, one must only be sure to get the sign right since a and b can be on either side of ν_L , and check for a and b on opposite sides of ν_L .

Type 4

$$T_4 \int_a^b e^{-(\nu - \nu_L)^2/W^2} / (\nu - \nu_f)^2 d\nu \quad (87)$$

To the present, we have found no adequate analytic approximation for (87). It is integrated numerically.

5.7 OSCILLATOR STRENGTH.

5.7.1 Oscillator Strength for Real States.

In the foregoing sections, f_{2k} is oscillator strength for allowed transitions, and is input data for the calculation. To account for an intuition that higher multiple moments should be more effective for electrons than for photons, we introduce the arbitrary rule that for electrons

$$f_{2k} = \max \{ \text{data for optically allowed transition, } f \} \quad (88)$$

where f is taken to be 10^{-3} . This cavalier treatment of optically forbidden transitions should be improved someday, but the above is how it stands at present.

5.7.2 Oscillator Strength to the Artificial State.

In order to calculate transition rates between some real eigenstate with index ℓ and the artificial state with index a , an oscillator strength, $f_{\ell a}$, must be calculated. This can be done by assuming a model for population distribution among the component states of the artificial state, summing the transition rates to all of them, and finding that value of $f_{\ell a}$ which yields the same total rate.

The model assumed is that eigenstate members of the artificial state are hydrogenic and have a Boltzmann distribution for all principal quantum numbers above some value, b .

The first step, then, is to find b . This is accomplished by comparing the sum of all spontaneous radiative transitions to lower states (easy to approximate) to the electron collisional excitation rate to the next higher state (also easy to approximate). The idea is that spontaneous radiation is the only process tending to drive state populations out of equilibrium and it drives electrons downward. So a state can be in equilibrium relative to its neighbors only if other processes, in particular those driving electrons upward, dominate spontaneous emission. The simplest such process to consider is electron collisional excitation from state b to state $b+1$. It would be more elegant and a little better to use the sum of all upward collisions but that is mathematically cumbersome and further, for hydrogenic states the widest energy gap to bridge is to the adjacent state, thus that single transition should serve as a good measure of the sum to all upper states.

Of course, it is possible that electron density or temperature could be so low that photon induced upward transitions dominate electron induced transitions and should be used in the comparison. Radiative

transition rate is more expensive to calculate than collisional rate even for the b to $b+1$ transition, but given an arbitrary line spectrum, one cannot assume any single transition to be typical, so the full sum would have to be approximated somehow. This elaborate process seems unnecessary; for if radiative transitions dominate, making our estimate of b too large and thus our estimate of $f_{\ell a}$ too small, it is probable that radiation will be intense enough to drive state ℓ toward equilibrium with state a even with a somewhat low value of $f_{\ell a}$.

If V is the vacuum ionization potential of a hydrogenic ion then the energy difference between the hydrogenic state b and some lower hydrogenic state ℓ is

$$E_b - E_\ell = V(b^2 - \ell^2)/b^2 \ell^2 \quad (89)$$

And Kramer's formula for hydrogenic oscillator strength is about

$$f_{\ell b} = 2\ell b^3 (b^2 - \ell^2)^{-3} \quad (90)$$

Substitution of (90) and (89) into (48) and recognition of the fact that hydrogenic state statistical weights are proportional to principal quantum number squared yields the transition rate due to spontaneous radiation,

$$r_{sp}(b, \ell) = 2A_r V^2 [b^3 \ell (b^2 - \ell^2)]^{-1} \quad (91)$$

To get the sum of all transitions from b , to states 1 through $b-1$ approximate the sum of (91) by an integral. For b large compared to unity the integral is approximated by

$$S = \sum_{\ell=1}^{b-1} r_{sp}(b, \ell) = 2A_r V^2/b^5 [\alpha + \beta \ln b] \quad (92)$$

where, if the normal integration limits of $\ell = 1/2$ to $b - 1/2$ are taken,
 $\alpha = .347$ and $\beta = 1.5$

A slightly better fit to the sum is obtained for the most important, low, range of b by taking

$$\alpha = 0.411 \text{ and } \beta = 1.516 \quad (93)$$

Substitution of (89) and (90) into (51) yields the electron collisional rate from b to $b+1$. After clearing

$$r_{EB}(b, b+1) = (2C_{Ec} N_e / \theta^{1/2} V) b^3 (b+1)^5 / (2b+1)^4 \exp(-\gamma) \quad (94)$$

where

$$\gamma = V(2b+1) / [\theta b^2 (b+1)^2]$$

After an appropriate value of the desired ratio of C to r_{EB} is chosen, one iterates (92) and (94) to find b . The ratio must be chosen empirically, on the basis of net ionization and recombination rates. A value of this ratio which yields good answers is 0.1.

The next step is to find the normalized population distribution. A Boltzman distribution is a good approximation for these states because the rate of collisional diffusion of electrons is very high among very highly excited states compared to the rate of transition from such states to lower ones. So we expect the individual state population n_k for some state k to be

$$p_k = C g_k e^{-E_k/\theta} = C \theta^2 \exp(-V/(k\theta^2)), \quad (95)$$

for k between b and the maximum S_m (from 3.3.3). To find the normalization constant, C , eq. (95) must be summed and set equal to the total population of the artificial state, p_a . As might be expected from the form of (95) the summation, even in an integral approximation, is pretty messy. An approximate function, accurate to better than 4% everywhere, is

$$C = 2 \rho_a (\beta/V)^{3/2}/F \quad (96)$$

with

$$F \in e^{x(b)}S(x(b)) - e^{x(S_m)}S(x(S_m))$$

1000 TURBOS

$$C_3 = 3.97 \times 10^{-3} + 1.04 \times 10^{-3} \ln \left(\frac{1}{\epsilon} \right) + 4.3 \times 10^{-4} \ln^2 \left(\frac{1}{\epsilon} \right) \quad (45)$$

THE BOSTONIAN SOCIETY

Digitized by srujanika@gmail.com

110 *Journal of Health Politics*

116 *Journal of Health Politics, Policy and Law* / March 2007

5.7.2.1 Radiation Oscillator Strength. To find the effective oscillator strength for radiation to the artificial state from some real state a we must now sum (48) over all states which make up the artificial state. Substitution of (89), (90), (95), and (96) into (48) and summing yields

$$R_r = \sum_k r_{sp}(k, \epsilon) = 4A_r V^2 (\alpha/V)^{3/2} p_a / (\epsilon F) \sum_b \frac{\exp(V/\epsilon k^2)}{k(k^2 - \epsilon^2)} \quad (100)$$

If the sum in (100) is replaced by an integral its value is

$$\begin{aligned} I &\equiv \int_0^{\infty} \exp(V/\epsilon k^2) / [k(k^2 - \epsilon^2)] dk \\ &= \exp(V/\epsilon \epsilon^2) [E_1(\frac{V}{\epsilon^2} - \frac{1}{\epsilon^2}) - E_1(\frac{V}{\epsilon^2} - \frac{1}{S_m^2})] \quad (101) \end{aligned}$$

where E_1 is the exponential integral of the first kind. It is convenient that (100) can be approximated analytically but since the exponential integrals will be approximated, there is ample opportunity for truncation error. To handle this define

$$H \equiv \exp(-V/\epsilon \epsilon^2) I \quad (102)$$

Then evaluate H for two cases. Define

$$y \equiv V/(\alpha \epsilon^2) \quad (103)$$

Case 1 $y < 1$

$$H = \exp(\alpha)/(2\ell^2) [\ln \beta/\alpha + \gamma(a_1x + a_2(\alpha+\beta)x^2 + a_3(\alpha^2+\alpha\beta+\beta^2)x^3 + a_4\gamma(\alpha+\beta)^2x^4)] \quad (104)$$

where

$$a_1 = .99999193, \quad a_2 = -0.24991055, \quad a_3 = .05519968, \quad a_4 = -.00976004$$

$$\alpha \equiv 1/\ell^2 - 1/b^2, \quad \beta \equiv 1/\ell^2 - 1/S_m^2, \quad \gamma \equiv 1/S_m^2 - 1/b^2$$

Case 2 $y > 1$

If $\ell^2/b^2 < 10^{-2}$ $Ex(y)/y$ then

$$H = \frac{1}{2} (1/b^2 - 1/S_m^2) \exp(-V/\theta b^2) \quad (105)$$

If $\ell^2/b^2 \geq 10^{-2}$ $Ex(y)/y$ then

$$H = (\theta/2V\ell) (Ex(V\alpha/\theta)/\alpha - \exp(-V\gamma/\theta) Ex(V\beta/\theta)/\beta) \quad (106)$$

where, from Ref. 5,

$$Ex(x) \equiv (a_2 + a_1x + x^2)/(b_2 + b_1x + x^2) \quad (107)$$

$$a_1 = 2.334733, \quad a_2 = 0.250621, \quad b_1 = 3.330657, \quad b_2 = 1.681534$$

Then substitute (102), and (101) into (100) to find R . Then equate R to (48) evaluated for states ℓ and a to obtain at last, for radiation,

$$f_{\ell,a}^R = 2V^{1/2} \theta^{3/2} g_A \exp(V/\theta b^2) H / [(E_a - E_\ell)^2 \ell^3 F] \quad (108)$$

where g_A is taken from (7)

5.7.2.2 Electron Collision Oscillator Strength. To find the effective oscillator strength for electron collisions to the artificial state from real state ℓ , sum (52) over all states which make up the artificial state. Substitution of (89), (90), (95), and (96) into (52) and summing yields

$$R_e = C_0 \ell^3 \sum_b^{\infty} k^5 \exp[V/(\theta k^2)] / (k^2 - \ell^2)^4$$

$$C_0 \equiv 2C_{EC} N_e \theta p_a g_\ell / [V^{5/2} F] \quad (109)$$

The sum in (109) is also rather messy and gives an unrealistically large rate when b approaches ℓ (that is, when θ and N_e are almost but not quite high enough to drive the artificial state into equilibrium with the uppermost real state). This is not shocking since the assumption of zero populations for states below b and full Boltzmann population above is over simple. An approach which largely alleviates this problem is to neglect contributions from the first two terms in the sum; replace b with

$$B \equiv b + 2 \quad (110)$$

The sum in (109) can be approximated by replacing it with

$$R \equiv \sum_B^{\infty} k^5 \exp[V/\theta k^2] / (k^2 - \ell^2)^4 dk \quad (111)$$

Replacement of k by $(V/\theta)(1/\ell^2 - 1/k^2)$ as the variable of integration reduces the integral to a fourth order exponential integral, which can be reduced to a first order exponential integral by integration by parts. To avoid truncation problems the following cases are recognized.

Case 1 $V/(\theta B^2) \leq 0.1$ and $4\ell^2/B^2 \leq 0.1$

Then an adequate approximation is

$$R = (1/\ell^2 - 1/S_m^2)/2 \quad (112)$$

Case 2 Case 1 failed but $(V/\theta)(1/\ell^2 - 1/B^2) < 10$. Define

$$B \equiv (V/\theta)(1/\ell^2 - 1/B^2), \quad \tau \equiv (V/\theta)(1/\ell^2 - 1/S_m^2)$$

$$R = (12\ell^2)^{-1} [V/(\theta\ell^2)]^{1/3} [\exp[V/(\theta B^2)]^1 (1 - 1/\tau + 2/\tau^2 - \text{Ex}(\tau))/\tau - \exp[V/(\theta S_m^2)]^1 (1 - 1/\tau + 2/\tau^2 - \text{Ex}(\tau))/\tau] \quad (113)$$

where the function $\text{Ex}(x)$ is that of (107).

Case 3 Not Case 1 or Case 2

$$R = (2\ell^2)^{-1} [V/(\theta\ell^2)]^{1/3} [\exp[V/(\theta B^2)]^1 (1 - 4/\tau + 20/\tau^2 - 120/\tau^3 + 340/\tau^4 - 6720/\tau^5 + 60,480/\tau^6) - \exp[V/(\theta S_m^2)]^1 (1 - 4/\tau + 20/\tau^2 - 120/\tau^3 + 340/\tau^4 - 6720/\tau^5 + 60,480/\tau^6)] \quad (114)$$

Then finally substitute R into (109) and equate it to the form (52) to find for electron collisions

$$f_{e,a} = 2\theta^{3/2} (E_a - E_e) g_a e^3 R / (V^{5/2} F) \quad (115)$$

SECTION 6

BASIC DATA

In addition to normal mathematical and physical constants, the major data requirements of this calculation are quantities associated with energy levels and especially oscillator strengths for transitions among energy levels.

Energy levels and their associated principal, orbital, and spin quantum numbers are obtained primarily from Ref. 7. Oscillator strengths are obtained primarily from Ref. 8.

A significant amount of art is involved in this process. While not all needed data exists, particularly for oscillator strength, far more energy levels are known than can be modeled. It is necessary to combine many states together to reduce the total number modeled to about 10. In doing so, one tries to combine states whose energy levels are nearby, avoid creating artificial gaps in the distribution of energy levels, not mix levels with different spins, nor different principal quantum number. Occasionally conflicts arise among these criteria and are resolved by best judgement. Another problem arises when all eigenstates of a given principal quantum number are not described in the literature. In that case we use available data to determine modeled state energy, etc., and raise the statistical weight to account for the missing states.

Oscillator strengths are summed over upper levels and averaged over lower levels. For transitions allowed by LS coupling rules but which do not appear in Ref. 8, oscillator strengths are assigned at a value smaller than the majority which do appear in the list.

In Griem's formula for Stark broadening (Ref. 2), the energy gaps to the next lower and next higher orbital state appears. Since we frequently lump states of differing orbital angular momentum together, these gaps are inserted as data, averaged as best as we are able.

An example of the results of this process is given in Table 1 which shows data entered into the computer for singly ionized oxygen. In this case 63 eigenstates from Ref. 7 were reduced to 10. For the upper 5 model states, preservation of spin was given up, as can be seen from the non-half integer values.

Table 1. O^{1+} Data. The first column is state index, k , the second state energy (cm^{-1}), then designation, statistical weight, g , principal quantum number, n , orbital quantum number, ℓ , spin quantum number, s , mean energy difference to $\ell-1$, w^- (cm^{-1}), energy difference to $\ell+1$, w^+ (cm^{-1}), and oscillator strengths where the number in parentheses is the value of k for the upper state.

k	Energy	Designation	g	n	ℓ	s	w^-	w^+	f	f	f
1	0	$2p^3 \ ^1S^0$	4	2	1	1.5	0	119,933	.43 (4)	.171 (6)	.32 (8)
2	36,317	$2p^3 \ ^3P^0$	10	2	1	.5	0	93,166	.25 (5)	.067 (7)	.141 (8)
3	40,467	$2p^3 \ ^3P^1$	6	2	1	.5	0	79,466	.186 (10)		
4	119,933	$2p^4 \ ^1P^0$	12	2	1	1.5	79,466	0	.22 (5)	.063 (6)	.039 (7)
5	170,944	$2p^4 \ ^3P_1, \ ^1S$	12	2	1	.5	15,660	0	.142 (8)	.178 (10)	
6	186,604	$3s \ ^1P, \ ^3S$	18	3	0	1.17	0	15,660	1.034 (7)	10^{-4} (8)	
7	208,712	various	64	3	.84	1.06	4,000	4,000	1.5 (8)	.104 (9)	
8	230,389	various	128	3	1.69	.97	10,000	10,000	.409 (9)	.483 (10)	
9	271,252	various	430	4	1.08	.98	15,000	15,000	.059 (10)		
10	275,041	various	90	3	1.64	.94	10,000	10,000			

SECTION 7 SAMPLE RESULTS

To date little useful data for direct comparison of overall results has been found. Necessary basic comparisons have been made. For example, our fit to Lotz's curve has been checked; Lotz has compared his curve to electron collisional cross section data. And we have checked our photon ionization cross sections against Kramer's. This sort of fundamental comparison is required but accomplishes no more than assurance that the formulae were correctly encoded; such checks do not give evidence of the adequacy of the method to produce correct answers. The only way to check the total method is to compare to other calculations and to limiting cases over as wide a range as possible.

7.1 COLLISIONAL-RADIATIVE RECOMBINATION AND IONIZATION.

The most severe test of the method we have found is based on the fact that a complete temporal calculation of electron eigenstate populations must automatically account for both radiative and collisional ionization/recombination processes. The only prior calculations known which are in a form for ready comparison are those in Ref. 9 by Bates, Kingston, and McWhirter (hereafter, BKM). The BKM calculations are restricted to hydrogen or, separately, hydrogenic ions in an optically thin medium*, using an electron collisional cross-section derived from Grysinski's semi-classical ionization rate coefficient to back out state-to-state excitation cross sections for electron collisions.

* They also carry out a version of a calculation for a medium optically thick to series of lines. They do not seem to consider the ionizing effect of the radiation. We have not yet attempted to compare to this work.

Their calculations make the following major assumptions, which in the following will be referred to by the letters in parentheses:

- (P) Only the ground state is significantly populated
- (D) Only the ground state requires a differential equation solution, all others can be approximated as in quasi-steady equilibrium.
- (E) All energy levels are present at all electron densities, that is, no effect of plasma polarization is included.

Over the range of applicability of these assumptions, BKM expect their results to be accurate to about a factor of 3. Our method is more general in that it makes none of the three assumptions, P, D, or E but less accurate in that for practical reasons we are limited to principal quantum number of 3 or 4. To check our method we ran hydrogen using only the first four eigenstates as well as the first 10 eigenstates. If our method were perfect, we would get the same answers in both cases.

7.1.1 Recombination Coefficient for Hydrogen.

Figures 1 through 5 compare our calculated values of collisional radiative recombination coefficient, α , with that of BKM. In all figures a vertical bar indicates the value of electron density, N_e , at which one or more BKM assumptions begin to fail, for higher N_e the BKM approximation is not reliable. In Figures 1, 2, and 3 assumptions D and E fail first, in Figures 5 and 6 assumption ? fails first.

It can be seen that while our method is not perfect, the 4 state case is pretty consistent with the 10 state case and both are consistent with BKM over the range of N_e for which the BKM approximation holds. In the radiative recombination limit, at low N_e , our α is consistently below BKM because the Lotz rate is below that used by BKM, but is at least close to the factor of 3 BKM expects.

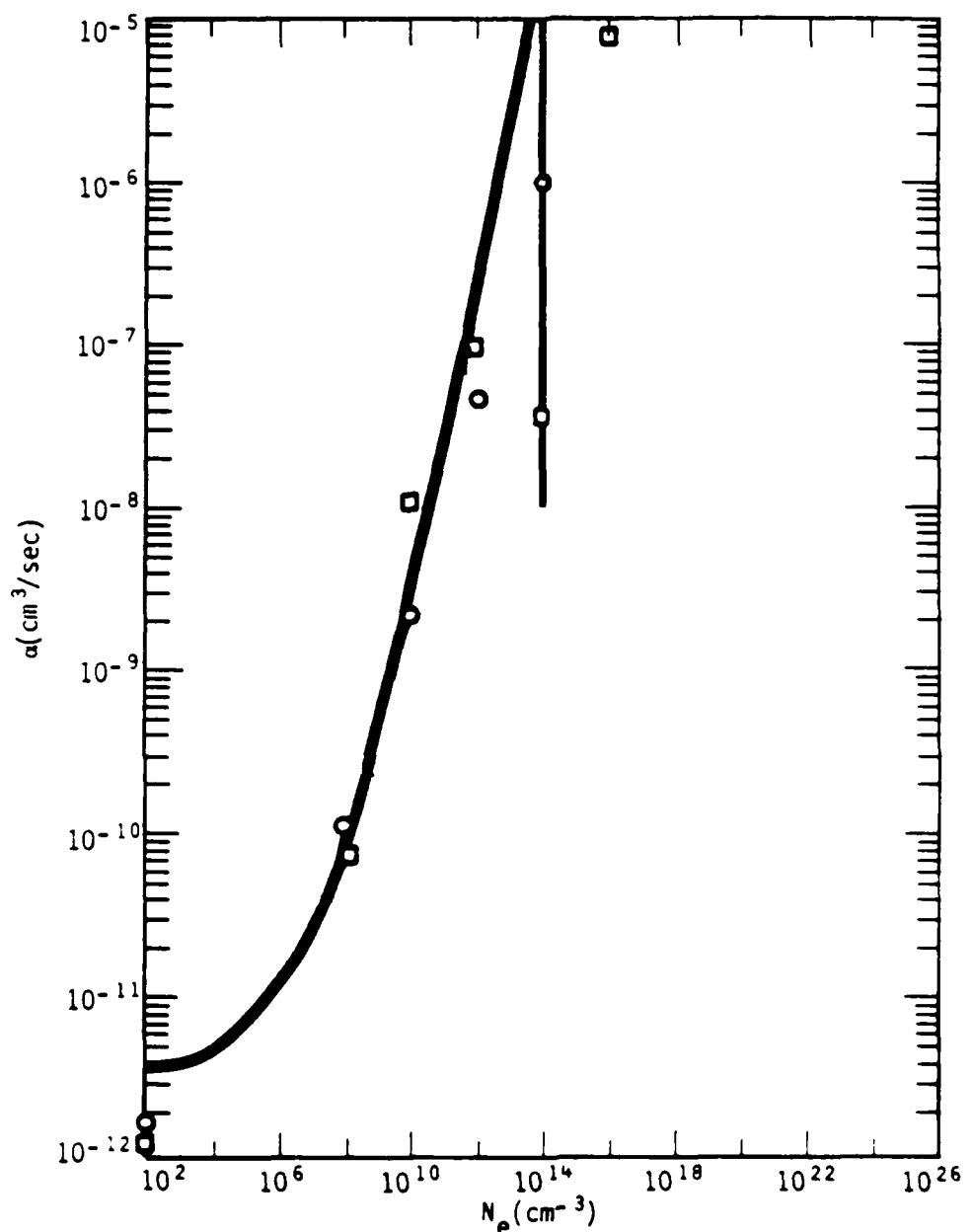


Figure 1. Hydrogen Collisional Radiative Recombination Coefficient at 250°K. The BKM coefficient is shown as a solid line. Our values for 10 states are shown as open circles, for 4 states as open squares. BKM is not reliable to the right of the vertical line.

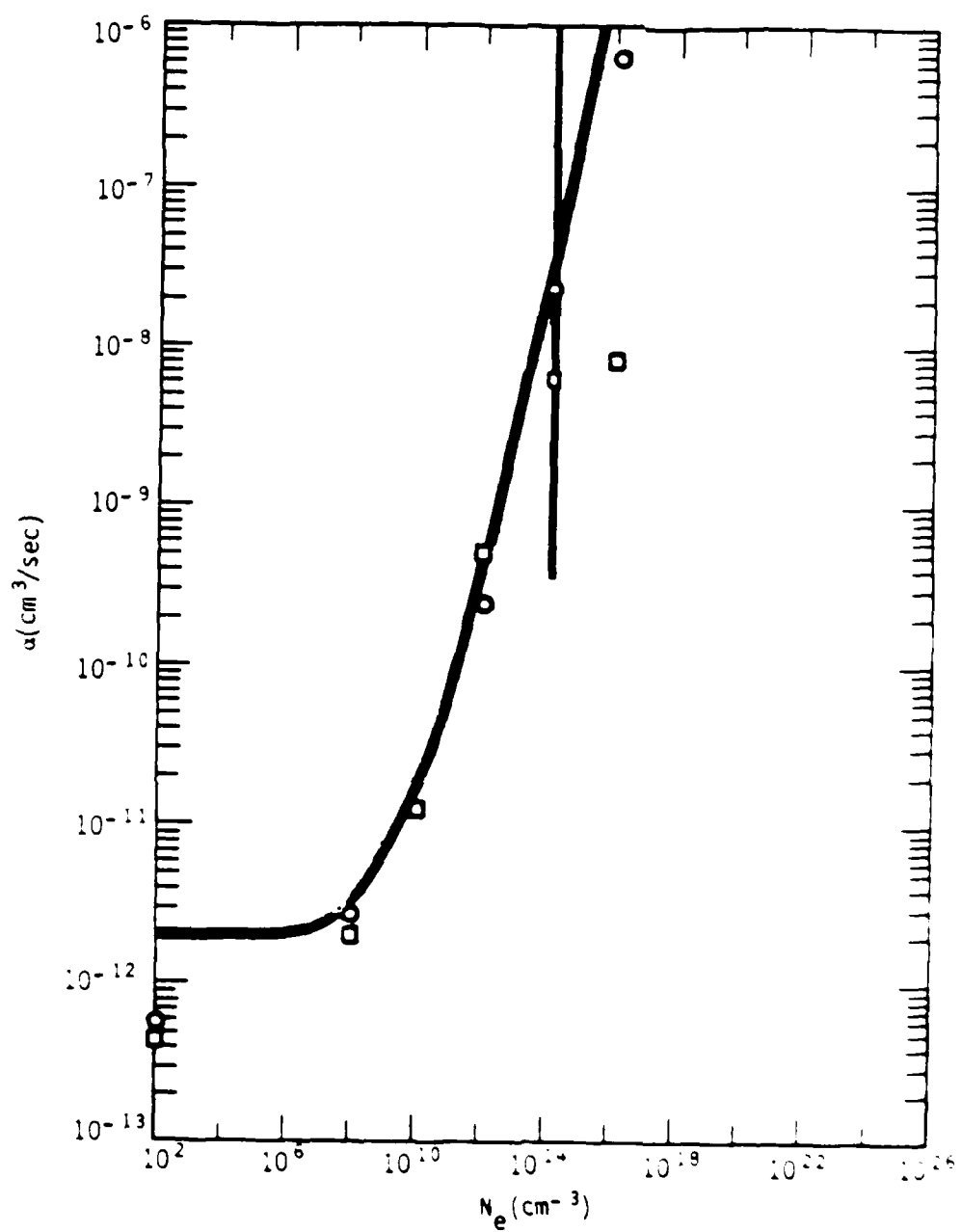


Figure 2. Hydrogen Collisional Radiative Recombination Coefficient at 1000°K. The BKM coefficient is shown as a solid line. Data values for 10 states are shown as open circles, for 4 states as open squares. BKM is not reliable to the right of the vertical line.

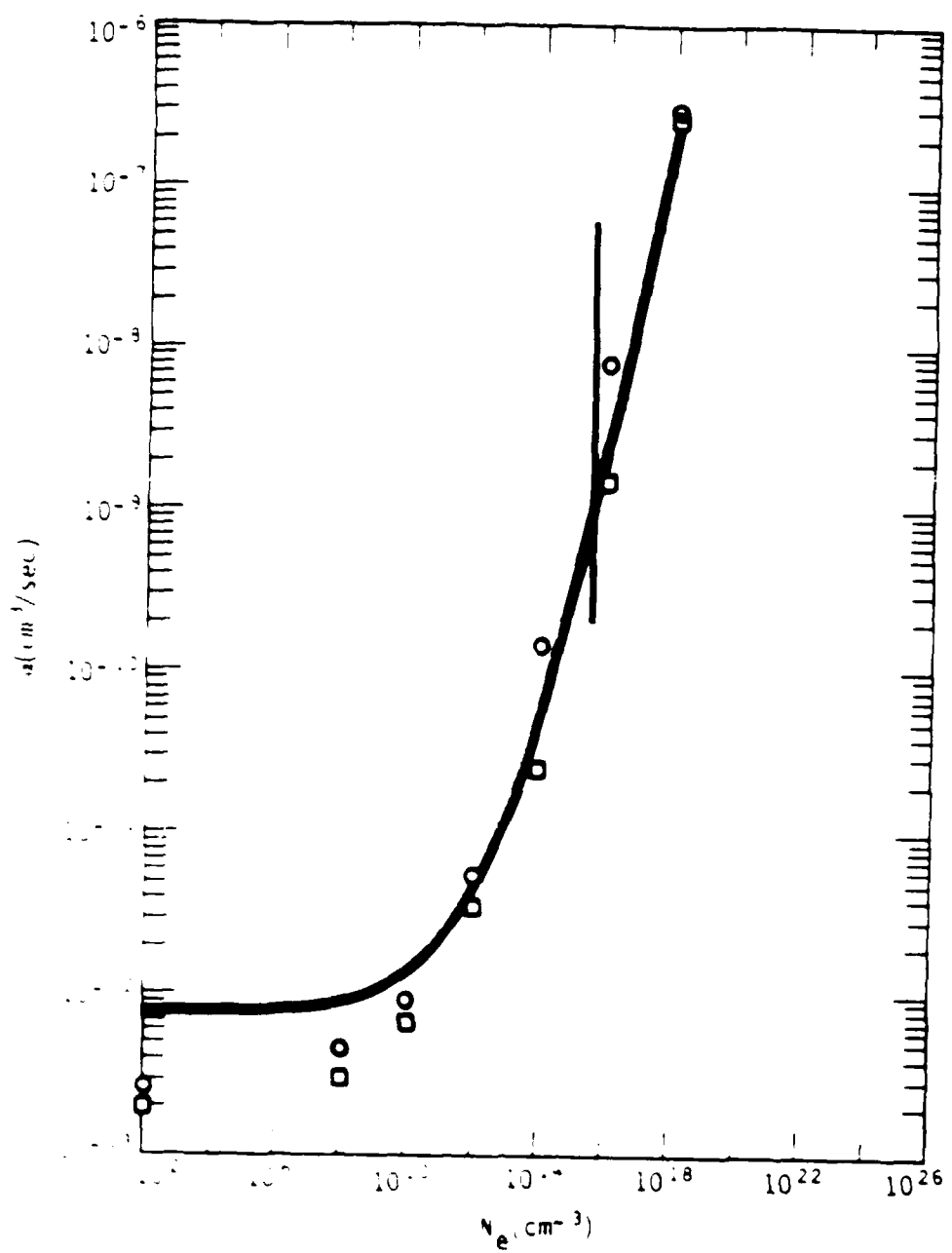


Figure 1. Hydrogen collisional Radiative Recombination Coefficient at $T = 10^4$ K. The BKM coefficient is shown as a solid line. Our values for 10 states are shown as open circles, for 4 states as open squares. BKM is not reliable to the right of the vertical line.

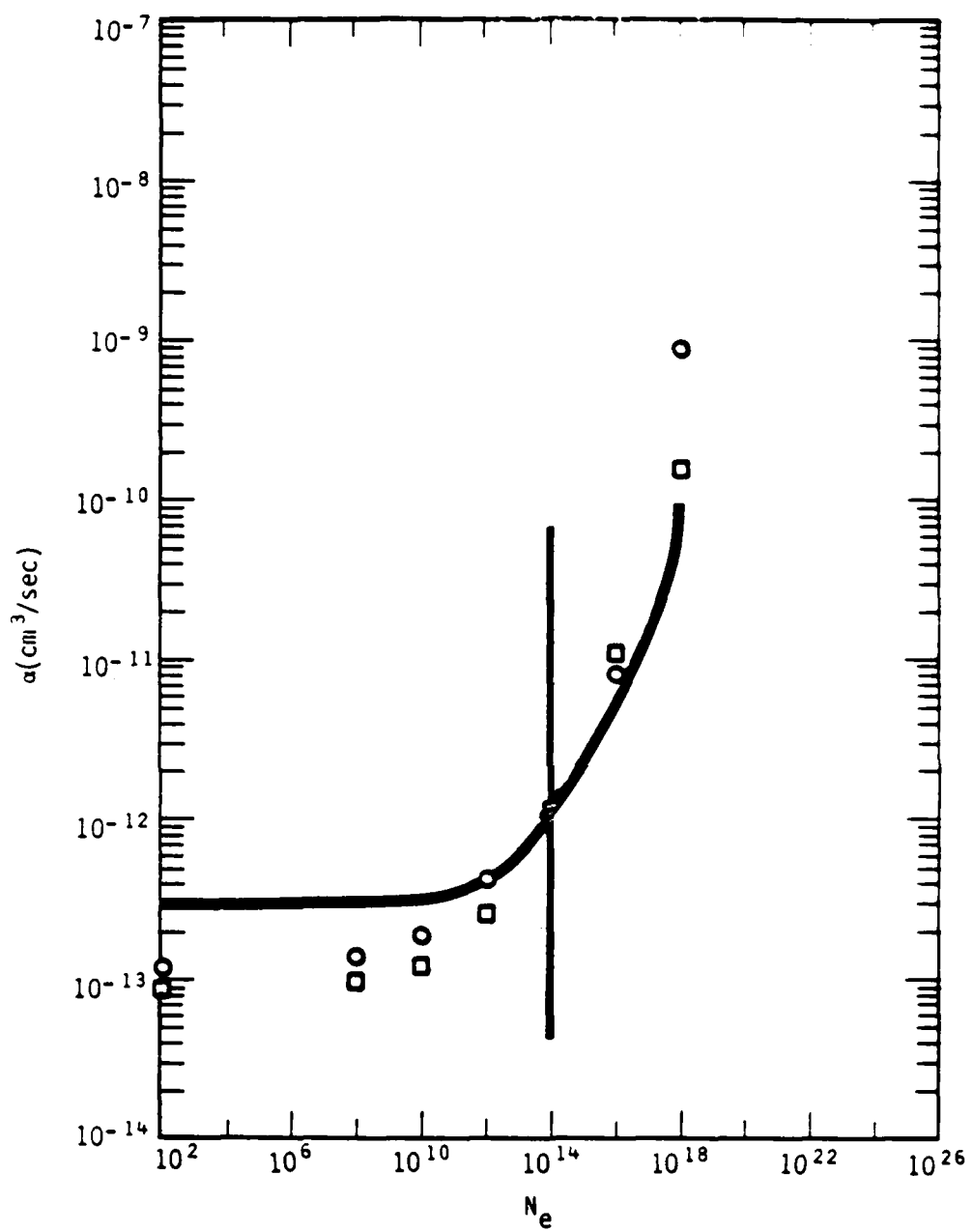


Figure 4. Hydrogen Collisional Radiative Recombination Coefficient at 16,000°K. The BKM coefficient is shown as a solid line. Our values for 10 states are shown as open circles, for 4 states as open squares. BKM is not reliable to the right of the vertical line.

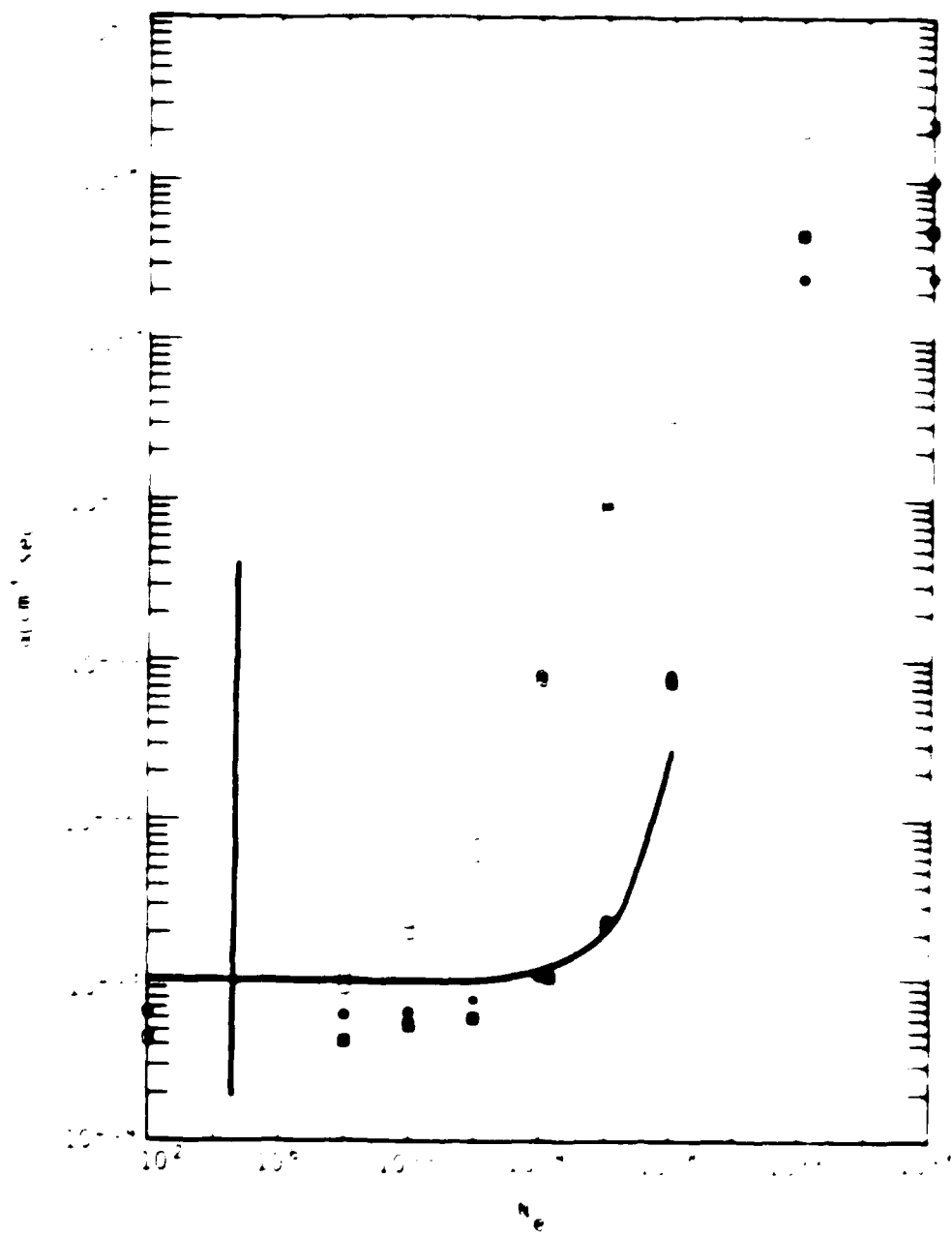


Figure 5. Hydrogen 3s states had at the reionization rate of $10^{10} \text{ cm}^3/\text{sec}$ and $54,000^\circ\text{K}$. The DFM effective coupling constant is shown as open circles, values for 10 states are shown as open circles, for 4 states as open squares. BKM is not reliable to the right of the vertical line. Solid circles and squares use BKM effective coupling.

At the two lowest temperatures, Figure 1 and 2, the 4 state calculation suffers a glitch at about the value of N_e for which BKM degrades. This is almost certainly a problem in our effective electron collisional oscillator strength from low lying states to the artificial state, due to the fact that the gap in energy between state 4 and the artificial state is about 40 times the electron temperature. This gap is reduced almost a factor of 6 for the 10 state case, and of course, is also reduced at higher electron temperature. We do not consider this a serious problem because we do not expect to encounter such high N_e at such low electron temperature. If this expectation is wrong, it will be necessary to either improve the method or carry more states.

At high electron temperature, especially Figure 5, our α climbs well above that of BKM at high N_e . In part this is due to a difference in our definition of α and theirs. We count recombination to any state as part of α , whereas BKM count only recombination to the ground state. When their assumption, P, is valid the two definitions are numerically equivalent, but when the upper states acquire a significant population, this is not true for the case of Figure 5 at high N_e , they are very different. Recombination coefficient to the ground state, to make a better comparison to BKM, is shown in Figure 5 as solid circles and it can be seen that the agreement is quite good, indicating that the BKM calculation is less sensitive to assumption P than might be imagined.

7.1.2 Ionization Coefficient for Hydrogen.

Figures 5, 7 and 8 show comparisons of our collisional-radiative coefficient, α , to those of BKM. Our values are uncomfortably high, which is at electron temperature for which BKM calculate values, Figure 6. This is at least partly due to a weakness in our treatment of the artificial state or oscillator strengths connecting to it;

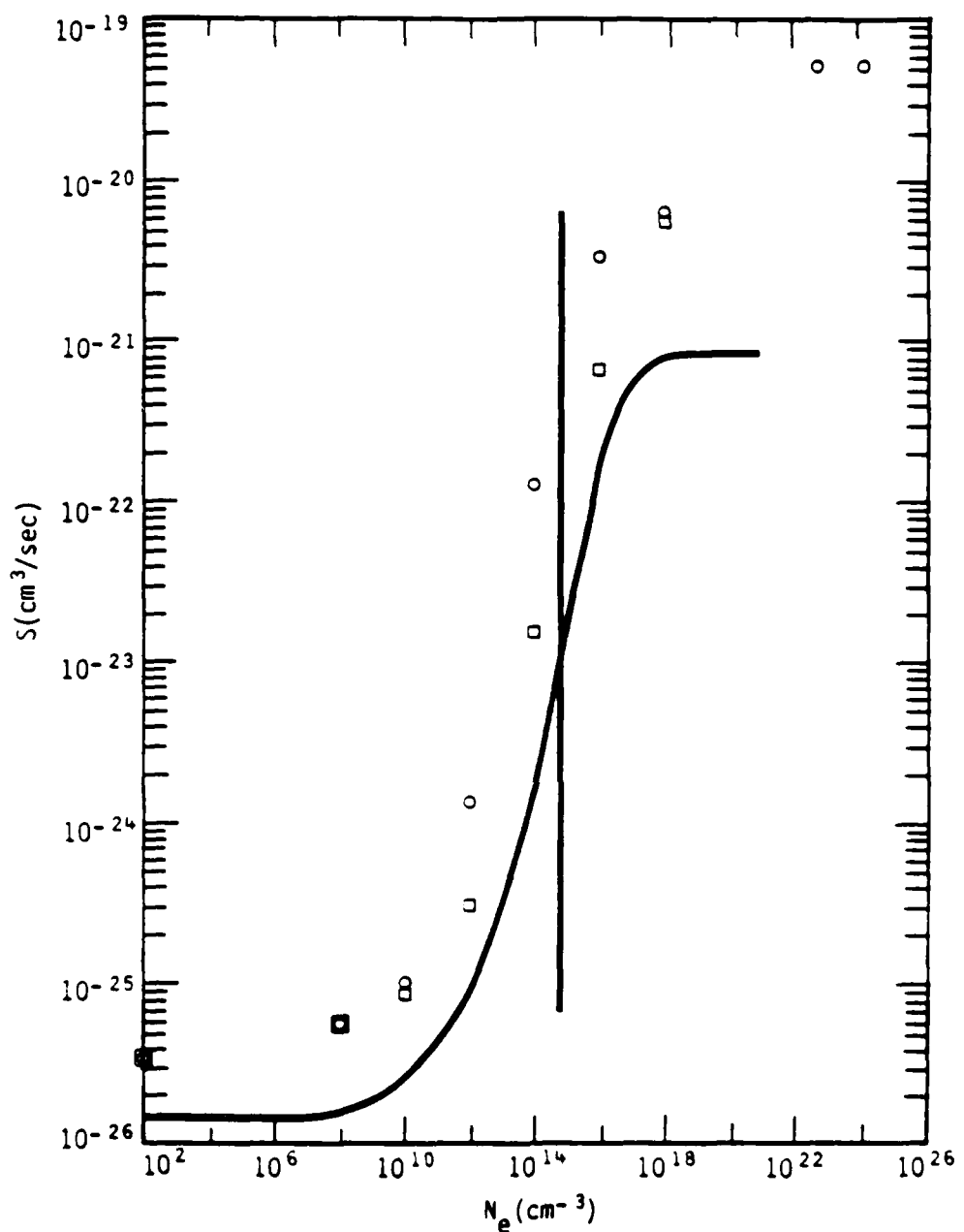


Figure 6. Hydrogen Collisional Radiative Ionization Coefficient at 4000°K. The BKM coefficient is shown as a solid line. Our values for 10 states are shown as open circles, for 4 states as open squares. BKM is not reliable to the right of the vertical line.

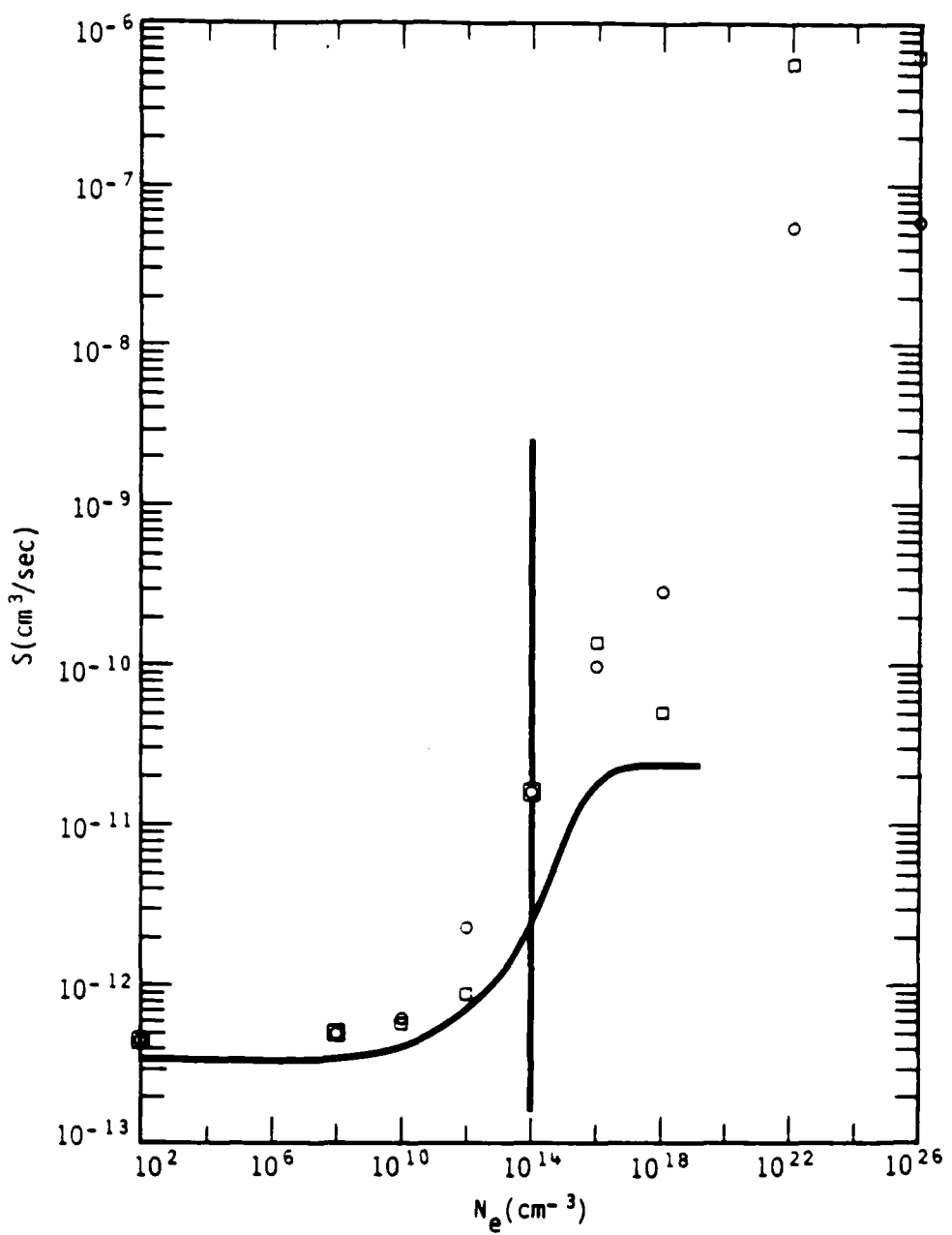


Figure 7. Hydrogen Collisional Radiative Ionization Coefficient at 16,000°K. The BKM coefficient is shown as a solid line. Our values for 10 states are shown as open circles, for 4 states as open squares. BKM is not reliable to the right of the vertical line.

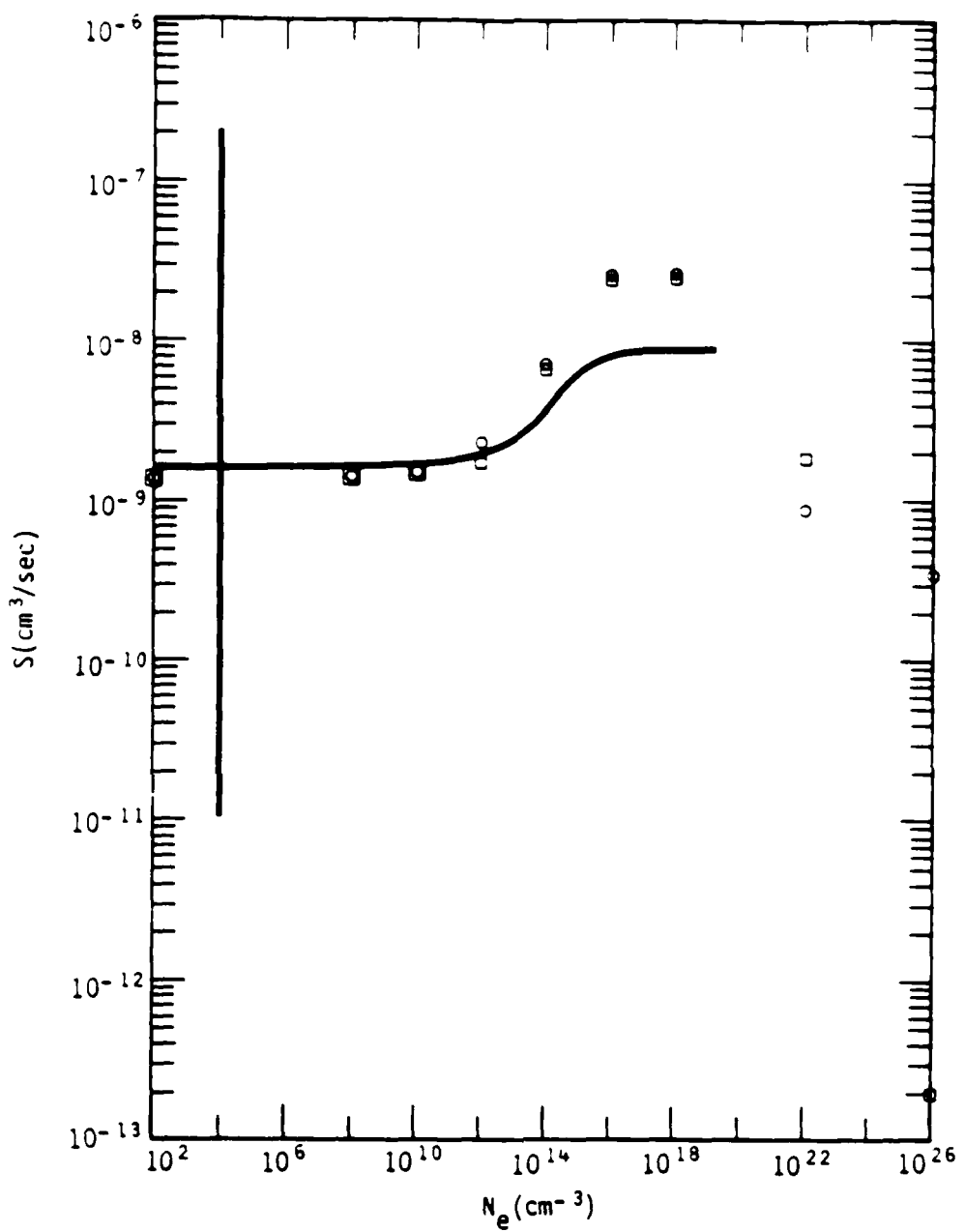


Figure 8. Hydrogen Collisional Radiative Ionization Coefficient at 64,000°K. The BKM coefficient is shown as a solid line. Our values for 10 states are shown as open circles, for 4 states as open squares. BKM is not reliable to the right of the vertical line.

test calculations modifying several aspects of the artificial state show that the value of S at 4000°K is sensitive to such details. For example, if the polarization depression energy of Eq. (3) were increased a factor of 4, essentially all discrepancies in S left of the vertical line would disappear for all three figures, 6-8. Although this would be the simplest way to eliminate the discrepancies, we don't feel qualified to argue the accuracy of (3), besides, there are other options for eliminating the discrepancy. Because S is so small at 4000°K, we don't feel it worth the effort to complicate the code.

More serious discrepancies occur in the region where BKM breaks down. Our value of S tends to be higher than BKM in this region because (1) polarization depression of ionization energy makes ionization more favorable when electron temperature is less than ionization potential and (2) as population of upper states becomes important, either in steady state or transiently during recombination, ionization of these states can dominate. The first of these effects occurs when BKM assumption (E) is violated, the second can occur transiently when their assumption (D) is violated and permanently when their assumption (P) is violated.

The scatter in our rates at very high N_e occurs due to breakdown of assumption (D). When the quasi-steady assumption fails for several excited states over a significant fraction of the time necessary for the process to go to completion, neither α nor S is a constant. The particular value obtained depends on the particular moment chosen for evaluation. The range of values obtainable is great, as illustrated by the orders of magnitude difference between S at $N_e = 10^{26}$ from Figure 7 and Figure 8, and by the difference in 4 state and 10 state values in Figure 8 at $N_e = 10^{26}$.

In summary, where the value of S is significant and the BKM assumptions valid, agreement is satisfactory. Where S is uninterestingly

small, our values are high. Where BKM assumptions fail, the normal concept of S breaks down and no calculations are available for comparison.

7.2 APPROACH TO STEADY STATE WITHOUT RADIATION.

In addition to comparison to the results of BKM, one can consider the "reasonableness" of the final steady state configuration for non equilibrium conditions and the rate and manner of approach to steady state.

A fairly serious problem with any such discussion is finding a straightforward and clear method of presentation of results for a system as complex as several dozen eigenstates distributed over several states of ionization for an element of interest such as nitrogen or oxygen.

In an attempt to invent an appropriate graphic technique, we have adopted the following.

Consider the partition function of some state, k , of an element at temperature θ and electron density N_e .

$$p(k) = (Q_e/N_e)^Z g_k \exp(-E_k/\theta) \quad (116)$$

where Q_e is the partition function for free electrons,

$$Q_e = 6.037 \times 10^{21} \theta^{3/2} (\text{cm}^{-3}) \quad (117)$$

θ (eV) is temperature, N_e (cm^{-3}) is electron density, g_k is statistical weight of the state k , E_k is energy of state k relative to the lowest eigenstate of the element (normally the ground state of the neutral, but, e.g., for oxygen, the ground state of O^-), and Z is the charge state of the ion to which eigenstate k belongs.

The total partition function of the element is

$$P = \sum_k p(k) \quad (118)$$

In equilibrium, the fraction of the element in state k is given by

$$f(k) = p(k)/P = \left[(Q_e/N_e)^Z g_k / P \right] \exp(-E_k/\theta) \quad (119)$$

or

$$F(k, \theta, N_e) f(k) = \exp(-E_k/\theta) \quad (120)$$

where

$$F(k, \theta, N_e) = P / \left[(Q_e/N_e)^Z g_k \right] \quad (121)$$

The form (120) is a rather versatile way to present results. One can graph the exponential of the RHS against E_k to obtain a straight line on semi-log paper, calculate F a priori, then use whatever $f(k)$ results from a calculation to evaluate the LHS and graph it. If the calculated $f(k)$ are in equilibrium at θ , the two curves will lie on top of each other, if not, one has a visual illustration of the degree of departure from equilibrium. The disadvantage of the presentation is that a curve of the LHS of (120) is effectively divorced from the actual values of $f(k)$, so that no clue exists as to which electron or ionization states are most populous.

7.2.1 Time Development of Hydrogen.

An introduction to this sort of presentation is provided by Figure 9 which shows the results for hydrogen initially neutral, bathed in 10^8 electrons at 1 eV with no radiation field. Our initialization over-populates the ground state ($k=1$) and the first excited state ($k=2$); as shown by the dashed line, relative to the 1 eV solid line. In slightly more than 10^4 sec the states have come to a steady configuration with electron collisional processes biased by spontaneous radiation, shown by the dotted line. In this case one might speak of an "effective eigenstate temperature" of about 0.4 eV to approximate the electron distribution. In the final state the actual fractional populations are 0.945 for state 1, 6.6×10^{-6} for the artificial state at about 13.6 eV, and 0.055 for H^{1+} at 13.6 eV. All the others range from 10^{-12} to 10^{-13} .

7.2.2 Hydrogen Steady State vs Electron Density.

Figure 10 shows the final configurations for hydrogen in a plasma of 1 eV electrons at several values of electron density. By $N_e = 10^{18}$ electron collisional processes dominate spontaneous radiation sufficiently that an equilibrium distribution is attained.

7.2.3 Time Development of Nitrogen.

A much more interesting and much more complex case is illustrated in Figure 11. Two calculations are illustrated. Both have electron density of 10^{14} cm^{-3} and temperature 3 eV. The first was initialized with all the nitrogen stripped to 7^+ , and the second was initialized with all nitrogen neutral. By 2.67×10^{-4} sec the first case has recombined enough to extend an erratic pattern of electron population down to N^{4+} , by 1.23×10^{-3} sec populations extend to 2^+ . By a few tenths of a

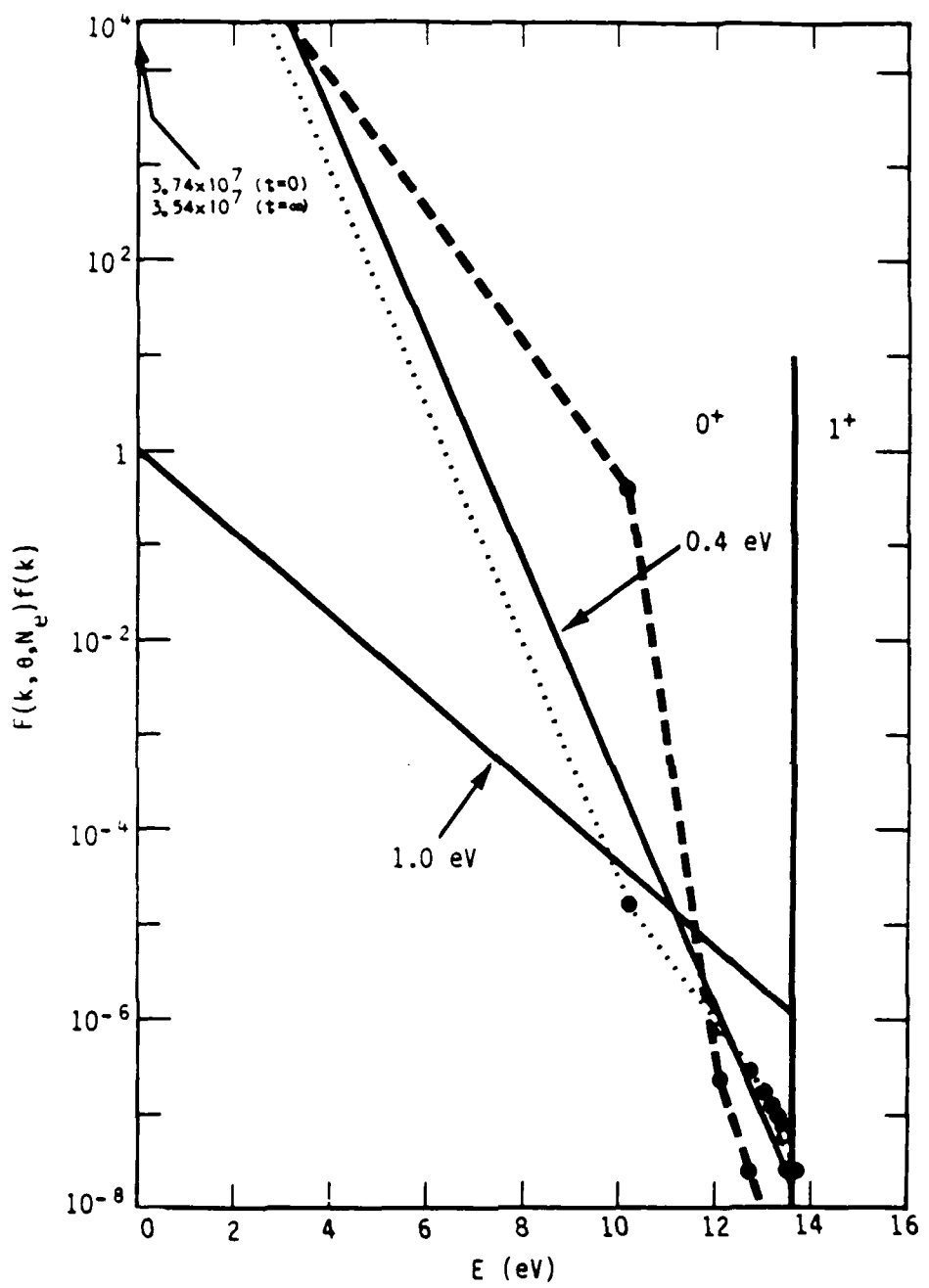


Figure 9. Hydrogen Ionization. At $N_e = 10^8 \text{ cm}^{-3}$ and $\theta_e = 1.0 \text{ eV}$, hydrogen is initially about as shown in the dashed line. The final steady state is as shown by the dotted line.

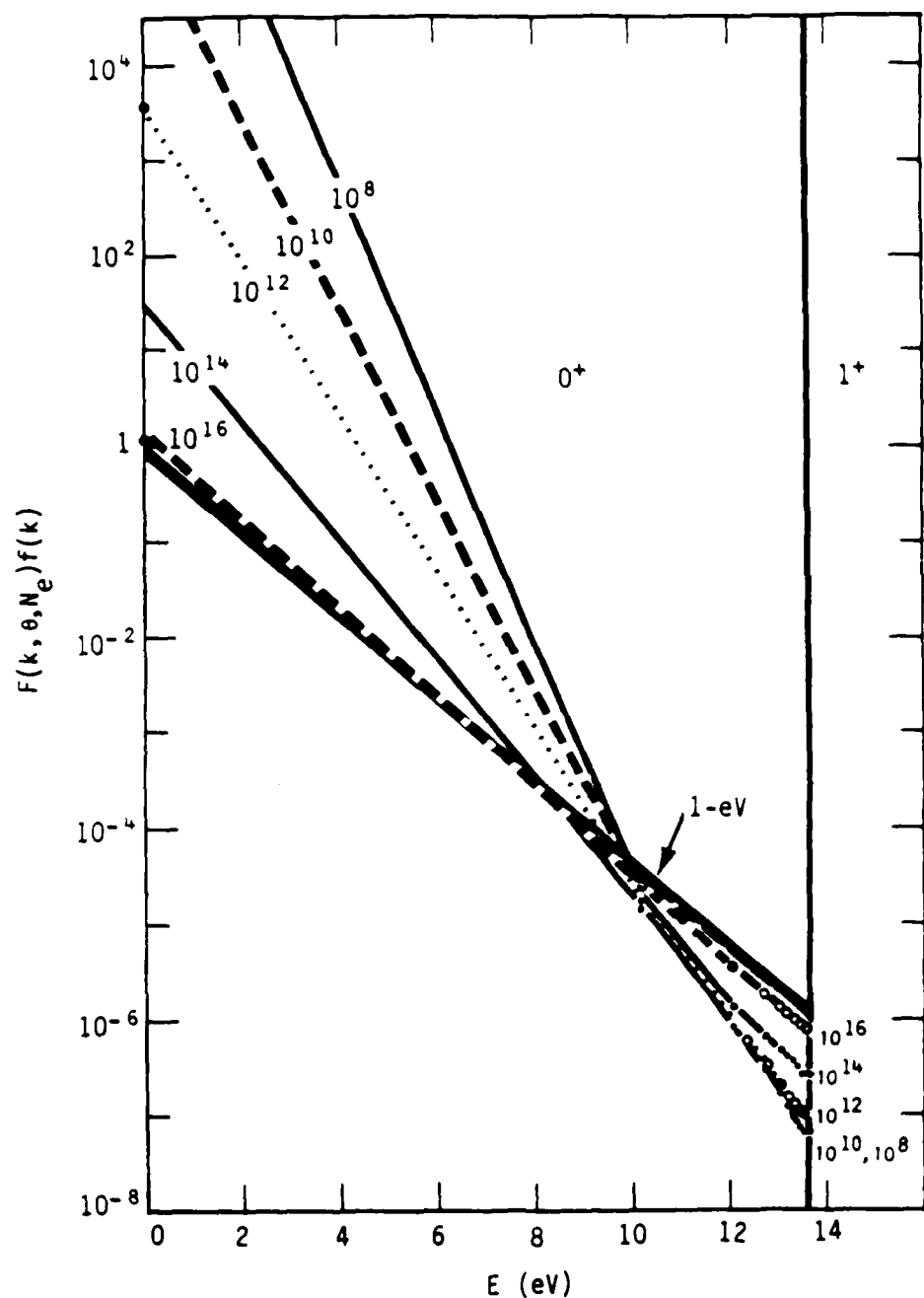


Figure 10. Steady State Hydrogen. For indicated electron densities (cm^{-3}) the steady state values of eigenstate populations are shown in the absence of a radiation field. For N_e of 10^{18} cm^{-3} or greater, all states lies on the 1-eV equilibrium line.

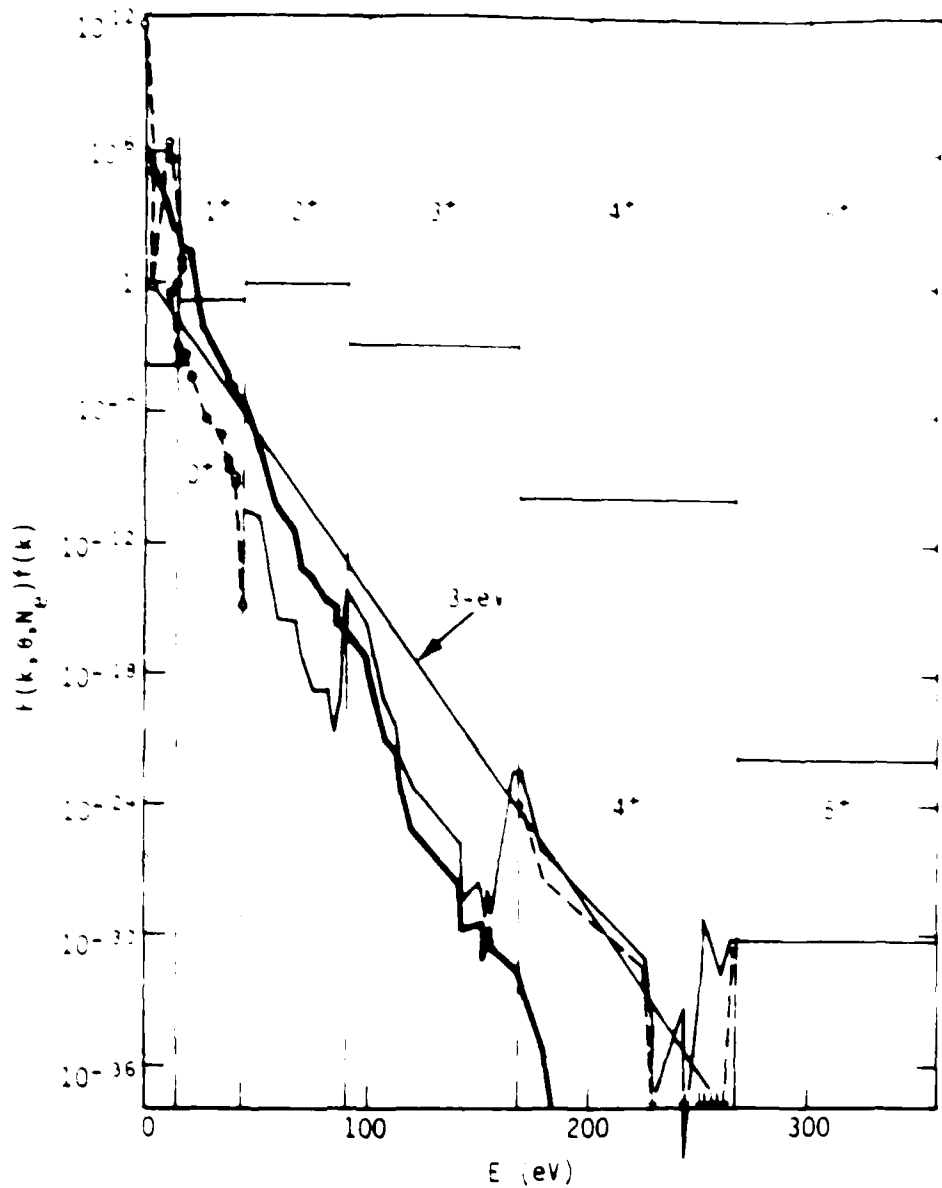


Figure 11. Nitrogen in 10^{14} electrons at 3 ev. The heavy solid line is the final steady state. The light broken line extending down to 4+ shows states at 2.67×10^{-4} sec after initialization with only 7+ nitrogen present. The light solid line extending down to 2+ shows states after 1.23×10^{-3} sec. The dashed line extending through 1+ shows states 1.87×10^{-11} sec after initialization with only 0+. Both cases approach the heavy solid line with total ion populations indicated by horizontal lines over the energy range corresponding to the state of ionization.

and the steady state is reached at the heavy solid line, which is better than the steady state temperature of 1 eV than the true electron temperature of 0.7 eV. The second case shows population through 1^+ by ionization and the steady state is reached at the heavy solid line by 1.87 sec (0.187 sec).

The relative population of states show much more structure than hydrogen does because oscillator strengths connecting the nitrogen states are arbitrary, in contrast to the smooth values appropriate for fully degenerate hydrogen states. Note that the first excited state of neutral nitrogen is underpopulated by nearly 4 orders of magnitude relative to the second state at 1.87×10^{-6} sec for the case initialized with neutral nitrogen. This is due to the fact that this state is optically forbidden with respect to the ground state. Our algorithm arbitrarily assigns an effective oscillator strength of 10^{-3} to such transitions for electron transitions, else it would be even more severely underpopulated.

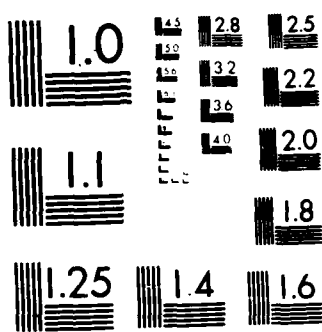
The effective ionization rate coefficient from N^{0+} to N^{1+} for this case is about $7 \times 10^{-10} \text{ cm}^3/\text{sec}$, about twice the BKM value for hydrogenic ions and about seven times Sappenfield's calculation for ground state ionization coefficient. The agreement with BKM is quite satisfactory, particularly in view of the fact that nitrogen is not especially hydrogenic. The discrepancy with Sappenfield is presumably due partly to differences in collision cross section and also is due in part to contributions from excited states, especially states 2 and 3, which acquire fairly large populations (0.6 of state 1 and 0.2 of state 1 respectively).

7.2.4 Nitrogen Steady State vs Electron Density.

Figure 12 shows steady state configurations for nitrogen in a bath of 1 eV electrons and in the absence of a radiation field, the optically thin limit. When electron density gets as high as $10^{16}/\text{cm}^3$

AD-A179 741 A METHOD TO OBTAIN TIME DEPENDENT ELECTRON EIGENSTATE 2/2
POPULATIONS WITH EL (U) MISSION RESEARCH CORP SANTA
BARBARA CA D H SOWLE 01 JUL 86 MRC-R-1006
UNCLASSIFIED DNA-TR-86-283 DNA001-85-C-0035 F/G 28/8 NL





MICROCOPY RESOLUTION TEST CHART
NATIONAL BUREAU OF STANDARDS 1964 A

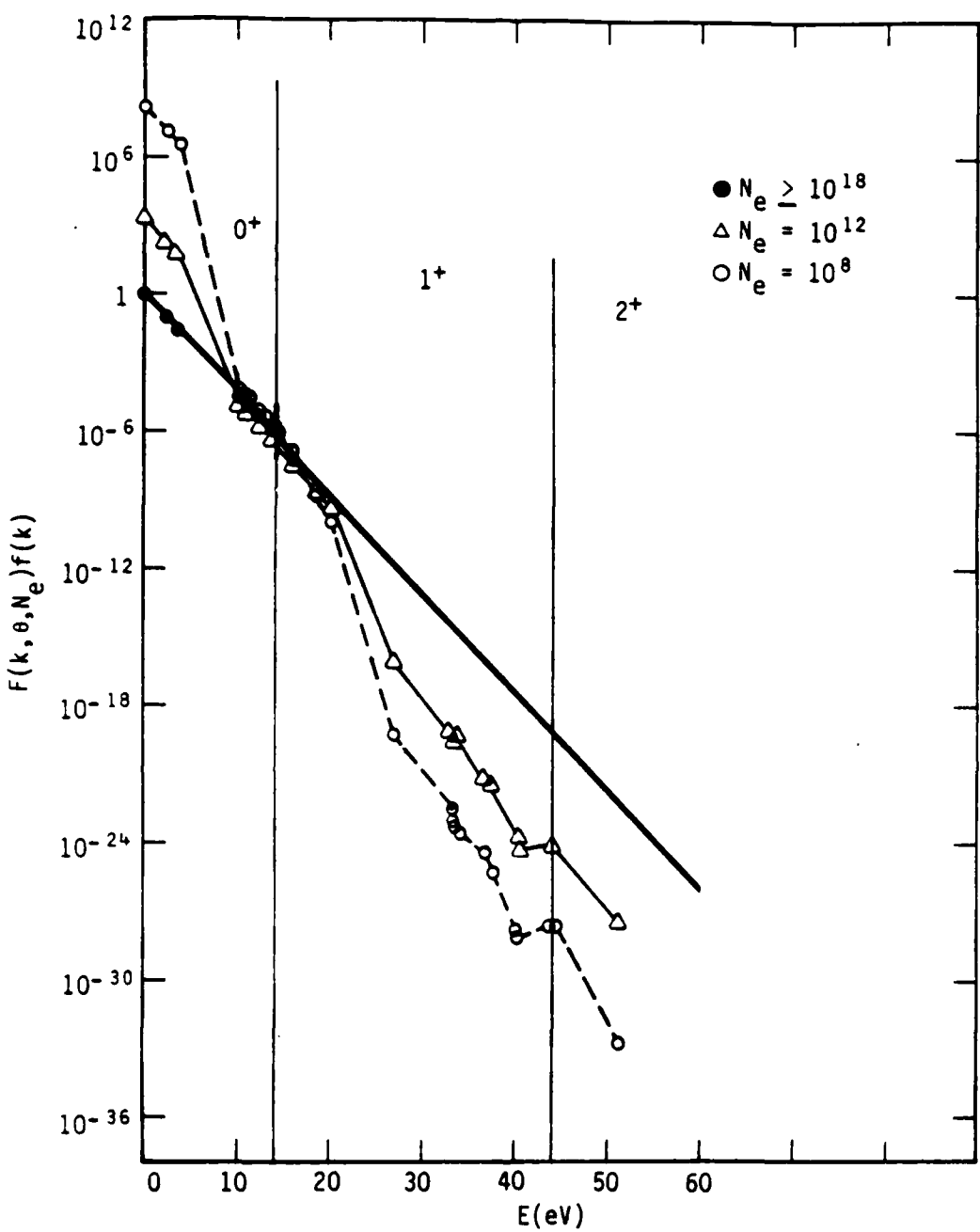


Figure 12. Nitrogen at 1-eV. Nitrogen steady state eigenstate distribution for 1-eV electrons and no radiation is shown for three values of electron density. Solid circles correspond to 10^{18} electrons/cm 3 or higher, open triangles to 10^{12} electrons/cm 3 and open circles to 10^8 electrons/cm 3 .

eigenstate populations follow the equilibrium exponential out to 20 eV or 30 eV before falling below it. By electron density 10^{18} cm^{-3} all states retained by the code are within 1% of equilibrium; states above 1+ are deleted as described in Section 3.3.4 at this high electron density.

Steady state distribution of nitrogen eigenstates for electrons at 10 eV are shown in Figure 13. Note that the abscissa is logarithmic, so the range goes from 10^{-70} to 10^{90} . The curves show the extreme sensitivity to electron density for weak plasmas, in that twelve orders of magnitude in electron density (10^{-2} to 10^{10}) result in 12 to 40 orders of magnitude difference in state population relative to equilibrium. It also illustrates the disadvantage of this presentation; the ground state of N^{0+} is overpopulated by an impressive factor of 10^{93} but even so, all N^{0+} states account for only 1 part in 10^{12} of the nitrogen.

The approach to equilibrium is shown in more detail in Figure 14. Here it can be seen that even 10^{18} cm^{-3} leaves the lower states about an order of magnitude overpopulated whereas 10^{20} cm^{-3} brings them into equilibrium. If the curves of Figure 14 were to be extended to higher energy, they would show that even at 10^{20} cm^{-3} , the excited states of N^{5+} around 700 eV to 800 eV would be severely underpopulated.

7.2.5 Value of Electron Density for Equilibrium in Optically Thin Plasma.

For electron collisions to drive the eigenstates into equilibrium in an optically thin plasma, it is clear that electron collisional excitation must dominate spontaneous radiation. Given a ladder of some dozens of eigenstates one would expect the downward bias to accumulate, so electron collisions might need to dominate spontaneous radiation by one or more orders of magnitude.

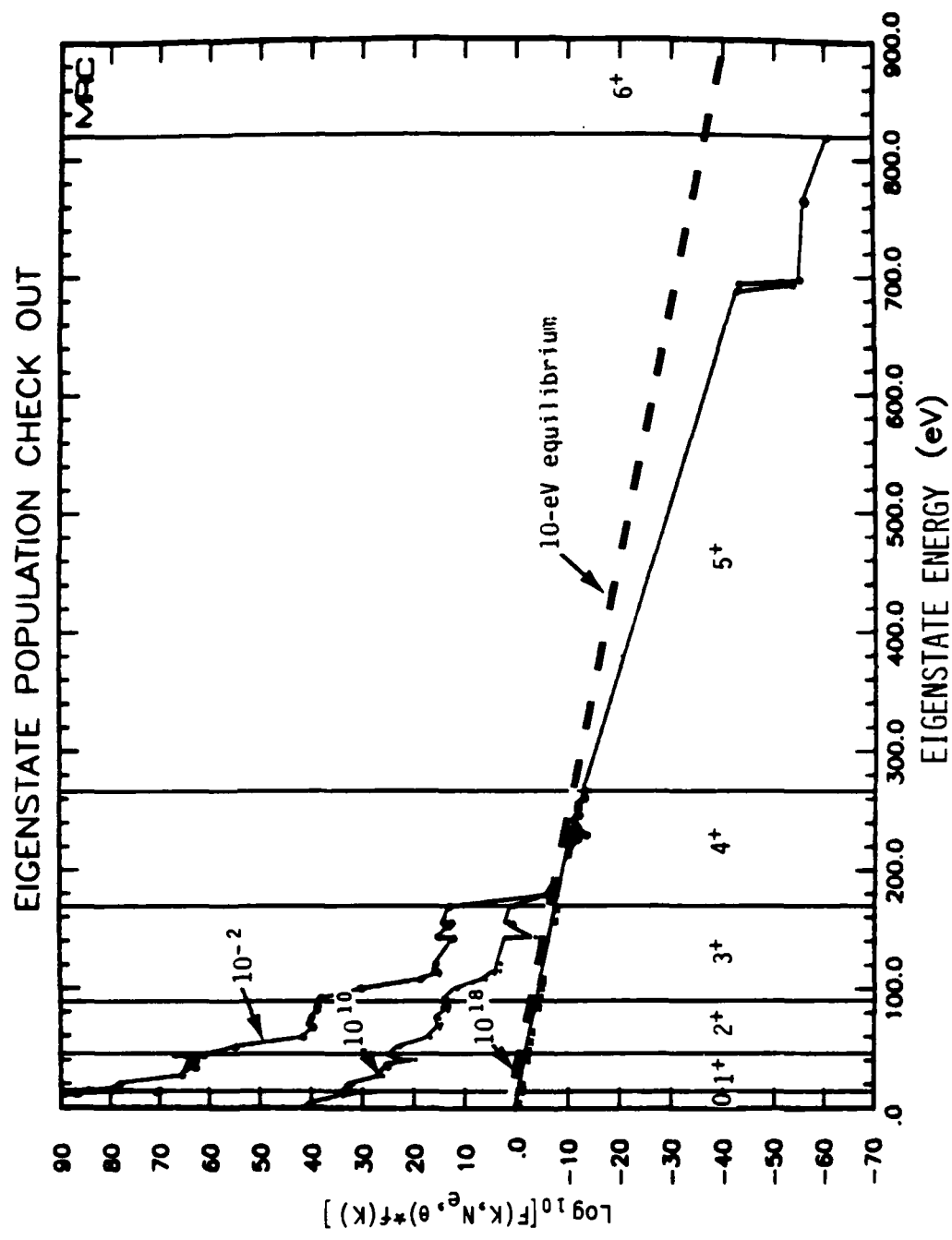


Figure 13. Nitrogen at 10-eV, optically thin. Electron density (cm^{-3}) is indicated for each line.

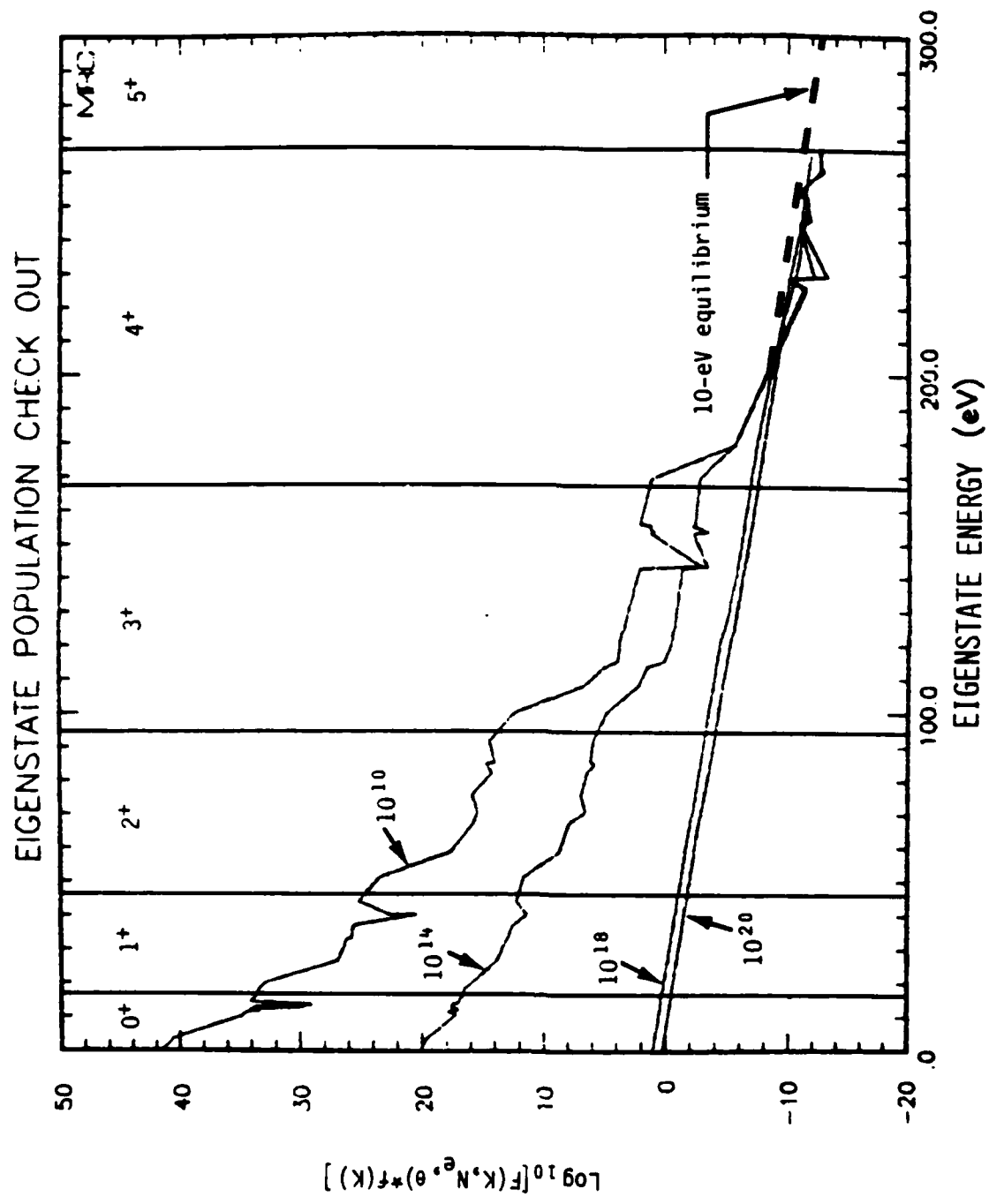


Figure 14. Optically thin nitrogen at 10-eV, more detail. Above the equilibrium curve, the 10^{10} curve is always above the 10^{14} , below equilibrium it lies below the 10^{14} curve.

The ratio of electron collisional excitation from lower state ℓ to upper state k to spontaneous radiation from k to ℓ is, from (48) and (51)

$$R_e = N_e (g_k/g_\ell) (C_{ec}/A_r) \exp[-(E_k - E_\ell)/\theta] / \theta^{1/2} (E_k - E_\ell)^3 - 1.5 \times 10^{-13} \exp[-(E_k - E_\ell)/\theta] / [\theta^{1/2} (E_k - E_\ell)^3] N_e \quad (122)$$

when θ and E are measured in eV and N_e in cm^{-3} , and the ratio of statistical weights has been taken to be unity. Then a distribution approaching equilibrium can be anticipated whenever $R_e \gg 1$, or

$$N_e \gg 6 \times 10^{12} \theta^{1/2} (E_k - E_\ell)^3 \exp[(E_k - E_\ell)/\theta] \quad (123)$$

If $E_k - E_\ell \sim 10$ eV as appropriate for lower ionization states of nitrogen, or for neutral hydrogen, one needs

$$N_e \gg 5 \times 10^{16} \text{ cm}^{-3} .$$

Thus one should not be surprised to see hydrogen states come into equilibrium at about 10^{18} cm^{-3} and the nitrogen line of Figure 14 parallel to the equilibrium line for the first few states of ionization at 10^{18} cm^{-3} .

On the other hand, if $E_k - E_\ell \sim 100$ eV as is the case for some states of N^{4+} and most of N^{5+} , one needs

$$N_e \gg 5 \times 10^{23} \text{ cm}^{-3}$$

for equality. These states aren't likely to be brought into equilibrium for N_e less than about 10^{25} cm^{-3} . Long before this electron density is reached: (1) equilibrium populations of highly ionized states are negligible ($< 10^{-20}$ for N^{4+}) and (2) our simple treatment of polarization effects has become inappropriate.

7.3 APPROACH TO STEADY STATE WITH PLANCK RADIATION.

The rate of excitation for an allowed bound-bound transition of energy, ϵ , by a Planck spectrum is

$$r_{BB} = \int \sigma(v) U(v) dv \quad (124)$$

If the line is reasonably narrow, as is almost always the case, the Planck spectral flux, $U(v)$, can be removed from the integral in (124) and the integral evaluated (Ref. 3, p. 59),

$$r_{BB} \sim U(v) \int_{-\infty}^{\infty} \sigma(v) dv = \pi r_e c f U(v) \quad (125)$$

where r_e is the classical radius of the electron, c the speed of light, and f the oscillator strength.

From (60), $U(v)$ can be written as

$$U(v) = C_p \epsilon^2 / (\exp(\epsilon/\theta) - 1) \quad (126)$$

Then for a transition of energy, ϵ , and nominal oscillator strength of 0.1, the time to reach equilibrium is of order

$$\tau_{BB} = r_{BB}^{-1} = 2 \times 10^{-7} (\exp(\epsilon/\theta) - 1) / \epsilon^2 \quad (127)$$

Thus, for a Planck spectrum at 1 eV temperature, we should expect equilibrium among bound states in about 10^{-5} sec if the biggest gap between states is about 8 eV, which is about the case for N^{0+} , N^{1+} , and N^{2+} , or about 1.5 sec for a biggest gap of 22 eV (N^{3+}).

To bring the states of ionization into equilibrium is more difficult. The cross section for photoionization is given by (67). If this value is substituted into (124) with proper care for units, one finds

$$r_{BF} = C_H C_p I_Z^2 / n \int_{I_Z}^{\infty} [\epsilon(\exp(\epsilon/\theta) - 1)]^{-1} d\epsilon$$

$$\approx C_H C_p I_Z \theta / n \exp(-I_Z/\theta) \quad (128)$$

or

$$\tau_{BF} = r_{BF}^{-1} \approx 2 \times 10^{-7} \exp(I_Z/\theta) / (I_Z \theta) \quad (129)$$

where (129) has assumed that $I_Z \gg \theta$ and $n = 3$.

If one assumes bound states to come into equilibrium before ionization states do, then we can apply (129) to the ground state and be within a few orders of magnitude of the right answer, since excited states lose in population all that they gain by the Boltzmann factor in (128).

Application of (129) yields 3^{-2} sec for N^{0+} to N^{1+} , 5×10^4 sec for 1^+ to 2^+ , 2×10^{12} sec for 2^+ to 3^+ , and 10^{25} sec for 3^+ to 4^+ for a 1-eV Planck spectrum. These numbers verify the assumption made above that eigenstates within a given ion should equilibrate faster than different ions.

Figure 15 shows nitrogen, initially neutral, bathed by a 1.0 eV Planck spectrum at 2×10^{-5} sec, 25 sec, and 10^{21} sec. To reduce effects of electrons to a minimum, electron density was taken to be 10^{-10} cm^{-3} , and to ensure that any appreciable collisional effect would show, at least on the steady state curve, electron temperature was set to 0.1 eV. One can see that eigenstates of 0^+ and 1^+ (the only ions present) are pretty well in equilibrium by 2×10^{-5} sec, as expected from (127) for

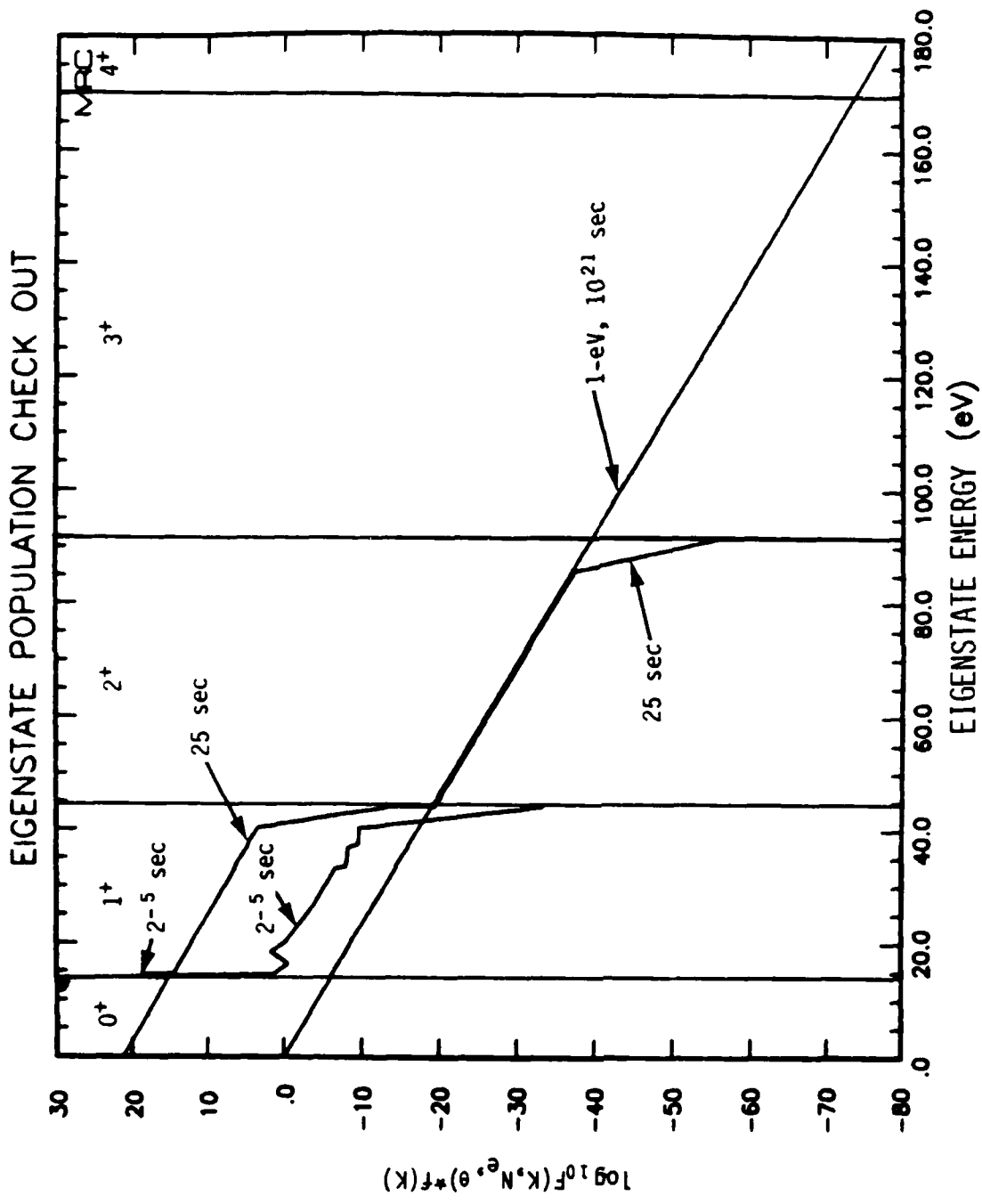


Figure 15. Nitrogen in a 1-eV Planck spectrum without collisions. Nitrogen, initially neutral, subjected to a 1-eV Planck spectrum yields distribution as shown at indicated times. To minimize collisional effects, electron temperature is 0.1-eV and electron density is 10⁻¹⁰ cm⁻³.

bound-bound transitions (their lines are parallel to the 1 eV line). By 25 sec the 0^+ ion state and 1^+ ion state are almost equilibrated (lines are parallel to the 1 eV and almost continuous), as expected from (129). By 10^{21} sec, all states are equilibrated, the curve is indistinguishable from an exponential at 1 eV. At 10^6 sec (not shown) 1^+ and 2^+ are in equilibrium as expected, while 2^+ and 3^+ are still far from equilibrium, as expected. The fact that 3^+ equilibrates with 4^+ by 10^{21} sec, rather than requiring 10^{25} sec is a bit mysterious. At least one order of magnitude is explicable by the distribution of eigenstate population in 3^+ , which makes (129) pessimistic.

Figure 16 illustrates a situation which is a bit more interesting physically, electrons hotter than radiation. Nitrogen, initially neutral, is bathed in a 1 eV Planck as in the case of Figure 15, but the electrons have a temperature of 10 eV and densities from 10^{-10} cm^{-3} to 10^{20} cm^{-3} . Shown are final steady state population distributions. For the case of 10^{-10} cm^{-3} the portion of the curve for 0^+ is an artifact of the computer plotting program and should be ignored; there is in fact so little 0^+ present (total ion fraction less than 10^{-23}) that the computer has zeroed out all 0^+ states. The negative glitch in the upper states of 1^+ should likewise be ignored - one state has too little population to be calculated. The other irregularities in the 10^{-10} curve are due to electron collisional effects on: (a) very closely spaced states, particularly that from the artificial state to the ground state of the next ion and (b) states so widely separated that the 1 eV Planck spectrum cannot bridge the gap even as well as 10^{-10} electrons/cm³. This latter is the case above about 250 eV eigenenergy. As electron number density increases the curve continues to parallel the 1 eV radiation temperature over some ranges of eigenstates until somewhere between 1 electron cm⁻³ and 10^{10} electrons cm⁻³ where the curve shape loses definition. Between 10^{14} cm^{-3} and 10^{18} cm^{-3} the electrons take over and by 10^{20} cm^{-3} the eigenstates through N^{4+} have been forced into equilibrium at 10 eV, despite the cooler photon flux.

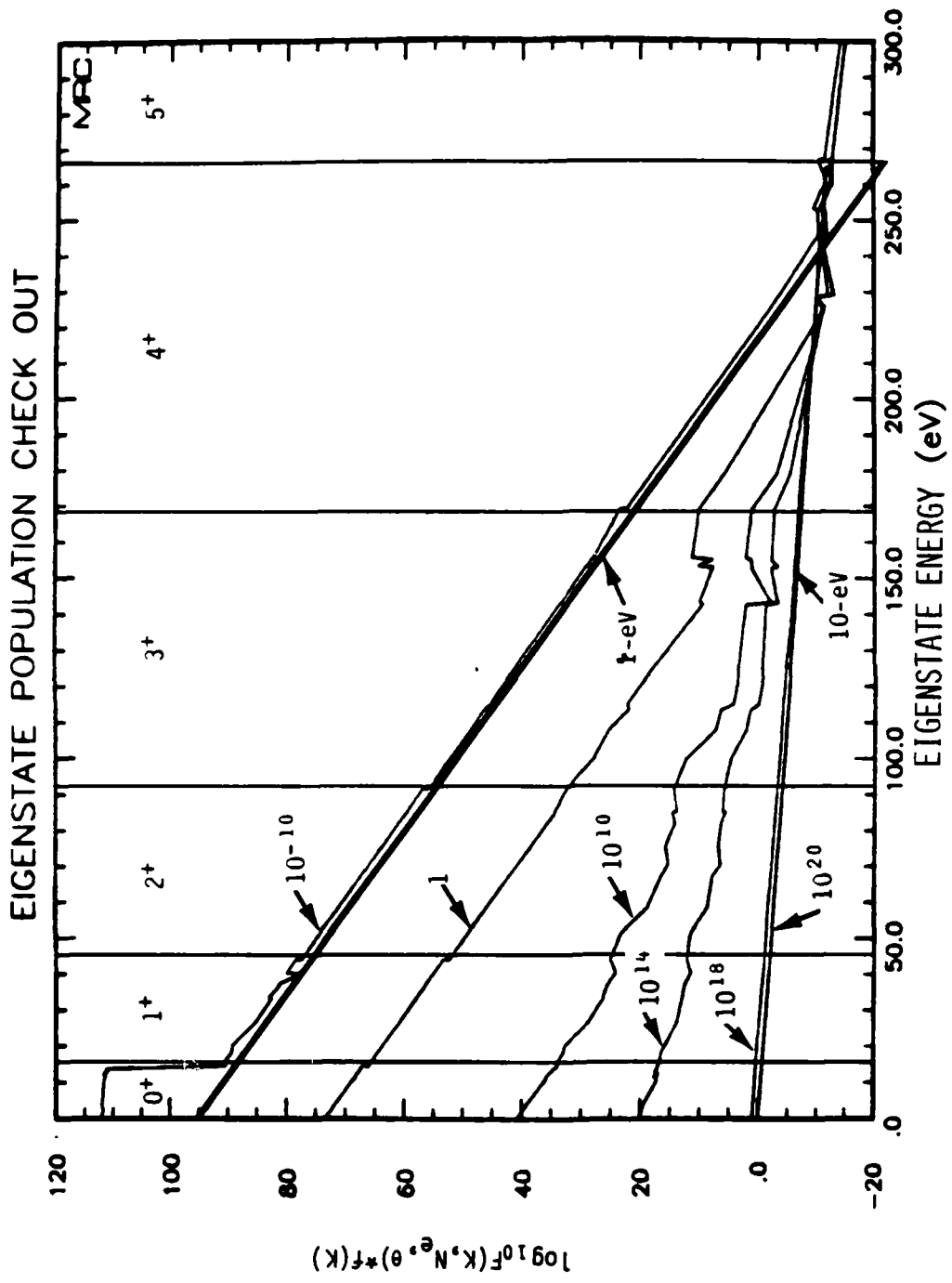


Figure 16. Nitrogen in 1.0 eV Planck radiation and 10-eV electrons. Electron density in cm^{-3} is indicated for each plot of F vs eigenenergy. An exponential at 1-eV is shown for reference near the 10^{-10} cm^{-3} curve. The curve at 10^{20} cm^{-3} lies on a 10-eV exponential through the N^{4+} states, after which F falls below the 10-eV line.

7.4 STEADY STATE WITH LINE RADIATION.

A situation of considerably more physical interest than the preceding examples, and one which has an important implication for the accuracy of previous calculations, is that in which line radiation is present with no continuum. To investigate the effect of a few strong lines, we chose an electron density of $10^{12}/\text{cm}^3$, corresponding to high enough altitude that the continuum should be extremely weak and not too many strong lines are expected. Electron temperature was taken to be 10 eV, a typical value expected when line radiation is an important energy loss mechanism. Under these conditions with no radiation present, initially neutral nitrogen approaches steady state in time of order 0.1 sec with state 4^+ dominant; fractional populations in steady state are:

0^+	1^+	2^+	3^+	4^+	5^+
6×10^{-12}	5×10^{-7}	2×10^{-3}	0.2	0.71	.087

Since 4^+ is the dominant ion we investigated the effect of adding a few lines which connect 4^+ states. All lines were taken to be saturated at the Planck limit for 10 eV. They were added in order of increasing energy.

The first case is illustrated in Figure 17 which shows the region of eigenenergy occupied by the electron states of N^{4+} . Two curves are shown, that for no radiation and that for a single line of 2.69 eV at the Planck limit connecting states 3 and 4 of N^{4+} . The cases are indistinguishable except that the line has raised the population of state 3 about a factor of 2. This is not an impressive effect, but perhaps one should not expect too much from a line whose intensity is over an order of magnitude down from the peak of the Planck spectrum and which connects states whose populations are rather small compared to the ground state.

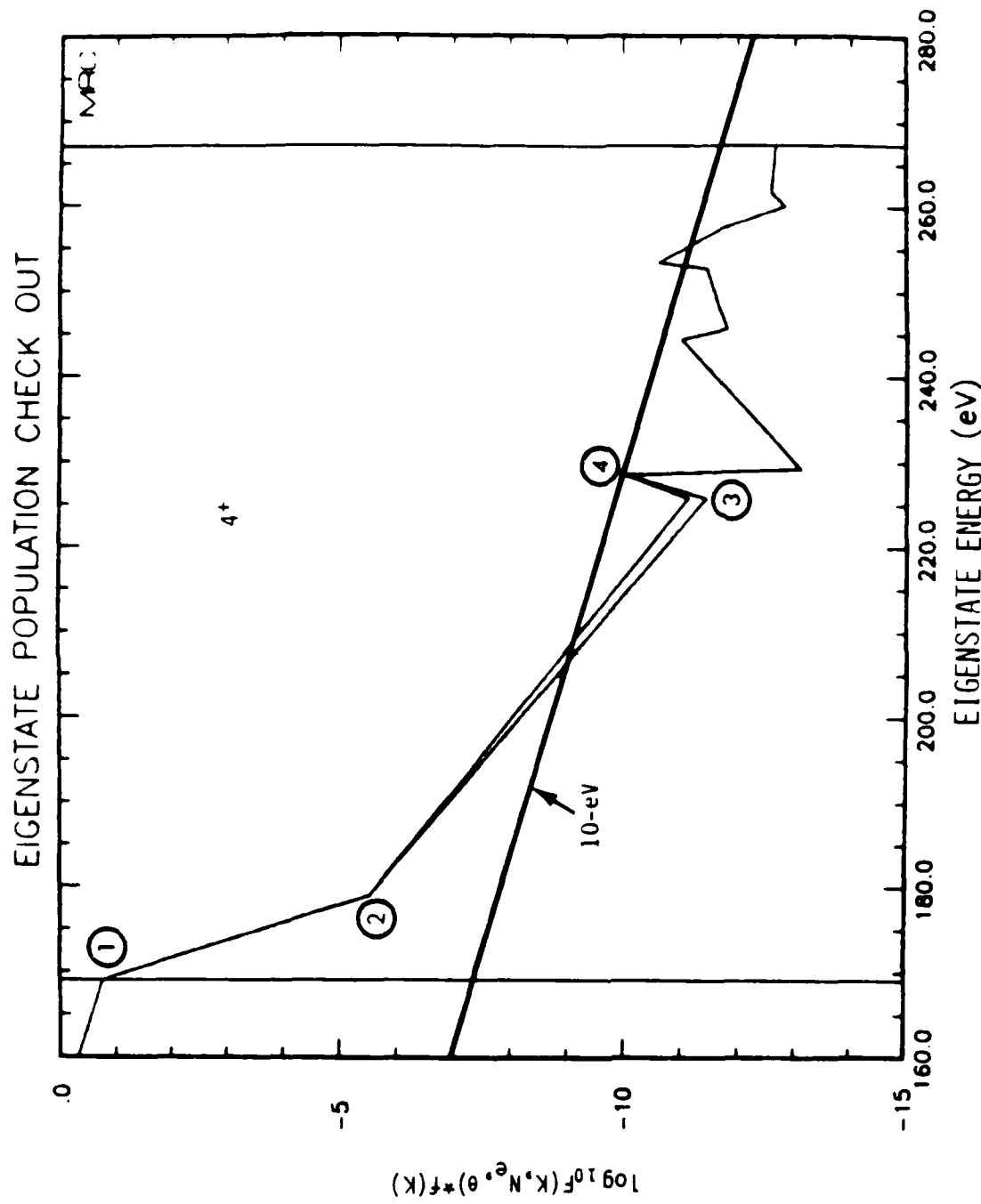


Figure 17. Nitrogen with 1 line. Nitrogen at 10-eV electron temperature and 10^{12} electrons/cm³ with and without a 2.69-eV line at the Planck limit, connecting states 3 and 4, is shown. True equilibrium values are shown by the straight line marked 10-eV. N_{4+} states are demarcated by vertical lines. The first 4 states are indicated by circled numbers. The case with 1 line is distinguishable only by increasing the population of state 3.

The next calculation, shown in Figure 18 is a little bit more impressive. Here we added a line at 9.9978 eV connecting states 1 and 2. One can see that state 2 is brought up to approximately the correct equilibrium ratio to state 1 (the line connecting state 1 to 2 in Figure 18 is nearly parallel to the 10 eV line). Further, several of the upper states, which have optically allowed transitions to state 2, have increased populations. This is the sort of result one would expect; in fact, a common method of assessing the effect of a medium optically thick to the line connecting ground state to first excited state is to set those populations in equilibrium ratio, then solve the remainder in the optically thin approximation. In an element with many ionization states such as nitrogen, however, the line has another effect which is at least as important as redistributing the 4^+ state populations. A line with about 10 eV energy is capable of ionizing the upper states of any nitrogen ion. Thus, this relatively weak line has also reduced the N^{3+} population from about 20% to about 13% and increased the N^{5+} population from about 9% to 18%.

In Figure 19 a line at 46.556 eV connecting states 2 and 3 has been added. This line has the expected effect of bringing state 3 into approximate equilibrium with states 1 and 2 but more importantly, it is capable of ionizing any state of N^{3+} or N^{1+} and all but the lowest states of N^{2+} , N^{3+} , and N^{4+} . The steady state configuration for this case is:

0^+	1^+	2^+	3^+	4^+	5^+	6^+
7×10^{-19}	4×10^{-11}	2×10^{-7}	10^{-4}	1.6×10^{-3}	.998	8×10^{-23}

The effect has been to raise the mean state of ionization from about 4 to 5. Under borderline conditions, radiation will virtually cease from affected regions. Both N^{3+} and N^{4+} are good radiators, whereas N^{5+} is an exceptionally poor one.

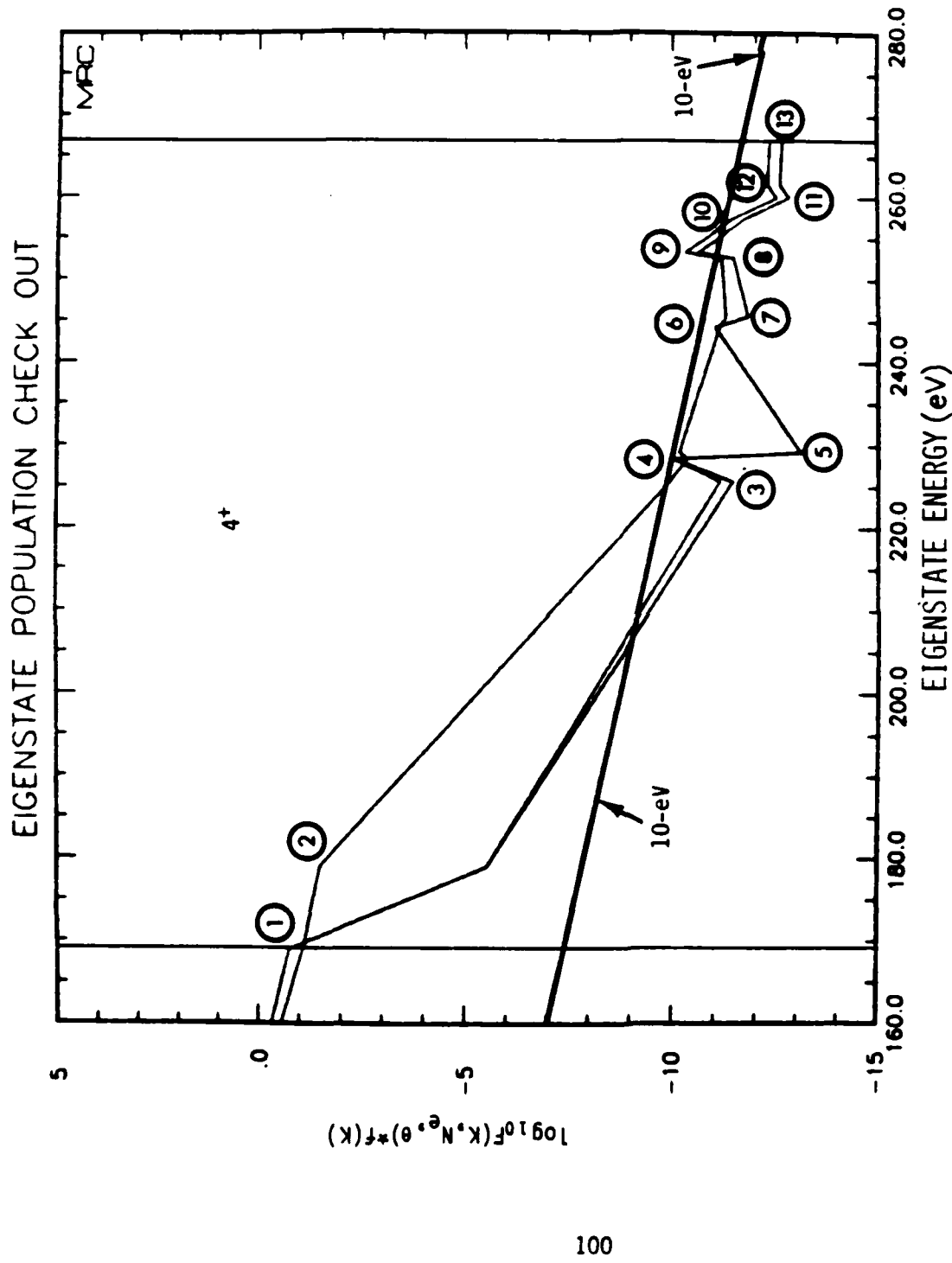


Figure 18. Nitrogen with 2 lines. A line at the 10-eV Planck limit intensity and 9.9978-eV energy has been added to the case shown in figure 17. This line brings states 1 and 2 into approximately their equilibrium ratio, causing upper states with good oscillator strength to state 2 to increase in population. It also ionizes upper states of all ion species, raising the average state of ionization.

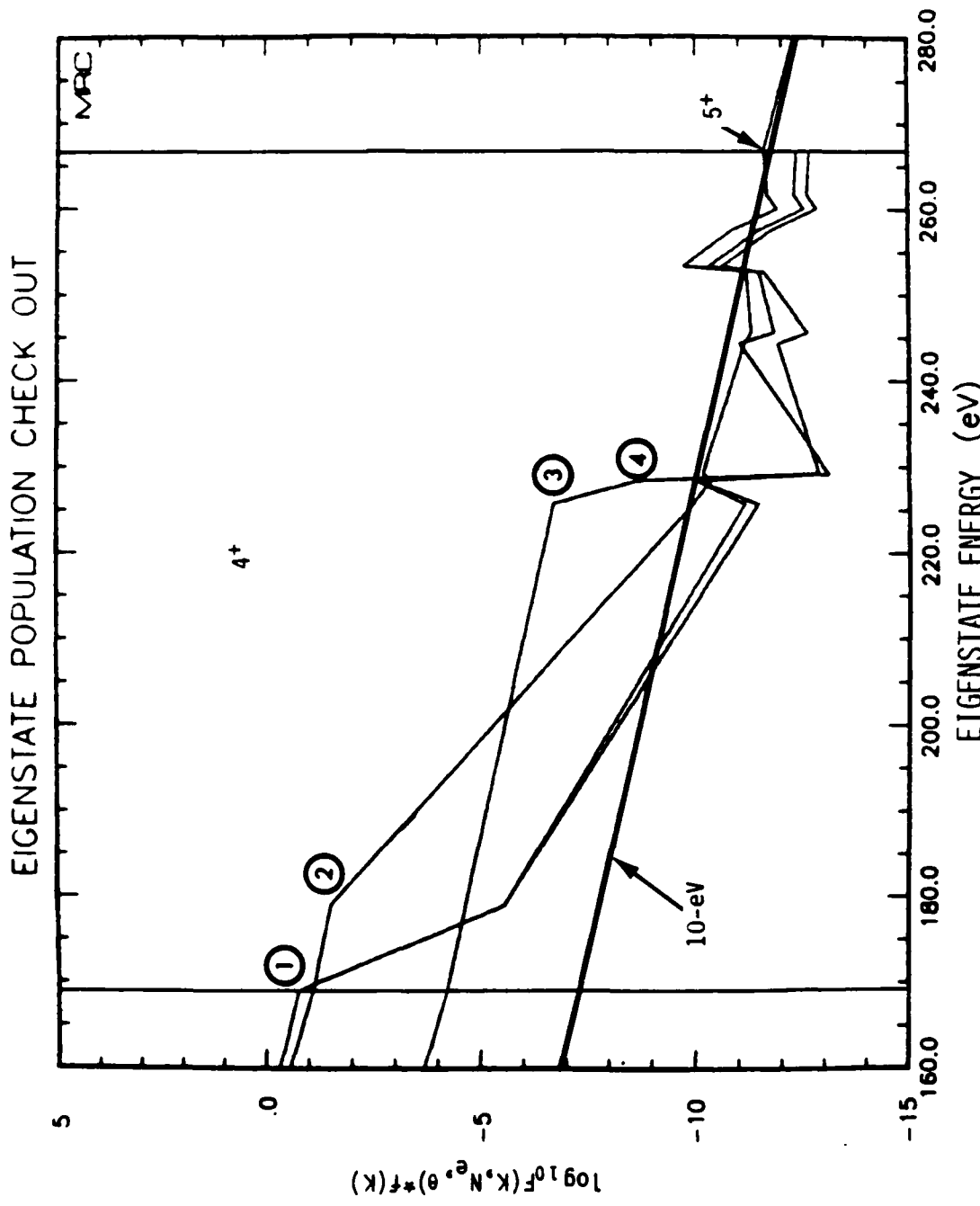


Figure 19. Nitrogen with 3 lines. A line at 46.556-eV at the Planck limit for 10-eV has been added to the case of figure 18. This line connects states 2 and 3. It brings the first three states close to an equilibrium ratio. Perhaps more importantly, it ionizes most states below N_{4+} and the upper states of N_{4+} , reducing the population of N_{4+} from 68% to 0.15%.

Figure 20 shows the barely noticeable effect of adding the 56.554 eV line connecting states 1 and 4 to the previous 3 lines. All states below state 4 are reduced in population by about a factor of 2 and no other discernable event occurs.

Finally, Figure 21 shows a comparison of the case with no radiation to that with all four lines over the full range of eigenstates. It shows that low ionization states are depopulated by up to 12 orders of magnitude by the radiation (either the 2-3 line or the 1-4 line would accomplish most of this), and the upper states of N^{3+} are brought into equilibrium with the lower states of N^{4+} .

The most important meaning of the series of calculations is hidden in the millimeter increase in the ground state of N^{5+} at 269 eV, bringing it from 9% to 99% of the population, and the 3 millimeter decreases in the ground states of N^{3+} and N^{4+} , reducing them from major ions to obscurity. Historically, cases similar to this have been calculated assuming line radiation drains energy from the system but does not appreciably affect state of ionization. The set of cases calculated here do not follow the dynamic behavior of shocked material and so a firm conclusion cannot be drawn, but certainly they call into question the previous method of calculation.

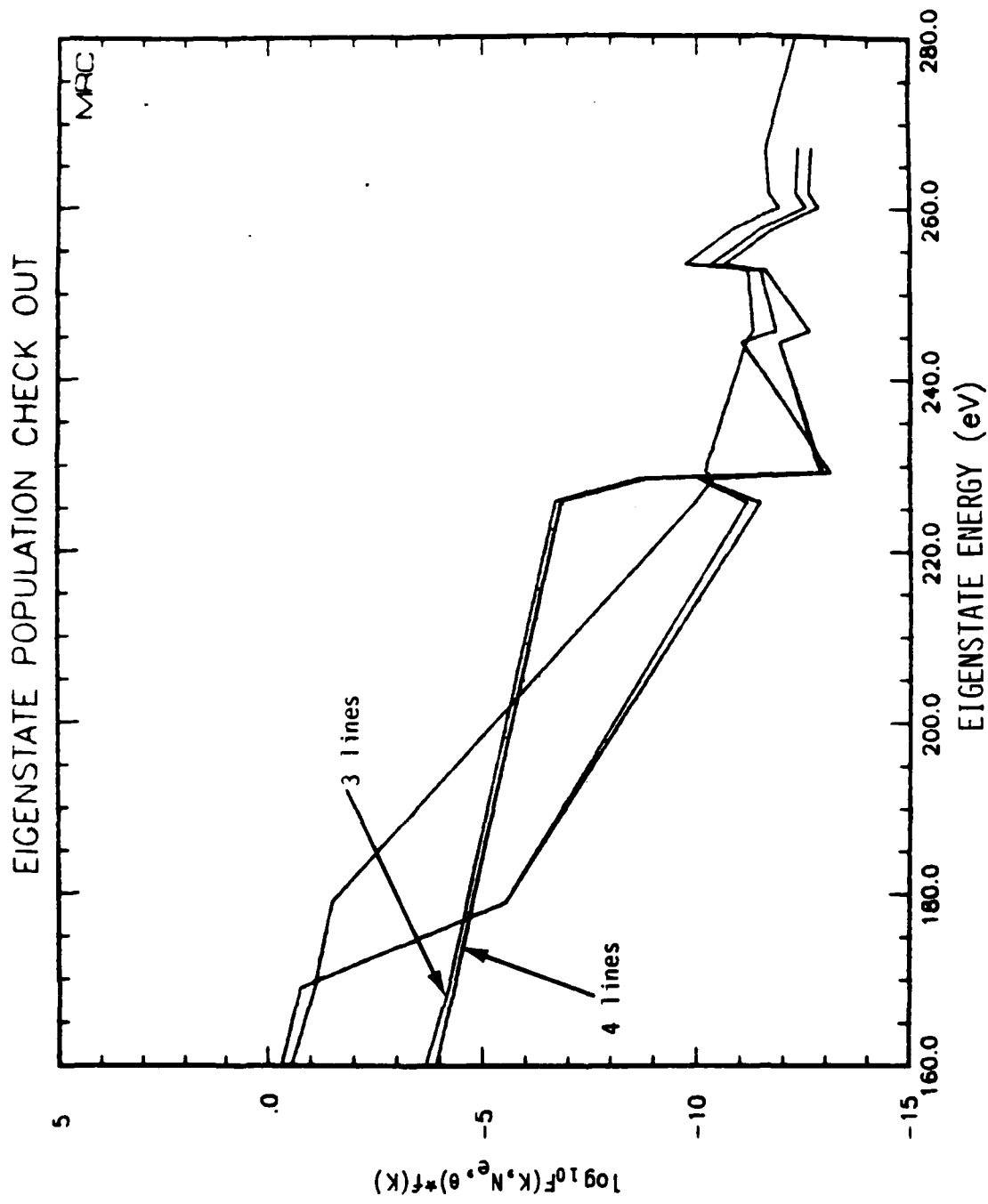


Figure 20. Nitrogen with 4 lines. A line at 56.554-eV connecting state 1 to state 4 has been added to the case illustrated in figure 19. The only effect is to decrease the population of states below the 4th state of N^{4+} by about a factor of 2.

EIGENSTATE POPULATION CHECK OUT

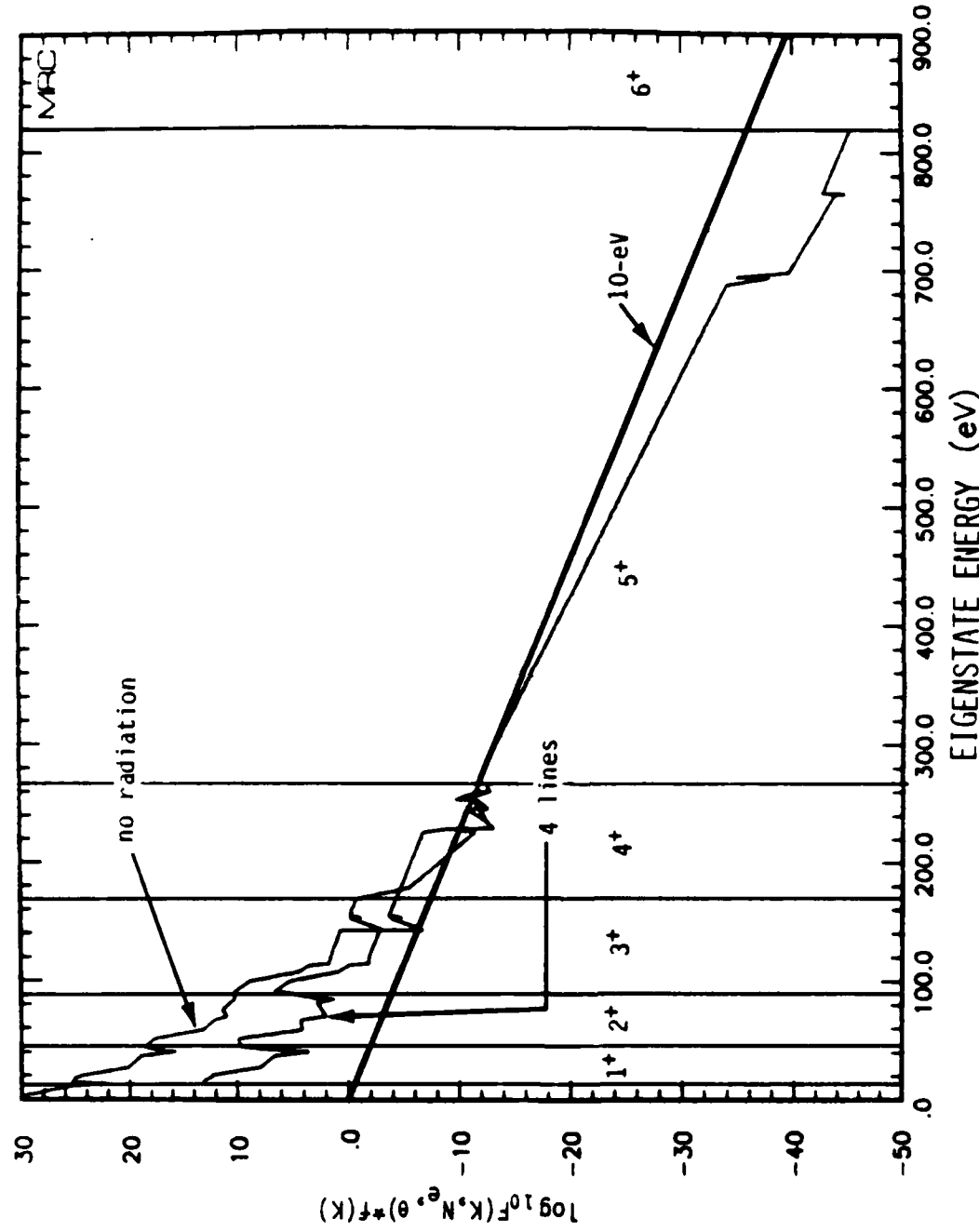


Figure 21. Nitrogen with and without 4 lines. Nitrogen at 10^{12} electrons/cm³ and electron temperature 10-eV is shown in steady state with no radiation field in the upper curve, extending to 269-eV. The lower curve extending to 820-eV has lines at the Planck intensity connecting $N_{\uparrow\uparrow}$ states 1-2, 1-4, 2-3, and 3-4.

SECTION 8
LIST OF REFERENCES

1. Greim, H.R., Plasma Spectroscopy, McGraw-Hill, 1964.
2. Greim, H.R., Spectral Line Broadening by Plasmas, Academic Press, 1974.
3. Allen, C.W., Astrophysical Quantities, Athlone Press, 1981.
4. Burgess, A., Stellar Spectra in the Far Ultraviolet, Int. Colloq. in Astrophysics, Liege, Belgium, 1961.
5. Abramowitz, M. and Stegun, I., Handbook of Mathematical Functions, National Bureau of Standards Applied Mathematics Series 55, Dec 1972.
6. Lotz, W., Electron Impact Ionization Cross Sections and Ionization Rate Coefficients for Atoms and Ions from Hydrogen to Calcium, IPP 1/62, Institut Fur Plasmaphysik, Garching bei Munchen, May, 1967.
7. Moore, C.E., Atomic Energy Levels, V1, National Bureau of Standards 467, 1949.
8. Wiese, W.L., M.W. Smith, E.B.M. Glennon, Atomic Transition Probabilities, V1, NSRDS-NBS4, National Bureau of Standards, May 20, 1966.
9. Bates, D.R., A.E. Kingston, and R.W.P. McWhirter, Recombination between Electrons and Atomic Ions. I Optically Thin Plasmas. Proc. Royal. Soc. London, Series A, 1962, pp 297-312.

DISTRIBUTION LIST

DEPARTMENT OF DEFENSE

ASSISTANT TO THE SECRETARY OF DEFENSE
ATOMIC ENERGY
 ATTN: EXECUTIVE ASSISTANT

BOSTON COLLEGE, THE TRUSTEES OF
2 CYS ATTN: CHAIRMAN DEPT OF CHEMISTRY
2 CYS ATTN: CHAIRMAN DEPT OF PHYSICS

DEF RSCH & ENGRG
 ATTN: DEFENSIVE SYSTEMS
 ATTN: STRAT & SPACE SYS (OS)
 ATTN: STRAT & THEATER NUC FOR. F VAJDA

DEFENSE INTELLIGENCE AGENCY
 ATTN: RTS-2B

DEFENSE NUCLEAR AGENCY
 ATTN: RAAE K SCHWARTZ
 ATTN: RAAE P CROWLEY
 ATTN: RAAE P LUNN
4 CYS ATTN: STTI-CA

DEFENSE TECHNICAL INFORMATION CENTER
12 CYS ATTN: DD

FIELD COMMAND
 ATTN: FCTT
 ATTN: FCTT W SUMMA

FIELD COMMAND DNA DET 2
LAWRENCE LIVERMORE NATIONAL LAB
 ATTN: FCL

DEPARTMENT OF THE NAVY

NAVAL POSTGRADUATE SCHOOL
 ATTN: CODE 1424 LIBRARY

NAVAL RESEARCH LABORATORY
 ATTN: CODE 2627 (TECH LIB)
 ATTN: CODE 4700 W ALI

DEPARTMENT OF THE AIR FORCE

AIR FORCE GEOPHYSICS LABORATORY
2 CYS ATTN: LS/R MURPHY
2 CYS ATTN: LSI/R SHARMA

AIR FORCE OFFICE OF SCIENTIFIC RSCH
 ATTN: AFOSR/NC
 ATTN: ASOSR/NP/MAJ JOHN PRINCE

AIR FORCE WEAPONS LABORATORY, AFSC
 ATTN: SUL

AIR UNIVERSITY LIBRARY
 ATTN: AUL-LSE

DEPUTY CHIEF OF STAFF/AFRDS
3 CYS ATTN: AFRDS (SPACE SYS & C3 DIR)

DEPARTMENT OF ENERGY

DEPARTMENT OF ENERGY
 ATTN: OMA, DP-22

LAWRENCE LIVERMORE NATIONAL LAB
 ATTN: L-10 A GROSSMAN
 ATTN: L-84 H KRUGER

LOS ALAMOS NATIONAL LABORATORY
 ATTN: D SAPPENFIELD
 ATTN: P364 REPORT LIBRARY
 ATTN: REPORT LIBRARY

SANDIA NATIONAL LABORATORIES
 ATTN: TECH LIB 3141 (RPTS RECEIVING CLRK)

OTHER GOVERNMENT

NATIONAL OCEANIC & ATMOSPHERIC ADMIN
3 CYS ATTN: E FEHSENFELD

DEPARTMENT OF DEFENSE CONTRACTORS

AVCO EVERETT RESEARCH LAB, INC
 ATTN: C VON ROSENBERG JR

BERKELEY RSCH ASSOCIATES, INC
 ATTN: J WORKMAN
 ATTN: S BRECHT

CALIFORNIA, UNIVERSITY AT RIVERSIDE
 ATTN: J PITTS JR

INSTITUTE FOR DEFENSE ANALYSES
 ATTN: E BAUER
 ATTN: H WOLFHARD

KAMAN SCIENCES CORP
 ATTN: E CONRAD

KAMAN TEMPO
5 CYS ATTN: DASIAC

KAMAN TEMPO
 ATTN: DASIAC

MISSION RESEARCH CORP
 ATTN: D ARCHER
2 CYS ATTN: D SOWLE
 ATTN: M SCHEIBE
2 CYS ATTN: TECH LIBRARY

MISSION RESEARCH CORP
 ATTN: C LONGMIRE

PACIFIC-SIERRA RESEARCH CORP
 ATTN: H BRODE, CHAIRMAN SAGE

DNA-TR-86-283 (DL CONTINUED)

PHYSICAL RESEARCH, INC
ATTN: T STEPHENS

PHYSICAL RESEARCH, INC
ATTN: J DEVORE

R & D ASSOCIATES
ATTN: F GILMORE
ATTN: H ORY
ATTN: R TURCO

RAND CORP
ATTN: B BENNETT

SCIENCE APPLICATIONS INTL CORP
ATTN: D HAMLIN

SRI INTERNATIONAL
ATTN: W CHESNUT

DIRECTORY OF OTHER

GOVERNMENT PUBLICATIONS LIBRARY-M
ATTN: J WINKLER

E N D

5 - 81

D T i C